LOAN DOCUMENT

PHOTOGRAPH THIS SHEET

AD-A241 416

DTIC ACCESSION NUMBER

LEVEL

INVENTORY

1

WL-TR-91-3086

DOCUMENT IDENTIFICATION

Oct 91

DISTRIBUTION STATEMENT

HANDLE WITH CARE

ACCESSION FOR

NTIS GRA&I ☒

DTIC TRAC ☐

UNANNOUNCED ☐

JUSTIFICATION

BY

DISTRIBUTION/

AVAILABILITY CODES

DISTRIBUTION	AVAILABILITY AND/OR SPECIAL	
A-1		

DISTRIBUTION STAMP

DATE ACCESSIONED

DATE RETURNED

91 10 9 027

DATE RECEIVED IN DTIC

91-12831

REGISTERED OR CERTIFIED NUMBER

PHOTOGRAPH THIS SHEET AND RETURN TO DTIC-FDAC

DTIC FORM 70A JUN 90

DOCUMENT PROCESSING SHEET

PREVIOUS EDITIONS MAY BE USED UNTIL STOCK IS EXHAUSTED

LOAN DOCUMENT

DISCLAIMER NOTICE

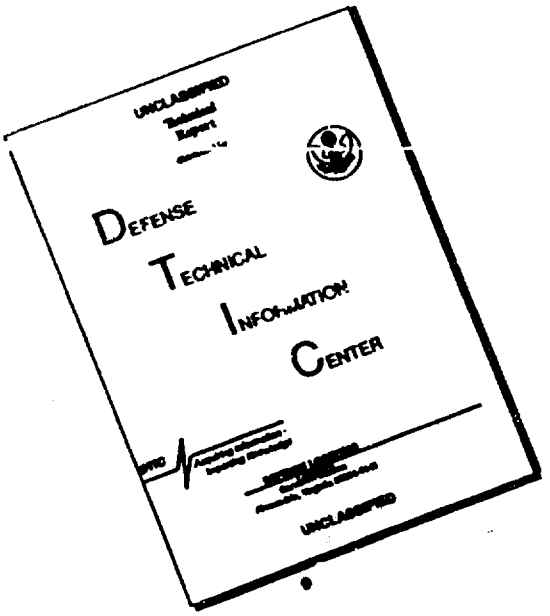

THIS DOCUMENT IS BEST QUALITY AVAILABLE. THE COPY FURNISHED TO DTIC CONTAINED A SIGNIFICANT NUMBER OF PAGES WHICH DO NOT REPRODUCE LEGIBLY.

WL-TR-91-3086

BEHAVIOR OF AIRCRAFT TIRE COUPONS UNDER VARIOUS LOADING CONDITIONS

V. Sarma Avva, P1
D. M. Pai
R. L. Sadler

North Carolina A&T State University
Greensboro, NC 27411

October 1991

Final Report for period September 1987 - December 1990

FLIGHT DYNAMICS DIRECTORATE
WRIGHT LABORATORY
AIR FORCE SYSTEMS COMMAND
WRIGHT-PATTERSON AIR FORCE BASE, OHIO 45433-6553

NOTICE

When Government drawings, specifications, or other data are used for any purpose other than in connection with a definitely Government-related procurement, the United States Government incurs no responsibility or any obligation whatsoever. The fact that the government may have formulated or in any way supplied the said drawings, specifications, or other data, is not to be regarded by implication, or otherwise in any manner construed, as licensing the holder, or any other person or corporation; or as conveying any rights or permission to manufacture, use, or sell any patented invention that may in any way be related thereto.

This report is releasable to the National Technical Information Service (NTIS). At NTIS, it will be available to the general public, including foreign nations.

This technical report has been reviewed and is approved for publication.

FOR THE COMMANDER

If your address has changed, if you wish to be removed from our mailing list, or if the addressee is no longer employed by your organization please notify WL/FIVMA , WPAFB, OH 45433-6553 to help us maintain a current mailing list.

Copies of this report should not be returned unless return is required by security considerations, contractual obligations, or notice on a specific document.

REPORT DOCUMENTATION PAGE

Form Approved
OMB No. 0704-0188

1a. REPORT SECURITY CLASSIFICATION Unclassified	1b. RESTRICTIVE MARKINGS None
2a. SECURITY CLASSIFICATION AUTHORITY	3. DISTRIBUTION/AVAILABILITY OF REPORT Approved for public release; distribution is unlimited.
2b. DECLASSIFICATION/DOWNGRADING SCHEDULE	
4. PERFORMING ORGANIZATION REPORT NUMBER(S)	5. MONITORING ORGANIZATION REPORT NUMBER(S) WL-TR-91-3086
6a. NAME OF PERFORMING ORGANIZATION North Carolina A&T State University 6b. OFFICE SYMBOL (If applicable)	7a. NAME OF MONITORING ORGANIZATION Flight Dynamics Directorate (WL/FIVMA) Wright Laboratory
6c. ADDRESS (City, State, and ZIP Code) Greensboro, NC 27411	7b. ADDRESS (City, State, and ZIP Code) WPAFB, OH 45433-6553
8a. NAME OF FUNDING/SPONSORING ORGANIZATION 8b. OFFICE SYMBOL (If applicable) WL/FIVMA	9. PROCUREMENT INSTRUMENT IDENTIFICATION NUMBER F33615-87-C-3413
8c. ADDRESS (City, State, and ZIP Code) WPAFB, OH 45433-6553	10. SOURCE OF FUNDING NUMBERS PROGRAM ELEMENT NO: 62201F; PROJECT NO: 2402; TASK NO: 01; WORK UNIT ACCESSION NO: 53
11. TITLE (Include Security Classification) Behavior of Aircraft Tire Coupons Under Various Loading Conditions	
12. PERSONAL AUTHOR(S) Avva,V. Sarma; Pai, D.M.; Sadler, R.L.	
13a. TYPE OF REPORT FINAL	13b. TIME COVERED FROM SEP 87 TO DEC 90
14. DATE OF REPORT (Year, Month, Day) 1991 October	15. PAGE COUNT 147
16. SUPPLEMENTARY NOTATION	

17. COSATI CODES			18. SUBJECT TERMS (Continue on reverse if necessary and identify by block number)
FIELD	GROUP	SUB-GROUP	Tire Coupons Peel Test Flex Fatigue

19. ABSTRACT (Continue on reverse if necessary and identify by block number)

The aircraft tire is a complex composite structure containing reinforcing nylon cords in a rubber matrix. It experiences a very complex loading during usage. There are inflation induced stresses as well as the centrifugal and flexural stresses induced by rolling. The material is exposed to cyclic thermal loading from heat generated by distortion and braking. All of these influence the useful life and performance of the tire.

The tire designer needs to have an understanding of the constitutive properties of the aircraft tire and the influence of environment and loading on those

20. DISTRIBUTION/AVAILABILITY OF ABSTRACT ☒ UNCLASSIFIED/UNLIMITED ☐ SAME AS RPT ☐ DTIC USERS	21. ABSTRACT SECURITY CLASSIFICATION Unclassified
22a. NAME OF RESPONSIBLE INDIVIDUAL Gary J. Migut	22b. TELEPHONE (Include Area Code) (513)255-7258 22c. OFFICE SYMBOL WL/FIVMA

block 19 (cont'd)

properties. In this study, unused aircraft tires were cut open and specimens extracted to test for constitutive properties and a very important mechanical property called peel strength. The procedure for extracting the coupons, the fixturing and the simulated loading conditions used in the laboratory are discussed. Three kinds of peel test configurations were compared in a baseline study. The best configuration was then used to test conditioned coupons. The results and statistical analysis of these tests are presented. A scanning electron micrograph study of the peeled coupons shows that the fracture mode is a function of the type of loading and environment that the coupon were subjected to. Conclusions are made regarding the influence of loading conditions on peel strength. Recommendations for further study are offered.

EXECUTIVE SUMMARY

PURPOSE:

1. Develop suitable test methods for determining the peel strength properties of aircraft tire materials.
2. Develop fixtures and procedures for accelerated aging of coupons to simulate field usage conditions.

PROCEDURE:

1. Three potential peel methods were identified and fixturing was developed.
2. Coupons were designed and extracted from virgin tires.
3. Baseline results were analyzed to identify most consistent peel test configuration for use on conditioned coupons.
4. Conditioning parameters were computed and fixtures were designed and fabricated for conditioning by i) heating ii) flexing iii) flexing at elevated temperatures. In all cases, the coupon was conditioned while being pulled with a tensile load to simulate inflation pressure.
5. Effects of conditioning were determined.
6. Mechanism of failure was qualitatively studied through Scanning Electron Microscopy.

ACCOMPLISHMENTS:

1. Developed methods of coupon extraction from tires, built successful peel test fixtures and identified the most consistent peel method for the material.
2. Conditioning procedures and fixtures were developed to produce accelerated aging in coupons.
3. Coupons aged under conditions of tensile load, heating and flex fatigue degraded at the same rate as coupons aged only by tensile load and heating. Results were quite comparable to those of Clark (University of Michigan), where conditioning was done only by heating.

RECOMMENDATIONS:

1. Higher frequencies and amplitudes must be employed in flex fatigue conditioning for more accelerated aging.
2. Higher tensile load needs to be applied to simulate even higher inflation pressures.
3. Results for laboratory conditioned coupons need to be verified by correlation with peel strength results for tires used in the field.

FOREWORD

This final technical report was prepared by Profs. Avva, Pai and Sadler with the assistance of graduate student Mohan Singh Khabra and undergraduate student Cheryl Casper Sellers of the Center for Composite Materials Research, Department of Mechanical Engineering, North Carolina Agricultural and Technical State University for the Flight Dynamics Laboratory, Air Force Wright Aeronautical Laboratories, Air Force Command, Department of the Air Force, Wright Patterson Air Force Base, Ohio 45433 under Contract No. F33615-87-C-3413. The Air Force Monitors successively were Lt. Mark R. Boike, Mr Paul Wagner, and Gary Migut.

TABLE OF CONTENTS

LIST OF TABLES

LIST OF FIGURES

LIST OF SYMBOLS

A	Surface area
C	Distance from neutral axis to extreme fiber
C_{sp}	Specific heat
d	Internai diameter of tire
D	External diameter of tire
I	Moment of inertia of cross section
k	Thermal conductivity
L	Change in length
M	Bending moment
p	Inflation pressure
P	Applied force
Q	Heat flow
r	Radius of gyration
S	Stress
t	Effective carcass thickness
T	Change in temperature
w	Load per unit length
δ	Deflection at center of arm
Θ	Cord angle
σ_H	Hoop stress
σ_L	Longitudinal stress
σ_{normal}	Static tension load

Chapter 1

INTRODUCTION

A tire can be considered to be a composite made up of an elastomeric matrix of relatively low strength and high elongation, combined with a reinforcing material (tire cord) of high strength and low elongation[1]. This results in a high degree of complexity of the material characteristics of the tire components. The majority of the load is carried by the textile cord reinforcement, which is partially impregnated with and wholly embedded in rubber[2]. Some compressive loads are carried by the rubber elements in the tread but these are rather minor.

Testing of tires is a sophisticated and highly complex procedure. Like any other product, a tire has a life that is partially governed by the severity of its usage, but which is finite even under optimum use conditions[3]. Future aircraft tires will require higher velocity, horizontal takeoff and landing capabilities than those in current use. Presently, aircraft tires have a ground speed limitation of approximately 250 mph. The development of heavy transport and military aircraft with high performance characteristics has placed an increased demand on landing gear and tire components[4]. Developments in tire manufacturing such as improved tire reinforcing cord materials, rubber compounds and tire structural design have made the ratio of tire weight to aircraft weight decrease steadily. For instance, in one type of tire, the number of cord plies was reduced from 26 to 17

while retaining the same performance. In order to support future development of high performance aircraft, tests must be developed which accurately predict the performance of the tires on some rational basis.

During braking, power is applied to the wheels and is transmitted to the ground through the tire. Within the structure of the tire, the stresses involved must be transmitted across the interface between the rubber and the reinforcing textile cord. In addition, aircraft tires generate substantial temperatures from two sources, internal heat generated in the tire body due to flexing, and brake heat being conducted into the bead area of the tire. Both these heat generation mechanisms are important. Excessive temperatures can cause a tire to fail even if the stress levels are not very high.

Repeated takeoffs and landings cause a cyclical variation in tire stress and temperature. These phenomena are basically accompanied by a gradual degradation of strength and adhesion properties. A study of the literature has indicated that information related to this area of degradation is very limited. Tire retreading and replacement is often based on human judgment. The useful life of a tire is limited, but the limits are not well defined, and they may vary not only from one tire to the next, but from one application to another.

Significant advances have been made in the tire industry in calculating stresses in the tire cord network based on the load carried and tire inflation pressure. Temperature build up in the tire body due to flexing and braking is a major cause of tire degradation. In the design of new aircraft tires, reliable thermal

models are valuable in assessing the validity of the proposed tire, to meet aircraft weight, ground speed and taxi length requirements.

In the past, aircraft tires were tested in field tests which were very time consuming with many uncontrolled variables. Tires are tested nowadays by dynamometer testing and laboratory conditioning, which, too, have become increasingly expensive. For example, it is reported [20] that over 50 different tests are currently being run by the Goodyear Tire Company to characterize tire performance.

It is believed the tire coupon test methodology developed in this study may substantially enhance the quality of tire strength data and serve to expand present tire characterization capabilities in the tire industry. These test methods are viable without the use of relatively specialized and expensive equipment.

Chapter 2 describes the objectives of this research work. Chapter 3 discusses the theoretical background obtained from a survey of the literature. Chapter 4 describes the test procedures. Chapter 5 presents the results and analysis. Conclusions and recommendations are discussed in Chapter 6.

Chapter 2

OBJECTIVES

The primary objective of the project was to determine experimentally the role of temperature and flex fatigue in the degradation of peel strength of aircraft tire coupons. The coupons were to be aged under conditions simulating actual usage as closely as possible. In addition, the constitutive properties of the tread and the carcass materials were to be determined.

These objectives were achieved through the performance of the following major tasks:

2.1 Design of Test Matrix and Coupons

Test matrices were designed for measuring the constitutive properties of tread rubber and carcass, and for measuring the peel strength of virgin baseline coupons and conditioned coupons.

2.2 Develop Coupon Extraction Procedure

Coupons were cut from the tread part of unused aircraft tire. Sizes and shapes of the coupons were designed based upon the test conditions.

2.3 Determine Constitutive Properties of Tread and Carcass

Properties determined were tensile modulus, Poisson's ratio, shear modulus, damping coefficient, specific gravity, cord spacing, ply spacing, cord angle, specific heat and thermal conductivity.

These properties are required for advanced finite element modeling of static and dynamic modes of an aircraft tire.

2.4 Design, Fabricate and Evaluate Peel Fixtures

Two peeling fixtures were designed and fabricated for peeling at 90° and at 180°. A third type of peel test used (the +/-90° test) did not require special fixturing.

2.5 Evaluate Three Peel Test Methods

These tests were performed on unconditioned coupons to determine the strength of adhesion between different ply levels at various locations of tire tread, by use and modification of ASTM D413-1988 and ISO 36-1985(E) Standards.

Peel strength was measured using three different loading configurations to determine which method yield the most consistent data. Effects of several different factors were considered in the performance of these peel strength tests. The data from the baseline test was used to select the method that yielded the least scatter in data. The peel test on conditioned coupons was performed using this selected method.

2.6 Design, Fabricate and Evaluate of Coupon Conditioning Fixtures

Fixtures were designed and fabricated to thermally age virgin coupons in an oven. Combination compression plus bolting type coupon holders were used to hold the coupons in these aging fixtures. A flex fatigue fixture and a temperature controlled heater jacket were designed and fabricated for flex fatigue conditioning.

2.7 Condition and Peel Test Coupons in the Laboratory

The static pre-loads for thermal aging and flex fatigue coupons were determined from the inflation pressure of the tire by using hoop and longitudinal stress, modelling the tire as a thin walled pressure vessel.

2.7.1 Thermally Aged Coupons

A static tensile load was applied and maintained as the coupon was thermally aged at different temperatures for various time durations.

2.7.2 Flex Fatigue Coupons

A static tensile load was applied to the coupon and then it was flexed laterally (to simulate take off and landing conditions). Conditioning was performed at room temperature, elevated temperatures and at two different frequency levels. The number of flex cycles was based upon distance traveled by the tire and the number of takeoff and landing cycles. The amplitude was based upon tire deflection. The cycle frequency was based on the maximum landing and take off speeds. The objective of this test was to determine degradation due to inflation pressure, deflection due to weight of aircraft, rolling speed and distance of tire roll.

2.8 Peel Test the Conditioned Coupons

Adhesion strength tests were performed on a series of thermally aged and flex fatigued coupons (room temperature and elevated temperatures) by using the peel strength test method selected in article 2.5. The peel strength results were compared with those from virgin coupons.

Chapter 3

LITERATURE SURVEY

There is a lot of information available in the literature regarding tire construction and materials [5-8]. The aircraft tire is one of the strongest and toughest pneumatic tires made. It can be considered to be a composite of reinforcing cord material and a rubber matrix. During its running, the material experiences a variety of dynamic stresses and strains at varying frequencies, amplitudes, temperatures and other environmental conditions.

The construction of a typical bias ply aircraft tire is shown in Fig. 1. It consists of the following:

Tread: The tread is made up of synthetic and natural rubber compounds for toughness and durability. The tread pattern is designed in accordance with operational requirements. A circumferential ribbed pattern is widely used on aircraft tires because it provides good traction under uneven runway conditions. The tread and sidewall together protect the carcass from wear and tear, and from deterioration induced by oxygen, moisture, and sunlight.

Tread Reinforcement Plies: These are one or more plies of reinforcing fabric used in high speed aircraft tires to strengthen the tread.

Breaker Plies: These are extra plies of reinforcing cord fabric placed under the tread. These plies protect casing plies and strengthen the tread area. These plies

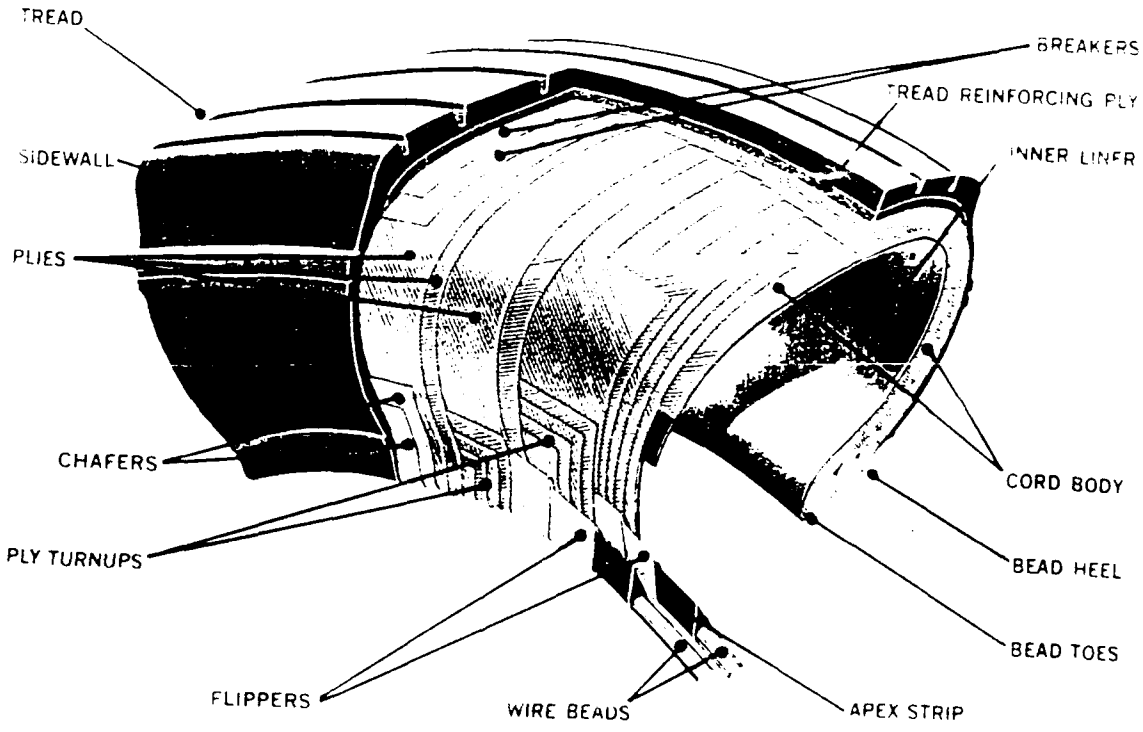

Fig.1 Bias ply tire construction [5]

are considered an integral part of the carcass construction and they break up and distribute road shocks.

Casing Plies: These are diagonal layers of cord fabric completely surrounded by a resilient rubber compound. They provide the strength of the tire. Each layer runs approximately perpendicular to its neighbors. The casing plies (plies) completely encompass the tire body and fold around the wire beads and back against the tire sidewalls ("ply turn-ups"). The cord angle with respect to the tire centerline, the number of cords per inch and the cord diameter are the fundamental factors that affect ply strength. The number and composition of the plies are useful in determining the ultimate strength of a tire.

Beads: Beads are made of steel wires embedded in rubber and wrapped in fabric. These may be considered as the foundation of the tire. Beads anchor the casing plies and provide a firm mounting surface on the rim.

Flippers and Chafers: These layers of fabric and rubber insulate the carcass from the bead wires. They also improve the durability of the tire.

Inner Liner: Used in a tubeless tire, this inner layer of rubber is less permeable to air and it acts as in a built-in tube. This prevents air from seeping through the casing plies. For tires with tubes, a thinner liner is used to prevent tube chafing.

Rubber composition plays a very important role in tire construction. The tread compounds provide wear resistance, toughness and resilience to minimize cuts, tears and cracks as well as to protect the carcass body from bruising impacts. The tire building process involves covering the tire cord sheet with a thin

layer of rubber and bringing such coated sheets together, often with considerable deformation. It is important that the adhesion developed between these sheets of rubber and cords be adequate to withstand the retraction forces caused by deformation. These forces give rise to complex stresses and the newly formed rubber to rubber joint is subjected not only to shearing stresses, but also to peel and cleavage stresses [2,11]. Due to the dissimilar nature of the matrix (low strength and high elongation) and reinforcing material (high strength and low elongation), an adhesive is required to ensure proper performance of the composite structure in the tire [10,12-13]. The system is nonhomogeneous and anisotropic. This leads to a complicated theoretical analysis. The deformations under actual loading conditions are large enough to require consideration of the large displacement geometric nonlinearities present in the structural behavior. The number of layers of plies are dependent upon the tire type, tire size and inflation pressure to be used.

There are three main arrangements for cords: woven cords, weftless cords, and cord material with light wefts [13] shown in Fig. 2. The tires tested in this project have cord material with light wefts. These fine wefts are not stress carrying members and serve only to hold the cords in their appropriate relationship during the manufacturing process.

Developments during the early years consisted principally of improved materials, better methods of component assembly, material shaping and improved vulcanization techniques. With increasing service demands, an analytical study of

WOVEN CORDS

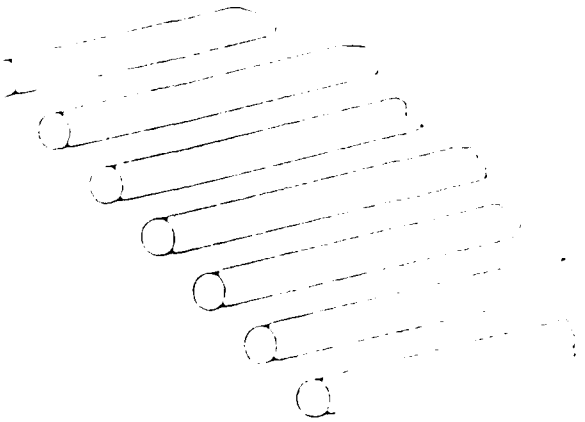

WEFTLESS CORDS

CORDS WITH LIGHT WEFT

Fig. 2 Filament arrangement in tire [13]

the finely balanced system of forces in a tire also becomes very important [14]. Significant advances have been made in the tire industry in calculating the stresses in the tire cord network based on the load carried and tire inflation pressure [4].

Tire modeling and analysis has been the subject of continuing research for the tire industry, but there is no simple and general tire model that exists for predicting the response of the tire under various loading conditions [15-17]. The constitutive properties of aircraft tires are very useful for advanced finite element modeling, both static and dynamic.

A mathematical analysis of the carcass based upon inflation pressure, centrifugal force and pavement contact loads is used to find the stresses on the cord network. Most of the current analyses of tire structural response make use of the micromechanics model given by the Halpin-Tsai equations. This model is very useful to find the influence of rubber modulus on the shape of an inflated tire carcass [18].

Advances in the development of heavy transport and military aircraft with high performance characteristics has placed an increased demand on landing gear and tire components. Improved tire reinforcing cord materials, rubber compounds and tire structural design have made the ratio of tire weight to aircraft weight decrease steadily [4]. There is a high degree of complexity of the material characteristics of the constituents of an aircraft tire. The majority of the load is carried by the cord network. Some compressive loads are carried by the rubber elements in the tread but these are rather minor. In addition to the strength

problem, aircraft tires generate substantial temperatures arising from two sources, internal heat generated in the tire body due to flexing, and brake heat being conducted into the bead area of tire. Clark[4] has developed an analytical model for predicting aircraft tire internal temperatures.

Testing of aircraft tires is a highly complex procedure. The best method is to subject them to actual field tests. However, this method is very costly and time consuming. Therefore, the tire industry is continually searching for indoor laboratory tests which simulate actual running conditions [20]. Dynamometer testing of aircraft tires is also very complicated and costly, because of the difficulty in simulating actual running (landing and takeoff) conditions [21].

Adhesion testing of tire components appears to offer a less burdensome alternative to some of the dynamometer tests [22]. These tests are based upon adhesion science technology. Building a tire involves adhesion between the tire cord and rubber [2,3] but rubber-to-rubber adhesion is also very important. When the tire deforms, the forces produce complex stresses and the newly formed rubber-rubber joint is subjected not only to shearing stress but also to peeling stresses. Peeling stress are stresses, normal to the ply length, that tend to separate plies from each other.

The major cause of degradation of tire composites is the loss of adhesion between cord and rubber and the loss of cohesion in the rubber matrix with temperature and time. Since cord adhesion is so important, many theoretical investigations have been conducted and published in this area [26-38]. This loss

of adhesion is followed by growth into a definite separation between plies, which is detectable by inspection techniques such as air needle or holography [3]. When the separations grow large enough, they can generate excessive local heat due to rubbing, thereby causing cord strength to degrade at a faster rate.

Many standards have been developed to find the peel strength between ply levels of tires. "Rubber, Vulcanized - Determination of Adhesion to Textile Fabric" ISO-36-1985(E) [23] gives a good discussion of the +/- 90° peel configuration described in detail in Chapter 4 of this thesis. ASTM D413 88 mentions three types of configuration [24]. Two of these, 180° and 90° are described in Chapter 4 of this thesis. The third configuration is ring specimen peeling which is a variation of peeling at 90°. Many different standards of interpretation are available to compute the adhesion peel strength from experimental data. "The Harcsar-Reiger Method for Determination of Tire Components Adhesion" [25] seems to best fit the present application. In this, the peel strength is determined from the average of the central region of each load-displacement data set.

Several papers [26-38] discuss the variables affecting peel strength. However, there are no recommendations regarding the test configuration to be used. Peel strength results depend strongly upon variables such as thickness of the substrate and adhesive, rate of testing, geometric configuration of the test, testing temperature, composition of the surrounding medium, and method of sample preparation [26,29]. Time and temperature are very important factors in static adhesion tests. At higher rates of peeling, the peel force is also increased

because the rate of deformation of the adhesive interlayer is also necessarily increased. Increase in thickness of the adherend also raises the peeling force [26-28,31].

Clark [3] has studied the effect of time and temperature on peel strength between the third and fourth plies of aircraft tires. In this study, samples were obtained from Type VII aircraft tires rejected by a retreader owing to cuts or damage by foreign objects. Tensile adhesion values were obtained by direct pull, using the +/- 90° procedure listed in ASTM D413-76. The initial adhesion value measured at room temperature was used as a baseline for comparison with subsequent data. Figure 3 shows the cord and adhesive strength retained as a function of time at an elevated temperature of 130°C (265°F).

These results show that adhesion strength retention is clearly less than cord strength retention. The adhesion strength between cord and rubber degrades more rapidly than the cord tensile strength. Figure 4 shows the variation in retained adhesive strength as a function of aging time in air at elevated temperatures between 175 and 300°F. Figure 5 and Fig. 6 show the variation in retained adhesive strength between comparable tires from two different manufacturers. An uncertain degree of oxidation is present at the interface of a propagating crack in an operating aircraft tire. Tires are usually inflated with nitrogen to reduce oxidation. Figure 7 and Fig. 8 show the variation in retained adhesive strength as a function of time in nitrogen at elevated temperatures between 200°F and 350°F. Nitrogen-aged specimens degraded slower than the air-

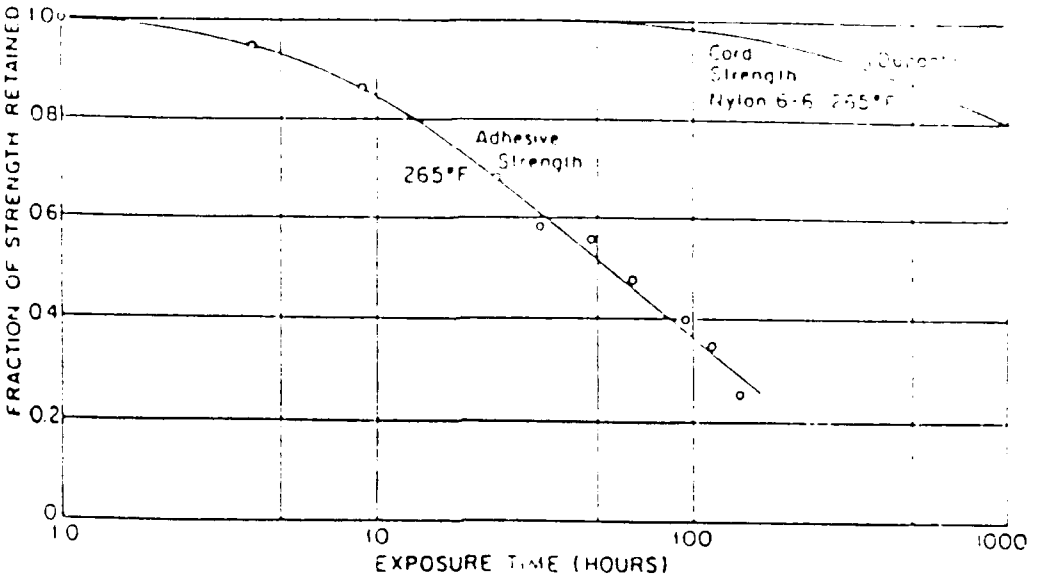

Fig. 3 Cord and peel strength vs temperatures [3]

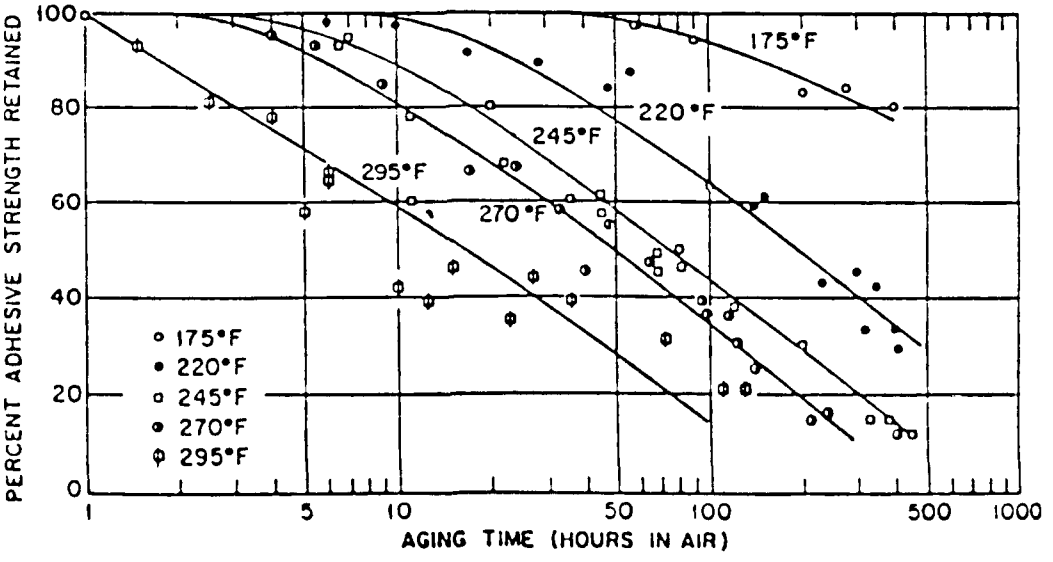

Fig. 4 Peel strength vs aging time in air [3]

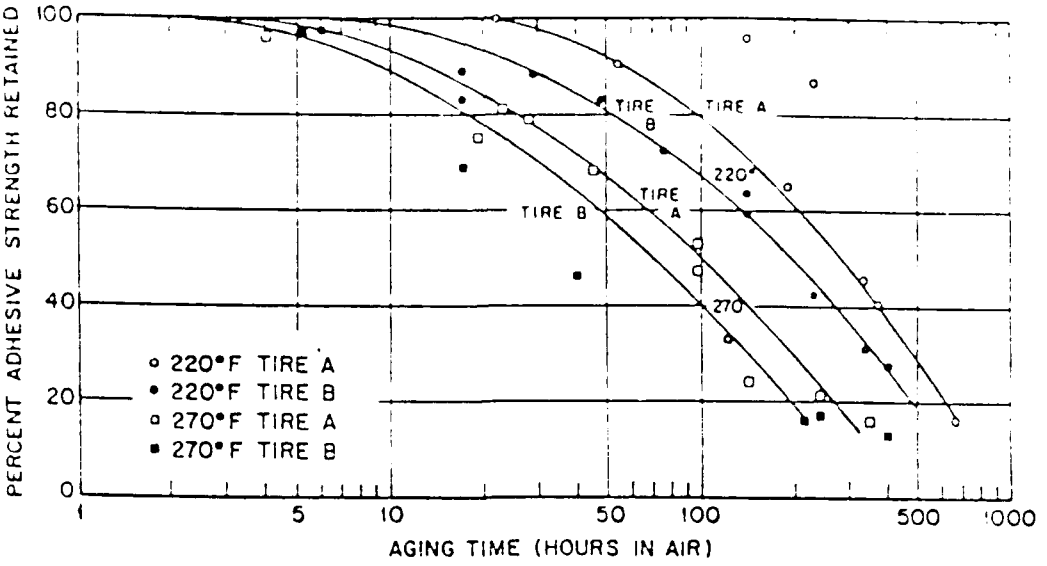

Fig. 5 Peel strength vs aging time in air [3]

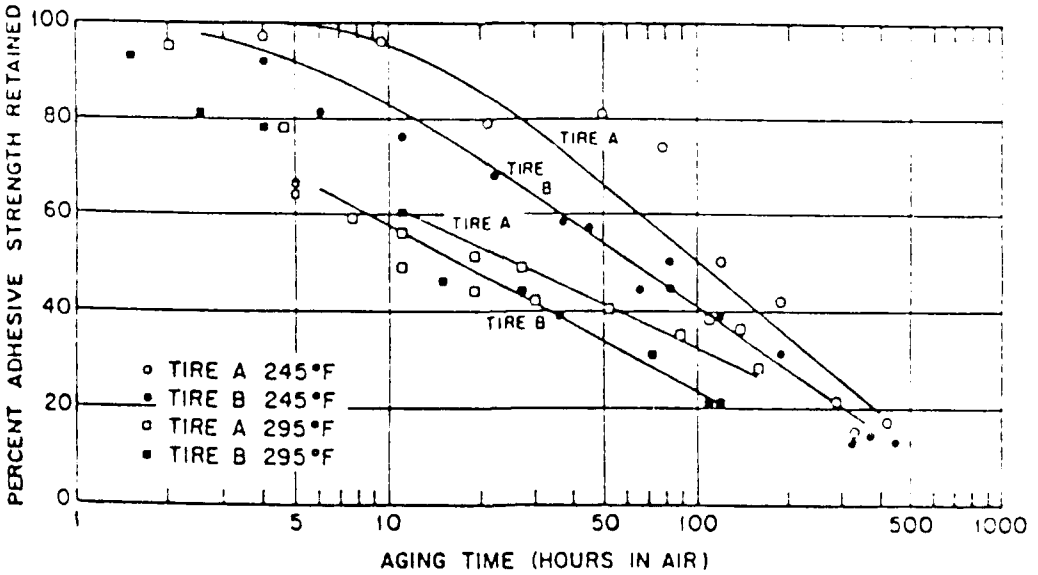

Fig. 6 Peel strength vs aging time in air [3]

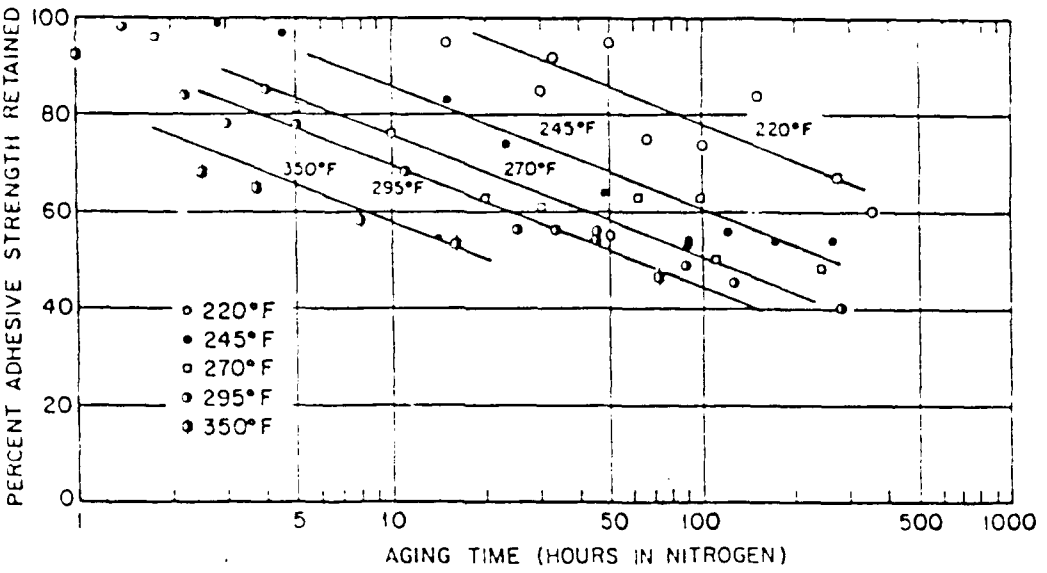

Fig. 7 Peel strength vs aging time in N_2 [3]

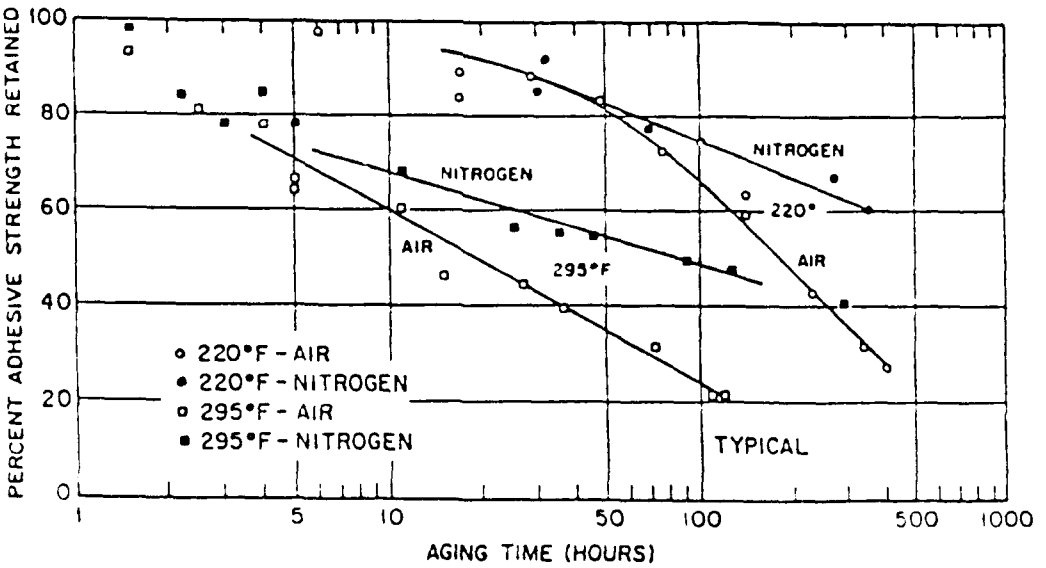

Fig. 8 Peel strength vs aging time in air & N_2 [3]

aged specimens.

In summary, the literature survey reveals a lot of information about tire construction, behavior of rubber and cord material, theory and mechanism of adhesion, peel configuration standards, and dynamometer and road testing methods. The test methodology developed during the present study expands upon the test methods developed previously in that the simulated service conditions such as inflation pressure, temperature, time, flex, tire rolling distance during takeoff and landing, and the number of landings are taken into consideration. The procedures for these modified tests are discussed in the next chapter.

Chapter 4

TEST PROCEDURE

Peel tests have been used to evaluate tire quality by determining the load required for failure to occur by growth of cracks (delamination) between ply levels. The tire constitutive properties have been measured using appropriate tests described later in this chapter.

The peel strength is a very important measure of tire strength. A peel test offers a less burdensome alternative to some of the dynamometer tests. Peel strength values depend strongly on some test variables such as the thickness of the substrate and the adhesive, rate of testing, geometrical arrangement of the test, testing temperature, composition of the surrounding medium, and the method of sample preparation.

The baseline peel tests in this study were done on test coupons from virgin (unused) tires using three different test orientations. The 180° and 90° peel tests were performed referring to ASTM 413-88 and +/-90° peel test was performed referring to ISO 36-1985(E).

The baseline test series was used to determine the best peel orientation. This best orientation was then used on conditioned coupons to determine the relationship between peel strength and the time-temperature environment to which the tire coupon had been exposed.

This work was divided into the following tasks:

4.1 Tire Sampling Plan

Testing was performed on coupons from the tread portion because of the relative ease of coupon extraction, property measurement and peel testing as compared to other portions of the tire such as the bead shoulders and sidewalls. The following is the specification of the tires used in this study:

Tire ID #:	NSN 2620005758893, Type VII,
	Goodyear 49 X 17 (outer dia. X width, inches),
	26 PR (ply rating), 195 knots, tubeless,
	ribbed tread design with 4 grooves.
Plies:	12 casing plies, 3 tread reinforcing plies,
	2 breaker plies.
Material:	Nylon reinforcing cords, synthetic & natural
	rubber tread.
Inflation pressure:	170 psi
(rated)	
Radial deflection:	3.7 in (at 39,600 lbf)

The tire sampling plan was as follows:

4.1.1 Constitutive Properties

Specimens were taken from the same tires as used for baseline peel tests. Properties for rubber and carcass were measured separately.

4.1.2 Baseline Coupons

The test was performed on three tires. Each tire was divided into five equal sectors. Three coupons were taken from each sector for each of the 3 test configurations (refer to Fig. 9), making a total of 5 * 3 * 3 = 45 baseline coupons. In the 180° and 90° configurations tests, layers 3-4, 7-8, 11-12 and 15-16 were peeled apart. In the other configuration (+/- 90°), layers 3-4, 7-8, and 11-12 were peeled apart. This plan of sampling allows an analysis of the influence of the following variables: manufacturing variations between tires, variation with position of a sector within a tire, difference between ply levels, and difference between the three test configurations.

4.1.3 Conditioned Coupons

Conditioned coupons were taken mainly from one tire, tire #6.

4.2 Tread Removal and Coupon Extraction

Many experiments were performed to find a satisfactory method for coupon extraction. It was finally determined that the tire tread could be removed most easily from the sidewall with a hand-held drill and a hand-held electric hack saw.

The procedure for separating the tread from the sidewall of the tire has been refined considerably. Two people and about two hours are required to remove one tread. The tire was placed on its side against the floor, and holes spaced 1 1/2" apart were drilled first with a 19/64" diameter drill and then the holes enlarged with a 1/2" drill. A water spray was used to cool and lubricate the drill bit

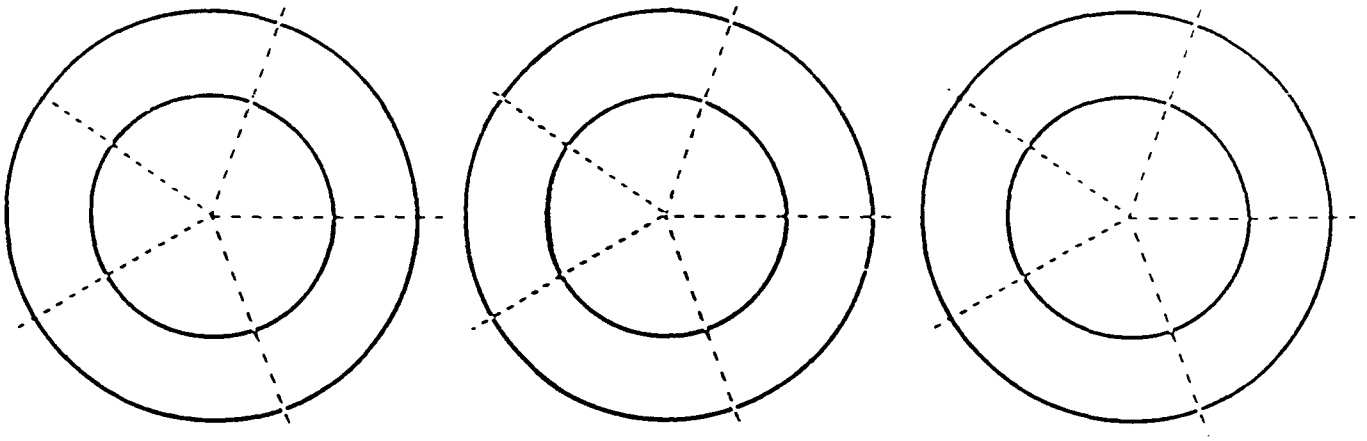

3 TIRE - 5 SECTORS/TIRE

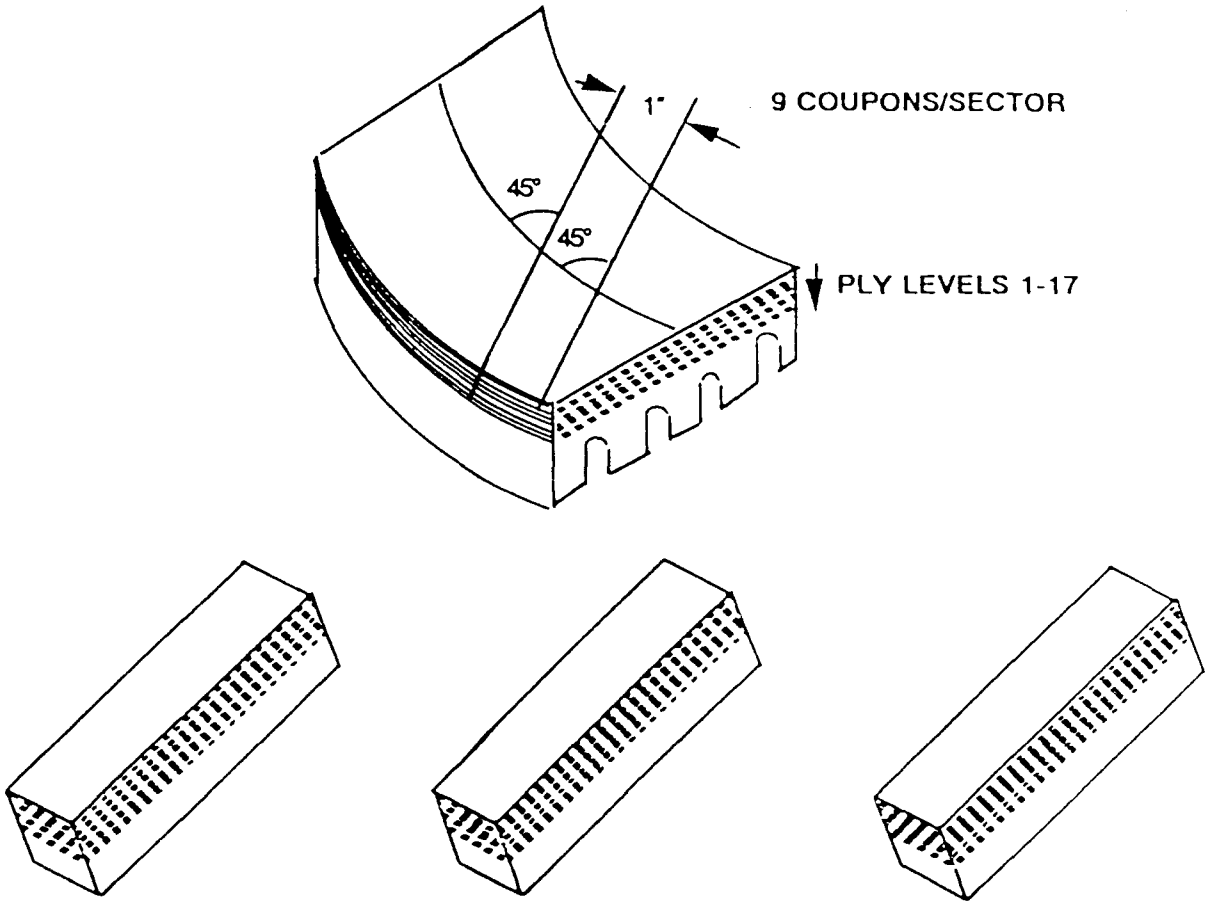

Fig. 9 Extraction plan for baseline coupons

to minimize rubber fumes. After drilling both sides of the tire sidewall,holes were also drilled in the read in a diagonai direction to maximize the number of test coupons extracted, which were to be cut parallel to the fibers in the second ply , as shown in Fig. 10.

The tread was separated from the sidewall of the tire by cutting both sides of tire with a hand-held power hacksaw. The saw connected a path through the 1/2 in. drilled holes. A water spray of was used to cool the cutting blade. The tread was cut into five equai sectors using the same method described above.

The rounded ends of the five tread sectors were trimmed off on both sides to leave a straight sided tread. This operation was performed on a vertical band saw with a blade speed of 1160 fpm, blade dimensions: width = 1/2", thickness = 0.025", teeth/in = 6 and high blade tension. The test specimens were extracted as follows:

4.2.1 Specific Gravity

Three specimens were taken from the rubber tread and three specimens from the carcass. The tire was first cut into 2 X 2" sections along the circumference. Then parallel lines spaced at 0.5" intervals were marked circumferentially and perpendicular to those lines on the sections with a white marker. The specimens were then cut along these scribed lines using the band saw. Each specimen contained tread and carcass. From this specimen, two separate specimens, one rubber and the other carcass, were obtained both having a 0.3" thickness. Each specimen was then 0.5 X 0.5 X 0.3" in size.

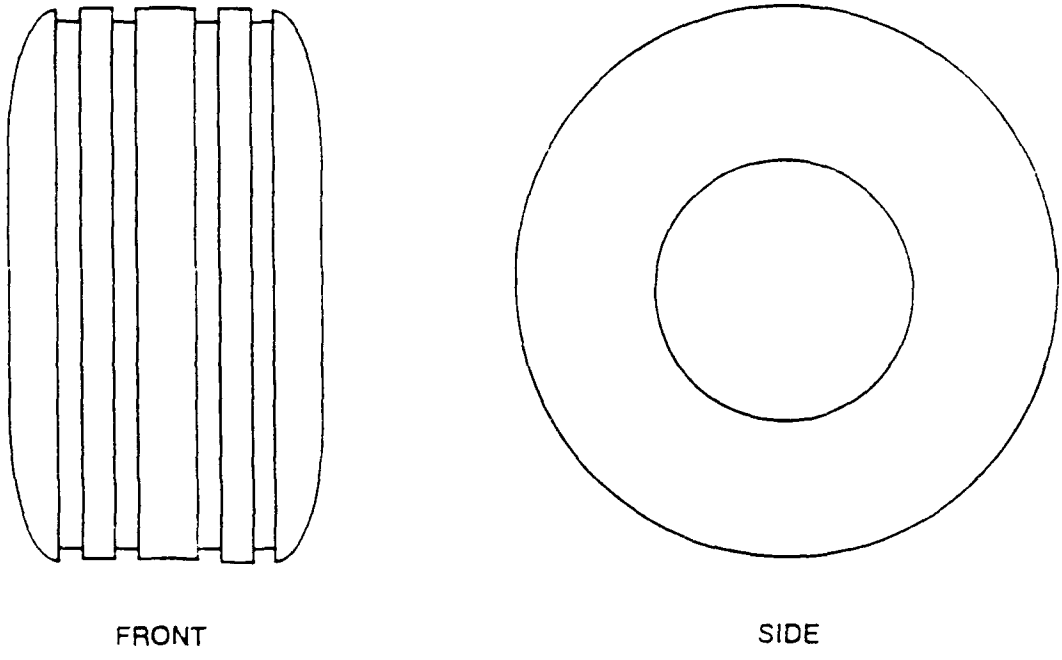

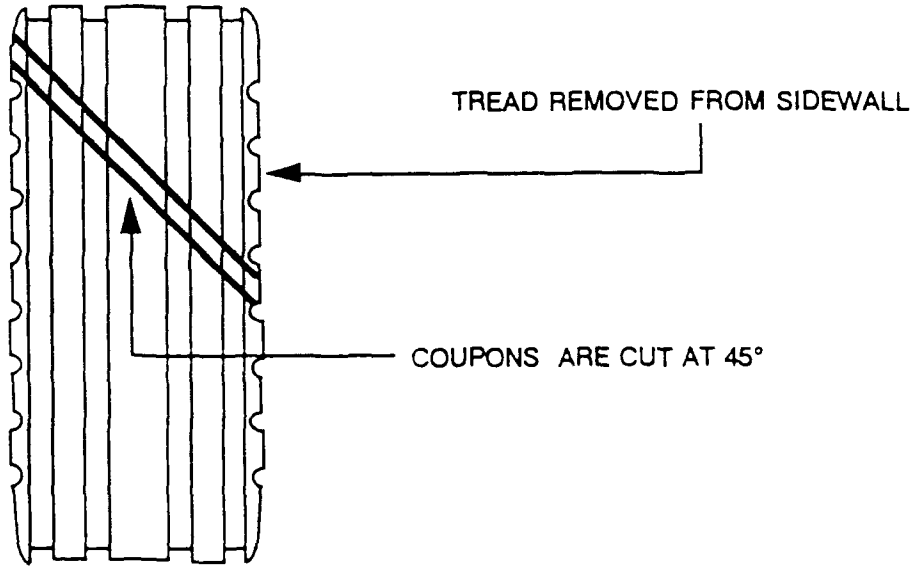

Fig. 10 Orientation of coupon

4.2.2 Cord Spacing Specimens

Cord spacing specimens were taken from three tires (3 coupons/tire). These coupons had already been used in baseline peel strength tests.

4.2.3 Ply Spacing

Specimens were taken from three different tires (3 coupons/tire). These coupons were cut circumferentially from each tire to a size 1 X 1 X 1 5/8" using a band saw.

4.2.4 Cord Diameter

Measurements were done on the ply spacing specimens described above.

4.2.5 Damping Coefficient and Shear Modulus

Specimens were taken from a single tire. The cutting procedure was the same as that for specific gravity specimens, but the size was 3 X 0.5 X 0.25". Each specimen had longitudinal fibers parallel to its length. For these tests two specimens each were taken from the rubber and the carcass.

4.2.6 Tensile Testing

Tread and carcass specimens were cut from a single tire with the dimensions of 1.0 X 0.5 X 10".

4.2.7 Thermal Conductivity and Specific Heat

Specimens were cut from tread and carcass with the dimensions of 4.0 X 4.0".

4.2.8 Baseline Peel Test

Coupons were taken from three virgin tires. The plan for extraction of

baseline test coupons is shown in Fig. 9. A center line was scribed along the length of the tread and then two parallel lines AB and CD, spaced 1 1/16" apart, were marked at about 45° to the center line as shown in Fig. 9. Final coupon dimensions are is shown in Fig. 11.

4.2.9 Thermally Aged and Flex Fatigue Aged Peel Test

Coupons were taken from a single tire. Coupon ABCD (path B-C, A-D)was cut as shown in Fig. 12. Once it was verified that the reinforcing cord was parallel to the coupon edges AD and BC, more specimens were cut parallel to AD. If not, the angle was modified slightly until the coupons had their reinforcing cords exactly parallel and perpendicular to the coupon length. Then bone-shaped coupons were made by cutting the coupon using the procedure in step 1, but with a width of 2.0 in. instead of 1.0 in., and tracing the path as shown in Fig. 12. The dimensions are shown in Fig. 11.

4.3 Test Equipment Description

4.3.1 Universal Testing Machine

The MTS 810 universal testing machine was used to find the peel strength of specimens. A technical description of the MTS - 810 Universal Testing Machine is provided in Appendix A.

4.3.2 Data Acquisition

Data acquisition was a crucial element of this work. Force and displacement data from the testing machine were acquired and stored on an IBM PC-XT

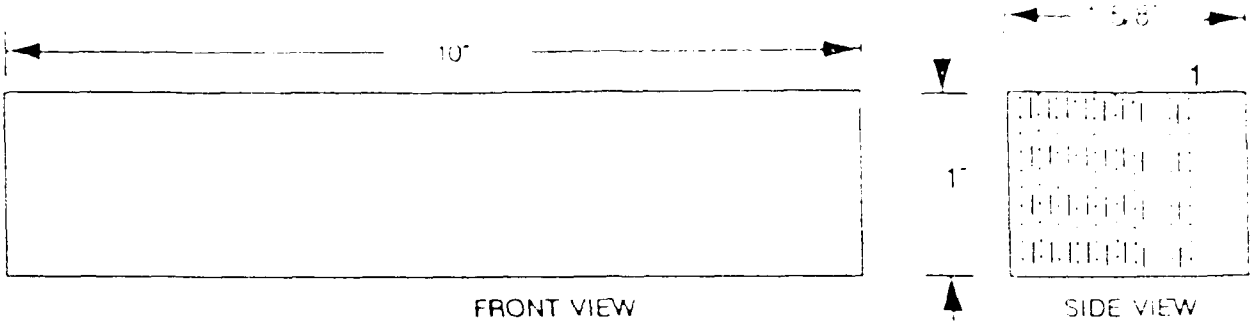

BASELINE COUPON

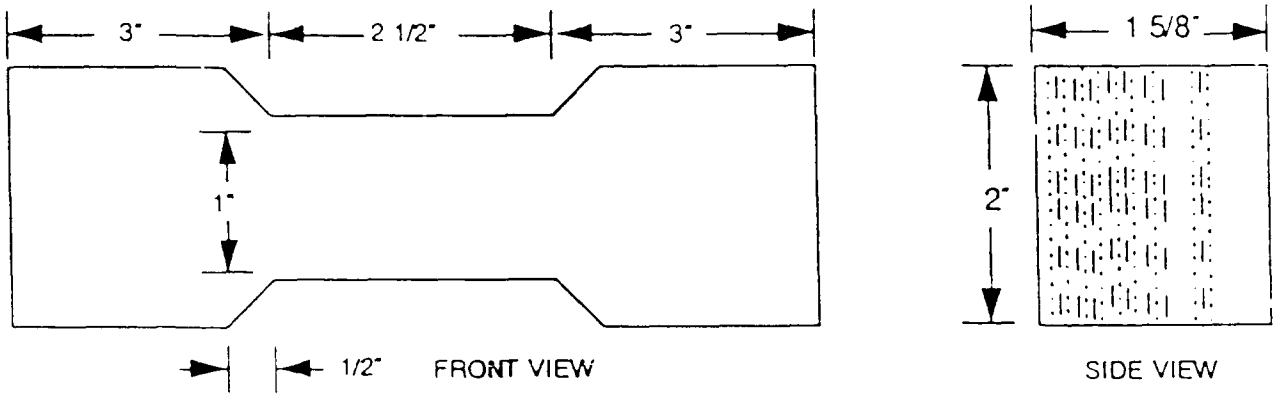

THERMALLY AGED COUPON

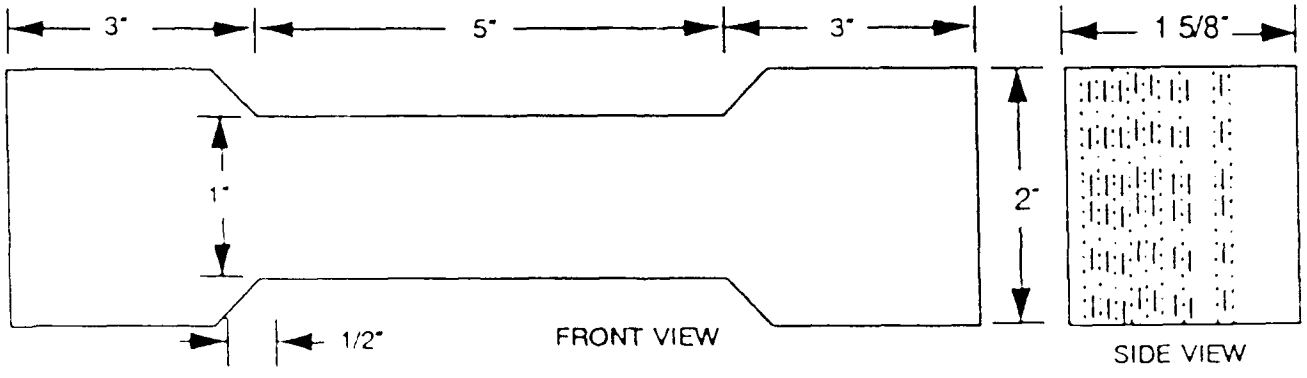

FLEX FATIGUE COUPON

Fig. 11 Coupon dimensions

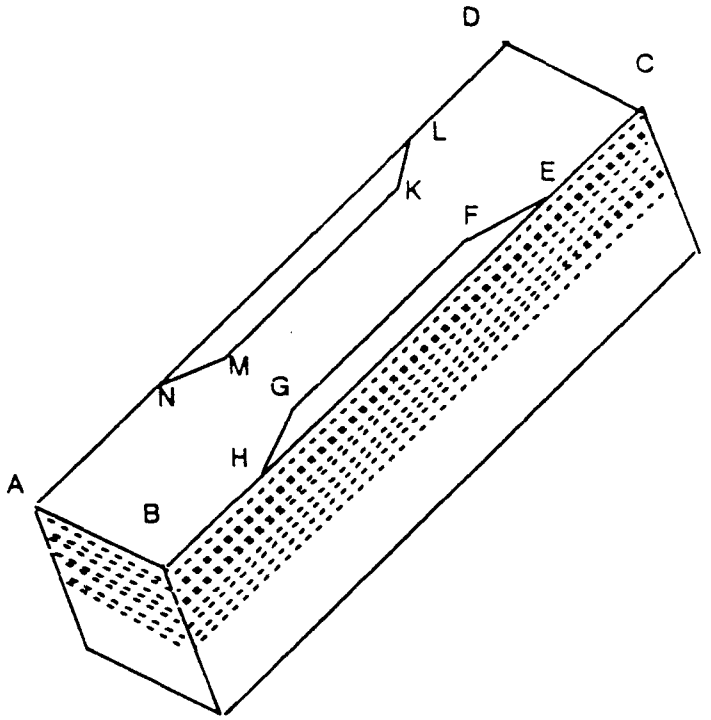

Fig. 12 Bone shaped conditioning coupon

microcomputer, using two different data acquisition software packages as described below.

Testlink 759 Data Acquisition Software: This data acquisition software, written in BASIC, is menudriven. It allows the user to set all the variables interactively. It can control the machine actuator movement for tensile, compression and flex fatigue tests.

The procedure is divided into the following steps:

From the main menu, the "Tensile Test" option is selected using the keyboard arrow keys.

From the "Tensile Test" submenu the "Prepare Test Control" option is chosen. This consists of creating or editing a file that includes parameters such as file name, operator's name, job number, specimen specifications, and environmental conditions under which the test will be run.

The specimen and station parameters such as gage length, width, thickness, full scale load, strain and stroke, and control mode (load or stroke) are input.

Next, "control parameters" such as load rate, final stroke rate, failure threshold and switch point strains are entered. The user then has to confirm whether the specimen is in place. The setup is verified by the software and the test is begun by typing "START".

During the test, the computer collects necessary data and the test is terminated by pressing the key <F5>. The data files that are generated are

converted into text files and into plots, both of which are used for data analysis.

LABTECH Data Acquisition Software: This software, also written in BASIC, is used to acquire data from two +/- 10V signal conditioners representing load and stroke. The menu driven software allows the user to set up all control parameters and data files from the screen. The menu is subdivided into four major sections control, display, data acquisition and data analysis.

The control section is used to input the rate, channel, full scale input, offset and scale factor in respective units.

The display sub-menu is used to format the real time output to the screen.

The data acquisition sub-menu is used to actually acquire data.

The data analysis sub-menu is used for curve fitting, plotting or data reduction.

Here the Microprofiler program of MTS machine needs to be run simultaneously to control the actuator movement.

Advantages of LABTECH Data Acquisition Software over Testlink 759 are:

i. Time per test is less.

ii. Number of channels from which data are to be acquired can be controlled, thus avoiding unwanted data and saving disk space.

iii. Easier to set up the parameters and begin test.

iv. No memory shortage problem.

v. Data file does not need any conversion.

4.3.3 Test Fixtures

Design of Peeling Fixtures:

180° Peel Fixture: The 180° peel test fixture was designed to suit the test configuration shown in Fig. 13. The peel angle (180°) should remain constant throughout the tests.

A 1" thick aluminum horizontal base plate is connected to the crosshead by five bolts. This plate has a slot in the center in which a vertical plate is fitted. This slot allows horizontal adjustment of the vertical plate to align the peeling ply at a constant 180°. The coupon holder is fixed on fixture plate using six nuts. This coupon holder has seven holes to hold the coupon and these are sufficient to keep the coupon from undergoing excessive deformation when the peel tests are performed. The ply holder (Fig. 14) was designed to hold the ply firmly without slipping and was connected to the load cell by screws. The load cell in turn was connected to the actuator.

90° Peel Fixture: The 90° peel fixture was designed according to the needs of peeling at a 90° configuration.

A horizontal base plate is connected to the crosshead grip. This plate is connected to two horizontal rods through vertical side plates. This horizontal fixture plate can glide on these rods using ball bearings so as to keep a constant peel angle (90°) throughout the test. The arrangement is shown in Fig. 15.

The coupon holder is fixed to the fixture plate using six nuts. This coupon

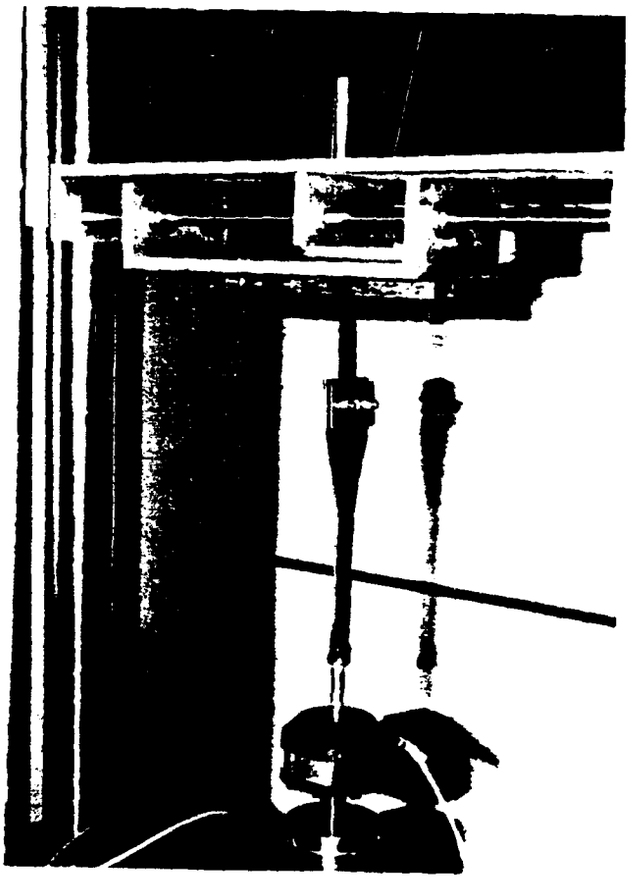

Fig. 15 90° peel fixture

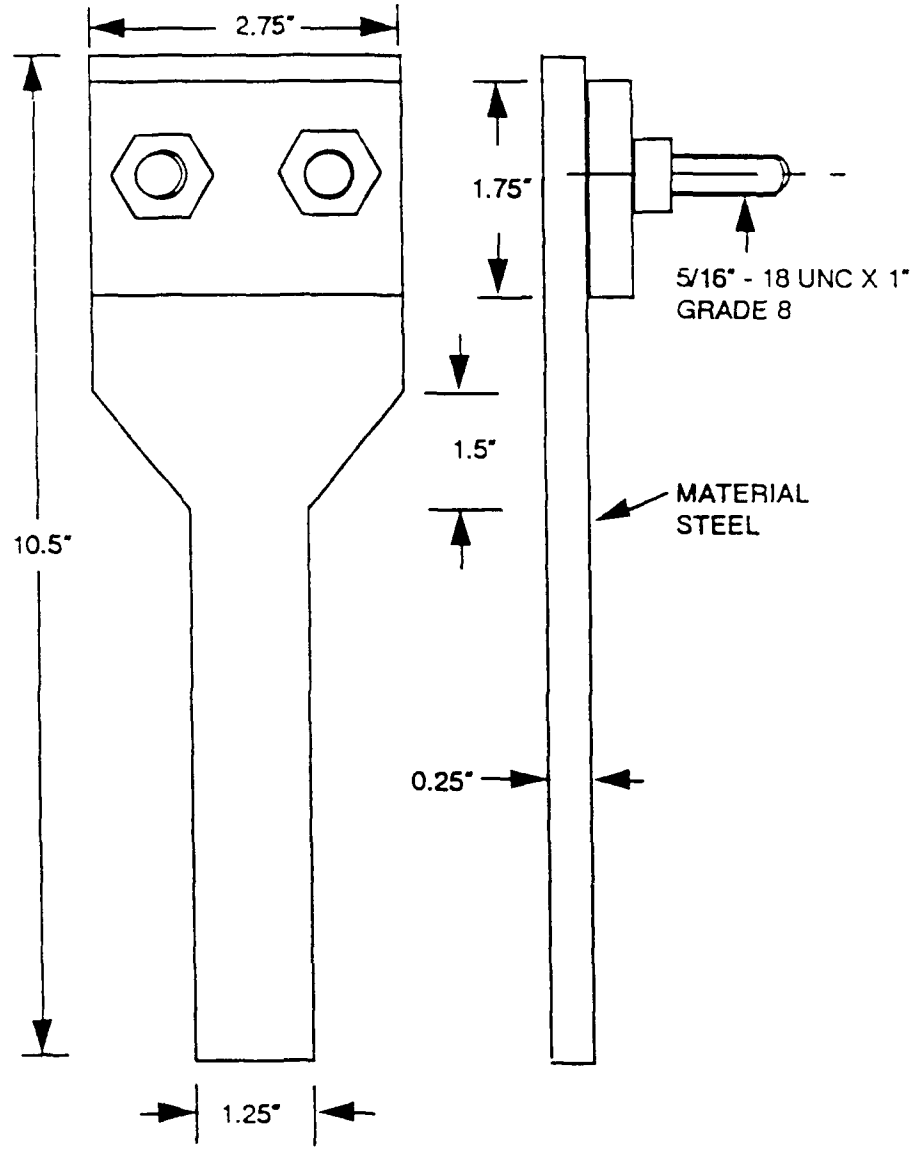

Fig. 14 Ply holder for peel test

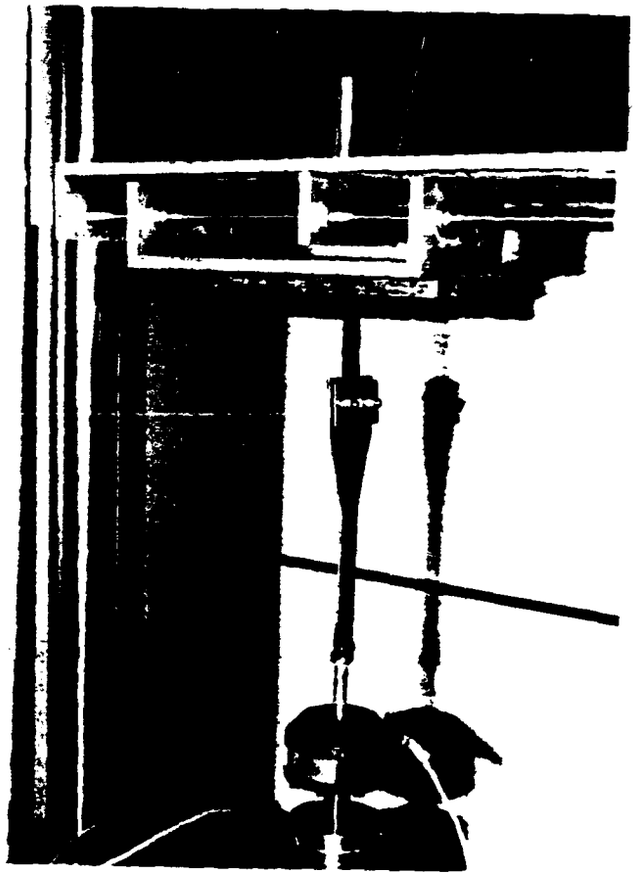

Fig. 15 90° peel fixture

holder has seven holes to hold the coupon and these were sufficient to keep thecoupon from undergoing excessive deformation when the peel tests were performed. The ply holder was designed to hold the ply firmly without slipping and was connected to the load cell by screws. The load cell is in turn connected to the actuator.

+/- 90° Peel Arrangement: For this test, two rigid coupon holders are used to keep the peel angle at 180° (+/-90°) throughout the tests. One coupon holder was connected to the crosshead grips and the other was connected to the load cell by screws. The load cell in turn was connected to the actuator. The procedure for this test is also described in the previous section. The arrangement of +/-90° peel test is shown in Fig. 16 and Fig. 17.

Thermal Aging Fixture: The thermal aging fixture was designed according to the requirements of the test such as

i Application of tension to the coupon

ii Stability at testing temperature

iii Ease of holding the specimens

iv Ease of moving the fixture subject to oven space limitation

The thermal aging fixture is shown in Fig. 18. The steel frame was made of two square tube elements with two steel rods threaded from ends. Two coupon holders were used at opposite ends of the fixture through holes in the square tube to hold the coupon. The design of the coupon holder is a very important part of this fixture. After many modifications, it was found that tension and lateral squeeze

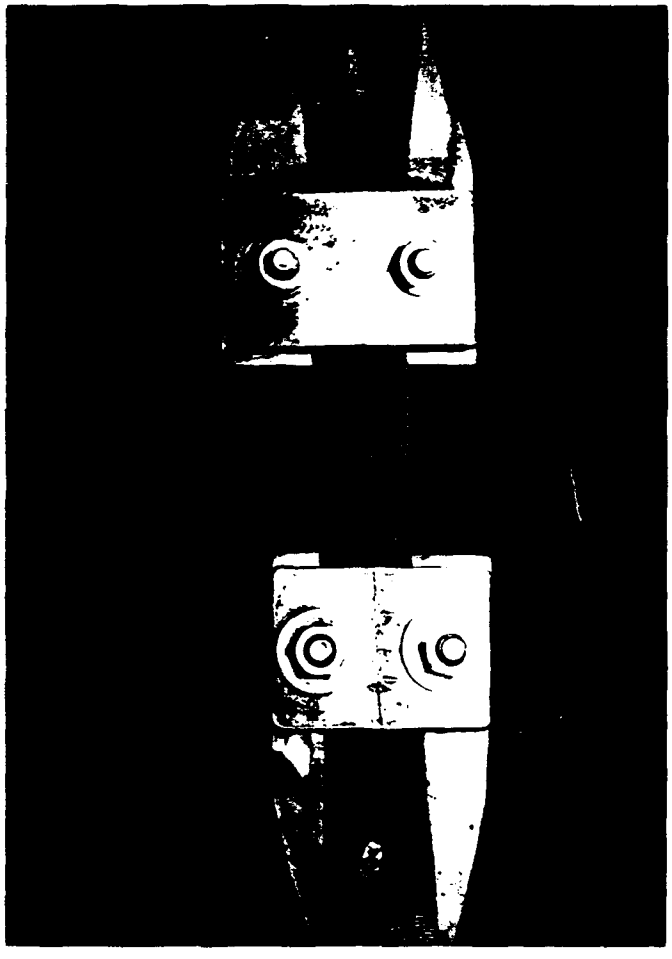

Fig. 16 +/-90° peel test arrangement (close up)

Fig. 17 +/-90° peel test arrangement

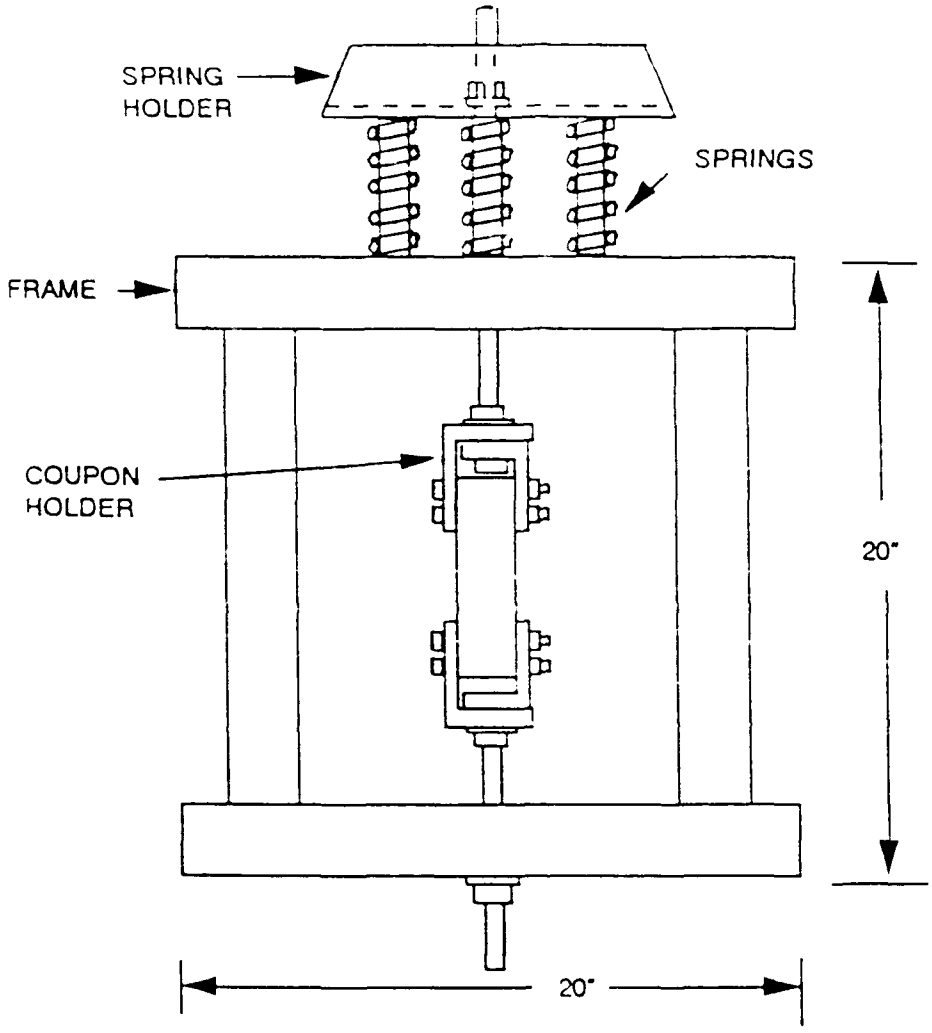

Fig. 18 Thermal aging fixture

type coupon holder (Fig. 19) was the best design to hold the coupon at required tension and testing temperatures.

The coupon holder consists of two L shaped gripper plates. The coupon was put into these plates and squeezed by fastening two bolts. These bolts (5/16" - 24 UNF) were passed through the flared end of the coupon. The tension was applied by compressing the three springs and fastening the tension bolts. The tension bolt specification (from Allen Hex-Socket Screw Hand Book):

Material	Allenoy steel series 60
Size	1/2 - 20 UNF (length = 8")
Yield load	24,460 lbf
Ultimate tensile load	27,200 lbf

These bolts passed through the gripping jaws. The three springs were compressed between the frame and spring holder (Fig. 20) made of carbon steel. The compression characteristics of all of these springs were tested and plotted and one of them is shown in Fig. 21.

Compression spring specifications:

Material	Chrome vanadium steel
Outer diameter	1.5"
Inner diameter	0.75"
Wire size	0.30" X 0.35"
Free length	2.0"
Maximum load capacity	1880 lbf.

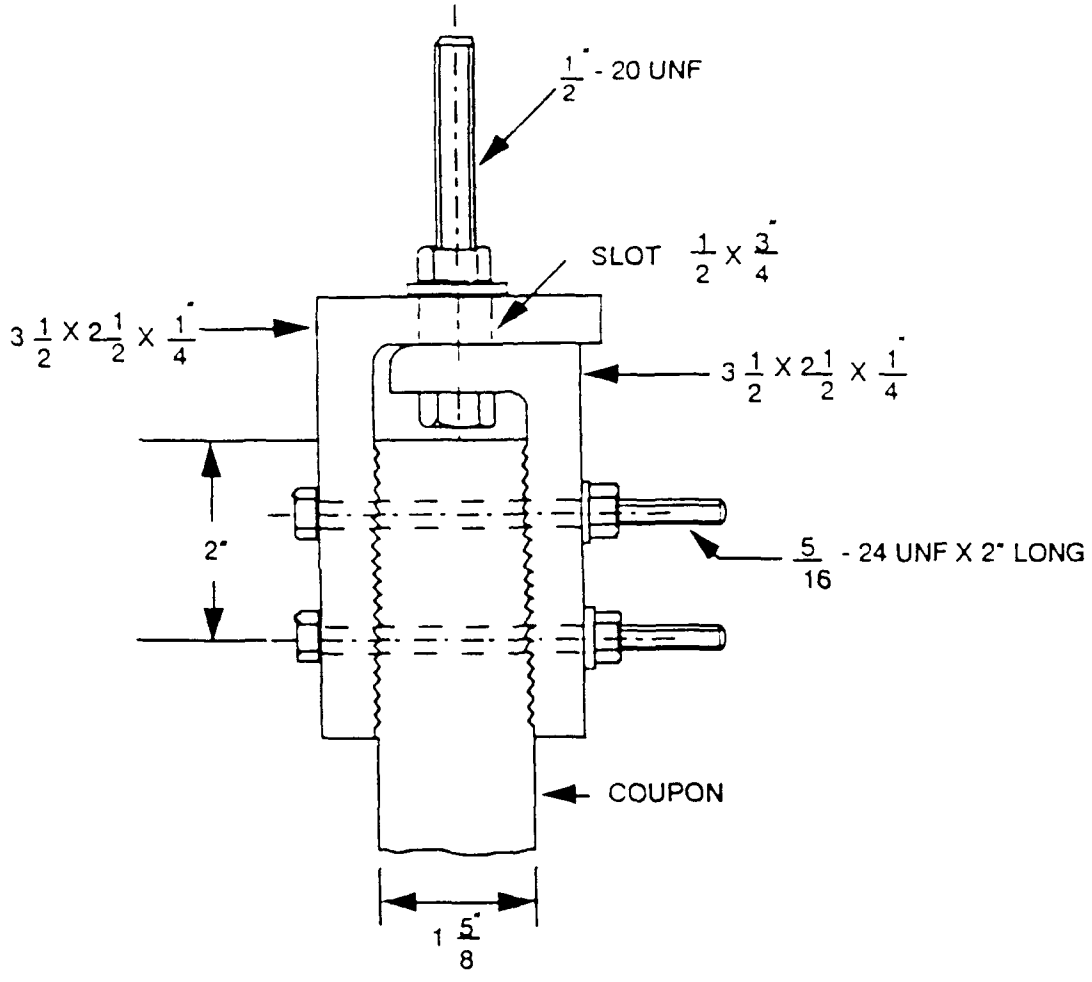

Fig. 19 Coupon holder for conditioning fixtures

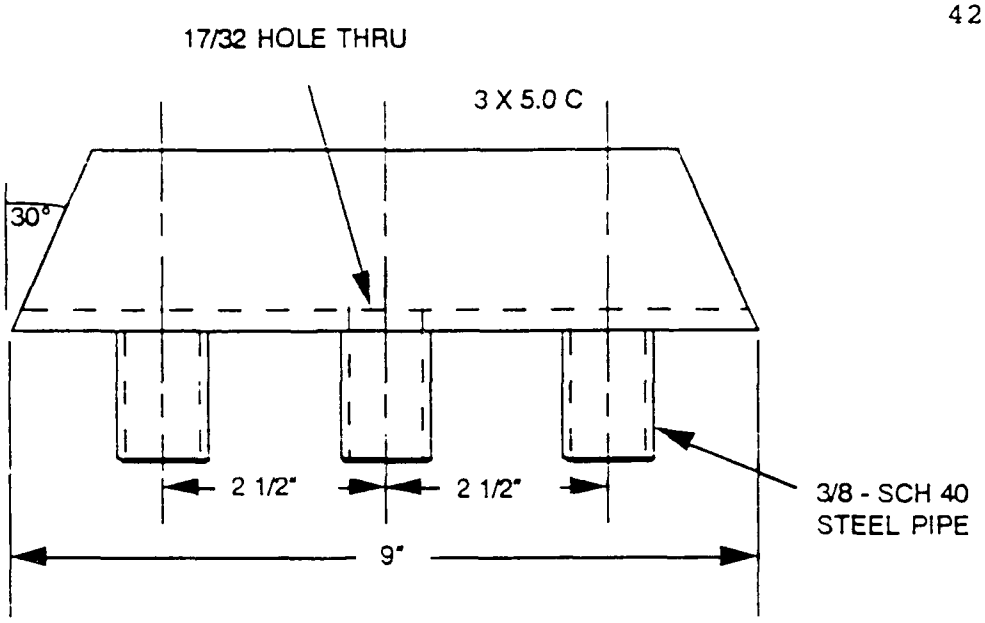

FRONT VIEW

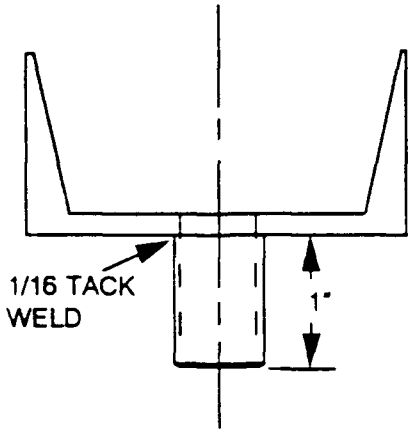

SIDE VIEW

Fig. 20 Spring holder for conditioning fixtures

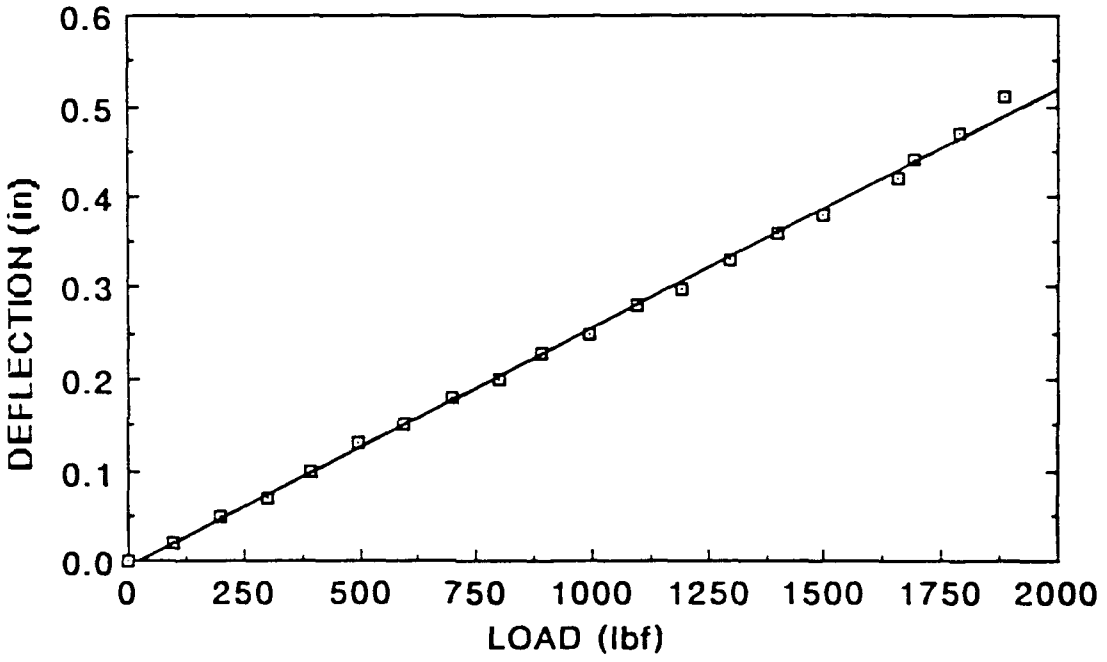

Fig. 21 Compression spring characteristic

The conditioning procedure is mentioned in the last section of this chapter.

Flex Fatigue Fixture: The flex fatigue fixture was designed according to requirements of the test such as:

i Application of tension to coupon

ii Lateral flexure of specimens

iii Stability at testing temperature, frequency and number of cycles

iv Ease of holding specimen in fixture

v Ease of mounting on MTS universal testing machine

The components in the fixture are:

Coupon holder frame

Base plate frame

Gripping roller assembly

Rigid side arms

Coupon holder frame is the same as in the thermal aging fixture except it is narrower because of testing machine space limitation and to facilitate heater jacket installation. All springs, spring holder, coupon holder and square tubular arms have the same specifications as in the thermal aging fixture.

Base plate frame is made of carbon steel and is connected to the crosshead by six bolts. The coupon holder frame is fixed to this plate horizontally through two columns by full penetration welding.

Gripping roller assembly has two side plates with 4 holes each, one stub

and two rollers. The coupon was gripped between rollers by fastening two screws to the side plates and stub. The stub in turn is screwed on to the actuator.

Rigid side arms are four square steel tubing assemblies fixed around the coupon holder and bronze bearing pads connected around tubular arms of the coupon holder frame to restrict any vertical movement. This vertical movement, if not restrained can cause bending and eventual breakage of the tensile bolts. The flex fatigue fixture is shown in Fig. 22 and Fig. 23. The flex fatigue fixture is shown in Fig. 24 without the heater jacket and Fig. 25 with heater jacket.

The procedures for room temperature and elevated temperature flex fatigue conditioning are described in the next section. The design of the heater jacket for flex fatigue is described later in this section.

Important design calculations (refer Fig. 26):

Bending moment at center of short arm of frame:

$M_{max} = PL_1/4 = (3000*8)/4 = 6000$ in.-lbf

P Force applied

M Bending moment

Bending stress at center of short arm of frame:

$S_b = MC/I = (3000*1)/0.5518 = 10874$ psi

S Stress

C Distance from neutral axis to extreme fiber

I Moment of inertia of cross section

$I = (1/12)(bh_1^3 - b_1h_2^3) = (b^4 - b_1^4)/12$

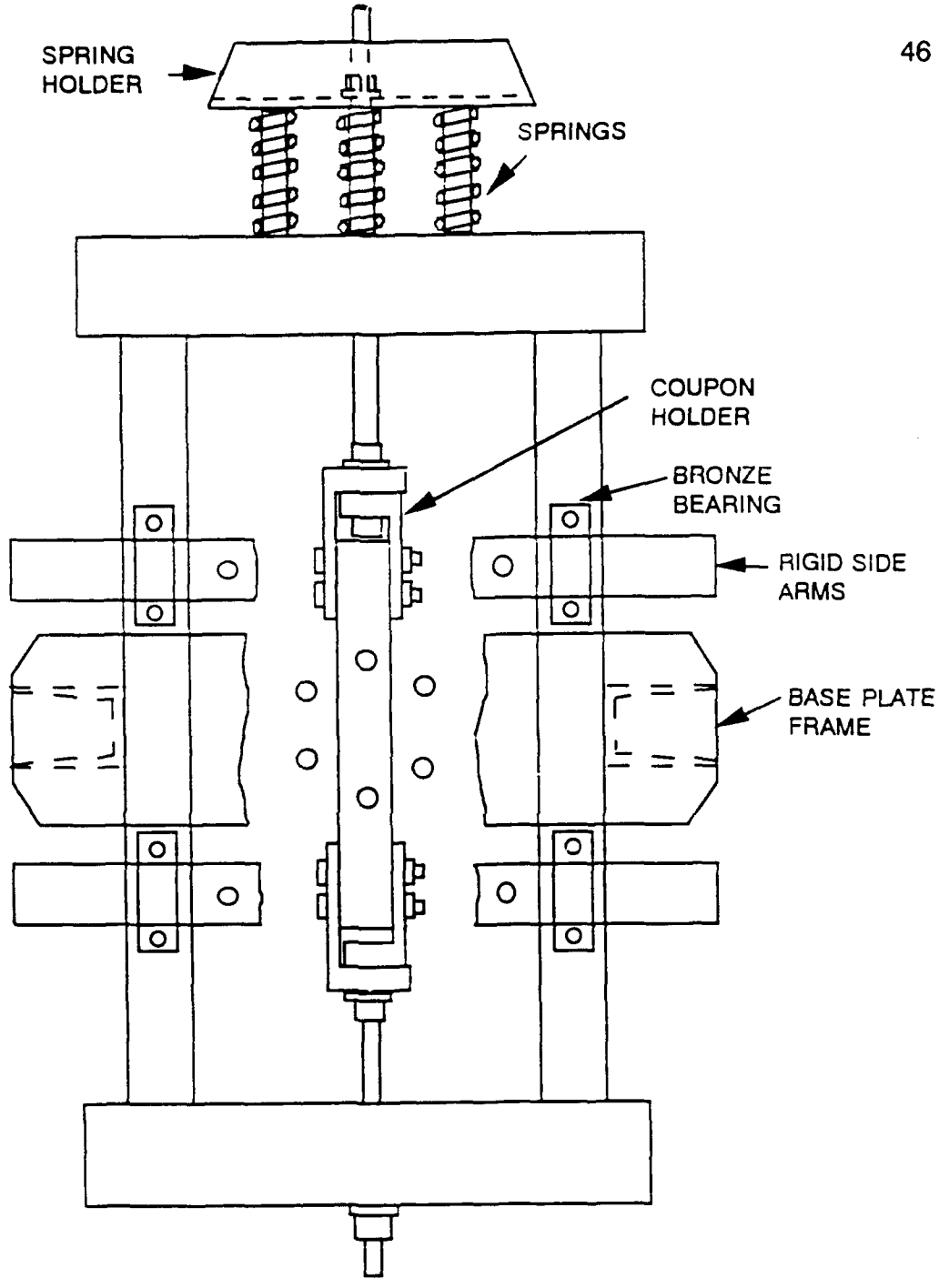

Fig. 22 Flex fatigue fixture (top view)

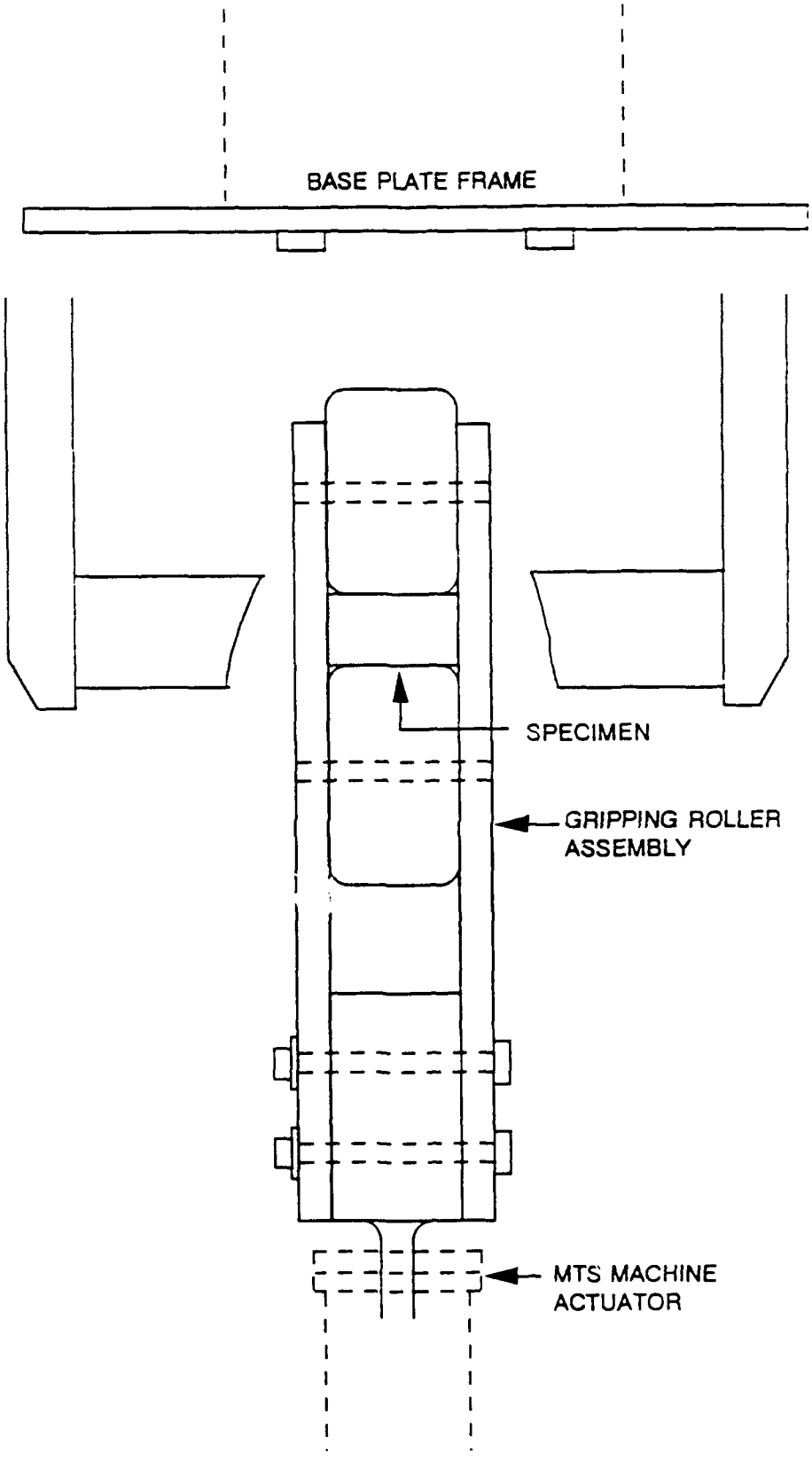

Fig. 23 Flex fatigue fixture (front view)

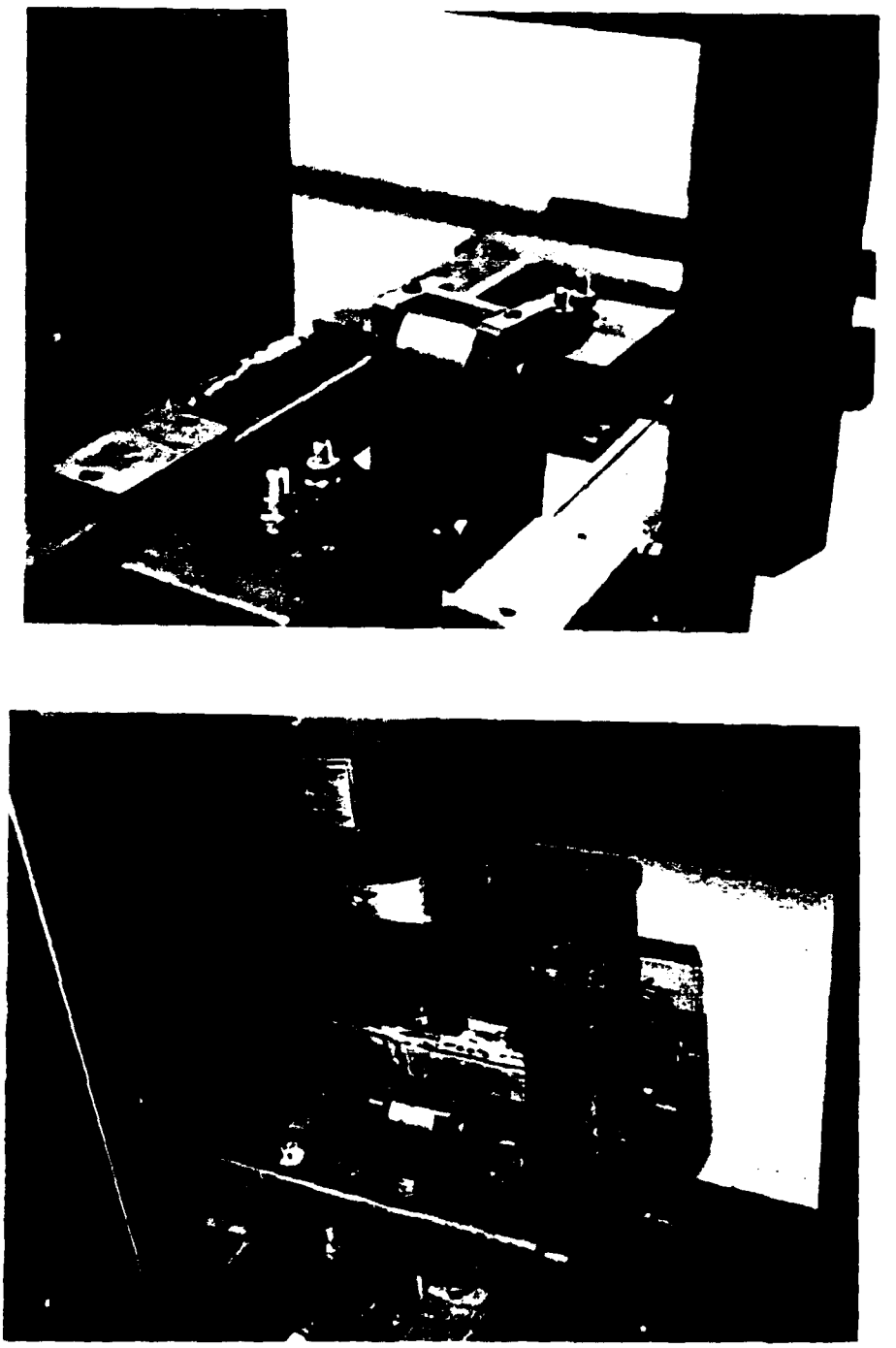

Fig. 24 Flex fatigue test arrangement

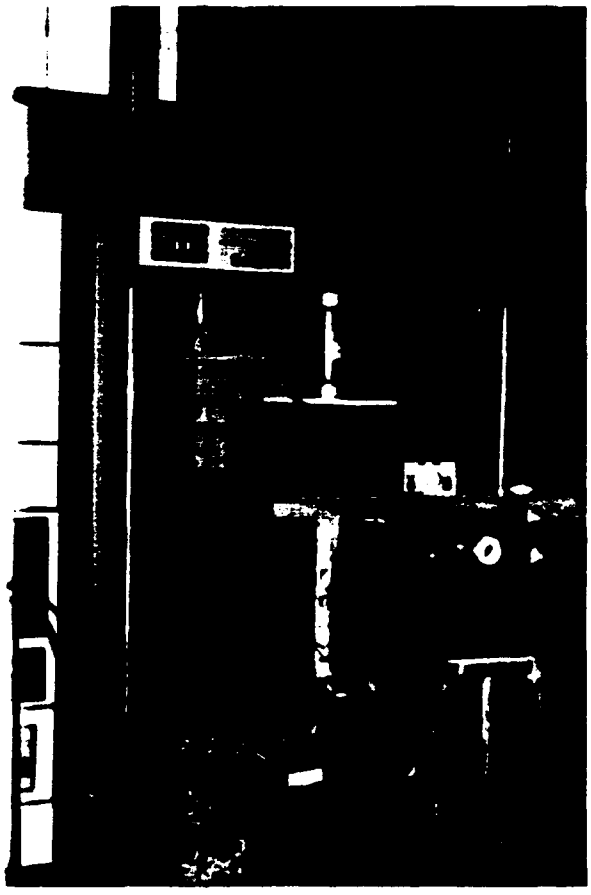

Fig. 25 Flex fatigue test arrangement with heater installed

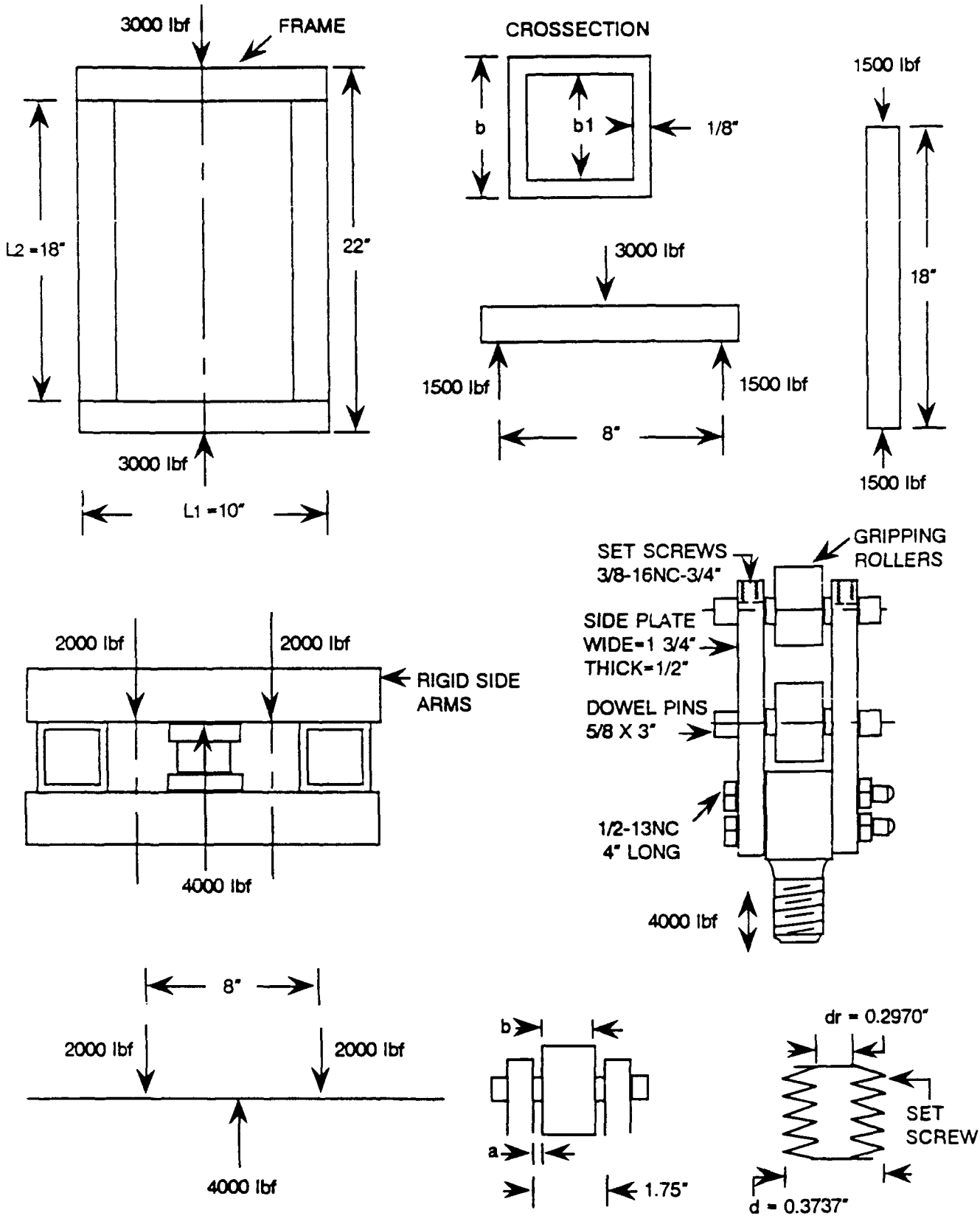

Fig. 26 Design of flex fatigue fixture components

$= (2^4 - 1.75^4)/12 \qquad = 0.5518\ in^4$

Here $h_1 = b$ and $h_2 = b_1$

Maximum deflection at center of short arm of frame:

(Assuming simply supported beam. This is a conservative assumption)

$\delta_{max} = (PL_1^3)/(192*E*I) = (6000*8^3)/(192*30*10^6*0.5518)$

$= 0.0005"$

δ Deflection at center of short arm

Radius of gyration (r):

$r = 0.289*(b^2 + b_1^2)^2 = 0.289*(2^2+1.75^2) \qquad = 0.768$

Buckling check for long arm:

$L_2/r = 18/0.768 \qquad = 23.4$

Allowable unit stress for long arm:

$P/A = 15{,}000 - 0.253*(L_2/r)^2$

$= 15{,}000 - 0.253*(23.4)^2 \qquad = 14{,}861\ psi$

Actual unit stress for long arm:

$P/A = 1500/(0.125*7.5) \qquad = 1600\ psi$

Tensile stress in bolts used for rigid side arms (size 3/8")

$S_t = P/A = 2000/0.0775 \qquad = 25{,}806\ psi$

(here 4000 lbf is estimated force applied on sample)

Stresses on side plates & rollers in gripping roller assembly:

Side plate stress in tension = $P/A = 2000/(1.75*0.5)$

$= 2285\ psi$

Dowel pin shear stress = P/A = 2000/(3.1415*0.625^2/4)

= 104294.4 psi

Point load at center of dowel pin (w) = 4000/1.625 = 2461 lbf

Maximum bending moment at dowel pin (M_{max}) =(w*b/2)(a+b/4)

(here a = 0.062" and b = 1.625")

= (2461*1.625/2)(0.062+1.625/4)

= 936 lbf.in

Maximum bending stress (S_b) = M_{max}*C/I

= (936*0.312)/(3.1415*0.625^4/64

= 40,000 psi

Thread stress in set screws:

Average shear stress in bolt thread:

S_{avg} = 2*P/(π*d_r*h) = 2*4000/(3.1415*0.297*0.62)

= 13,829 psi

Average shear stress in nut thread:

S_{avg} = 2*P/(π*d*h) = 2*4000/(3.1415*0.0.374*0.62)

= 10,981 psi

4.3.4 Heater jacket

The heater jacket is designed to heat the specimen for thermal flex aging test within the constraint of MTS machine space limitations and size of the flex fatigue fixture. The heater jacket is shown in Fig. 27.

This jacket is made of fiber glass (insulating material). It was designed so

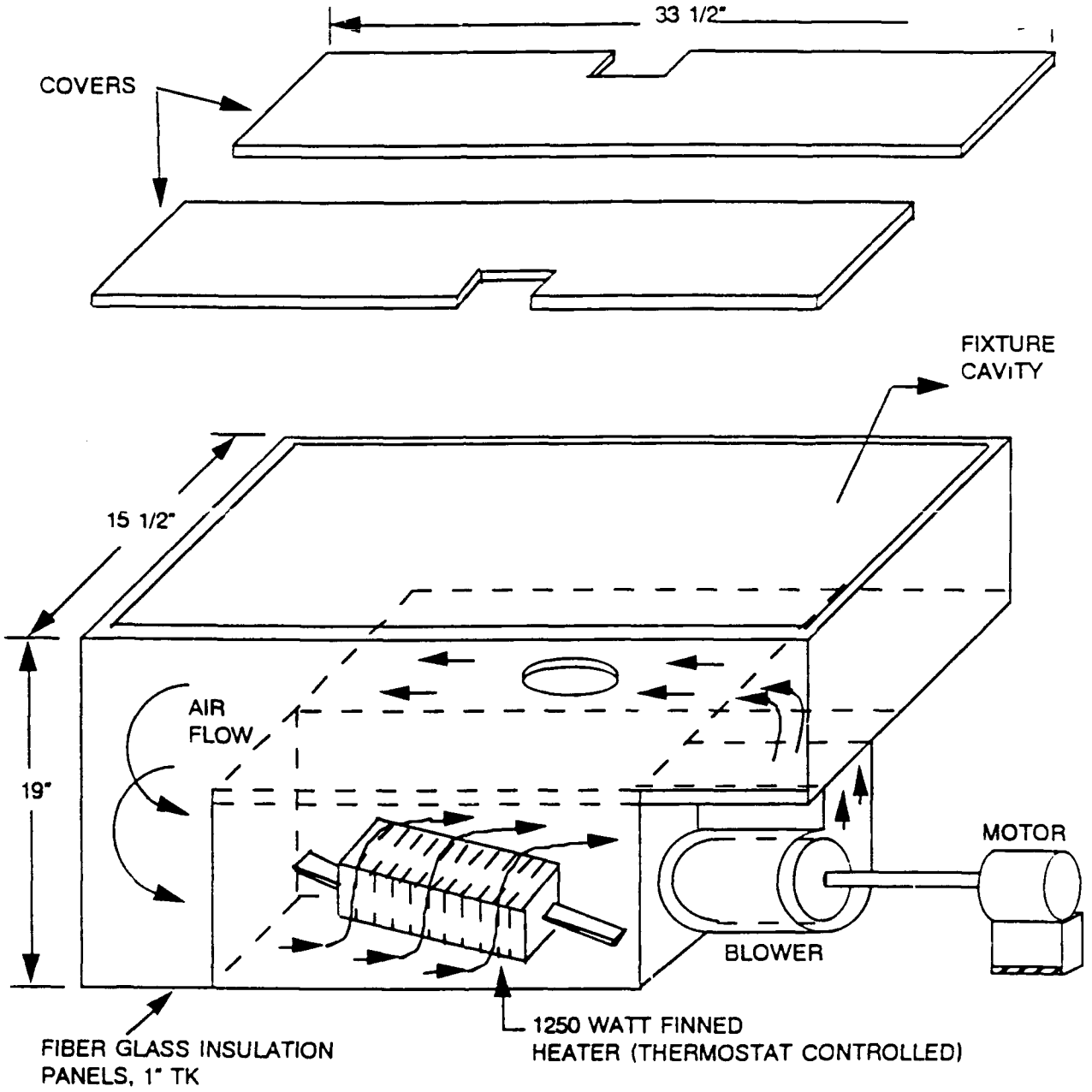

Fig. 27 Heater jacket for flex fatigue tests

that after equilibrium the heat would flow at a constant rate from heater cavity to fixture cavity. The fixture is lowered into the fixture cavity with the test specimen and covered. The 1250 W finned heater is fixed in the heater cavity by two screws. This heater is connected to a thermostat for controlling temperature.

The thermostat controls the heater. Its thermocouple tip is inserted in the inlet heat stream of the fixture cavity.

The squirrel cage blower with motor is fixed between heater cavity outlet and fixture cavity inlet. It sends heated air from the heater to the fixture cavity. The thermostat set point is fine tuned by reading specimen surface temperature off a separate thermocouple attached to the specimen surface. The procedure is described later in this chapter. The design calculations are as follows:

Outside temperature = 80°F

Inside temperature = 250°F

k (thermal conductivity) = 0.23 BTU/hr.ft^2.°F.in

Thickness of insulation = 1"

Surface area (A) = 18.2 ft^2

Total weight of fixture (m) = 50 lbs

Fixture material = steel

Specific heat of steel = 0.118 BTU/lb.°F

Specific heat of fiber glass = 0.20 BTU/lb.°F

Heat loss through oven panels by conduction

By Fourier's Law Q = - (k*A*T)/L

where k coefficient of heat transfer

C_{sp} specific heat

A surface area

T change in temperature

L change in length

- ve sign denotes heat leaving the system

Q_{out} = - (0.23*18.2*(250-80)/1

= - 711.62 BTU/hr

If a 1250 W heater is used the

Q_{in} = 0.057 BTU/min * 60 min/hr

= 4275 BTU/hr

Effective heating rate = 4275 - 711.62

= 3563.38 BTU/hr

Time required to heat up the oven to 250°F from 80°F can be found from the following equation:

$Q = m*C_{sp}*t$

Q_{steel} = (50 lb)(0.118 BTU/lb°F)(170 °F)

= 1593 BTU

$Q_{insulator}$ = $(6\ lb/ft^3)(18.2\ ft^2)(1/12\ ft)(0.20\ BTU/lb°F)(170°F)$

= 309.4 BTU

Total BTU/hr for heat up:

$Q_{steel} + Q_{insulator}$ = 1593 + 309.4

= 1902.4

Heat up time = Total heat of equipment / Heat input (by heater)

= 1902.4 BTU/4275 BTU/hr = 0.45 hr.

4.3.5 Ovens

In this project two commercial ovens were used with thermostat temperature controls were used as described below:

Hotpack oven: Capacity - 650°F, Timer - 24 hours.

Fisher isotemp oven (400 series model): Capacity up - 438°F,

Timer - 12 hours.

4.4 Constitutive Properties - Coupon Design and Test procedure

The results for all the tests described below are given in the next chapter.

4.4.1 Specific Gravity

For this test, rectangular coupons of size 0.3 X 0.5 X 0.5" were taken from the carcass and tread separately, because this size can be conveniently handled by the precision balance used for mass measurements. Six specimens (3 tread rubber, 3 carcass) were taken from virgin tires. Each specimen was first weighed in air and then in water using a Mettler PM400 precision balance as shown in Fig. 28. Measurements should be taken very quickly otherwise the rubber will start absorbing water. Specific gravity is the ratio of the weight of the specimen in air to its loss of weight in water.

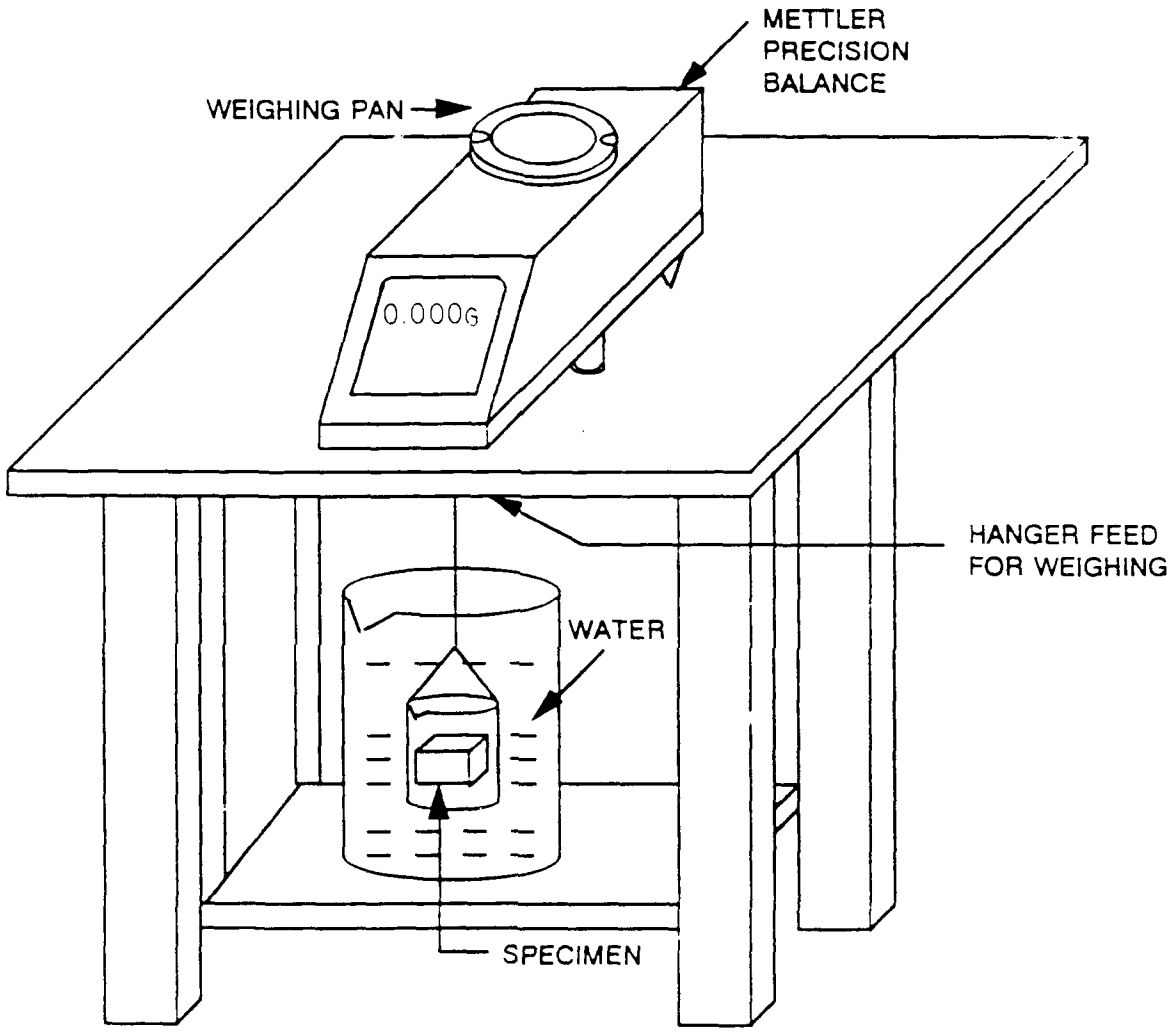

Fig. 28 Specific gravity measurement equipment

4.4.2 Cord Spacing Measurement

Coupon that had been used in baseline peel tests were used for cord spacing measurement. This is because peeling exposes the cords well for measurement under a toolmaker's microscope. Cord spacing is the center to center distance between neighboring cord in a ply. A typical coupon cross-section is shown in Fig. 29. Cord spacing was measured for nine coupons taken from three tires (3 coupons/tire). Cord spacing was measured using a toolmaker's microscope as shown in the figure. From each ply three readings were taken and the average was determined.

4.4.3 Cord Angle Measurement

Coupon that had been used in baseline peel tests were used for cord angle measurement. This is because peeling exposes the cords well for measurement under a toolmaker's microscope. The plies are not laid perfectly parallel to each other. Using the long edge of the coupon as a datum, the angle of cord orientation of the plies is called the cord angle. Ideally, longitudinal plies should have 0° cord angle and transverse plies should have 90° cord angle. Cord angle was measured for nine coupons from three tires (3 coupons/tire). The coupons used had already been peel tested. The cord angle was measured using a toolmaker's microscope as shown in Fig. 30. Plies are numbered (1 to 17) from the inner liner to the tread surface. The first 12 plies are the casing plies, next two are breaker plies and the last three are tread reinforcing plies.

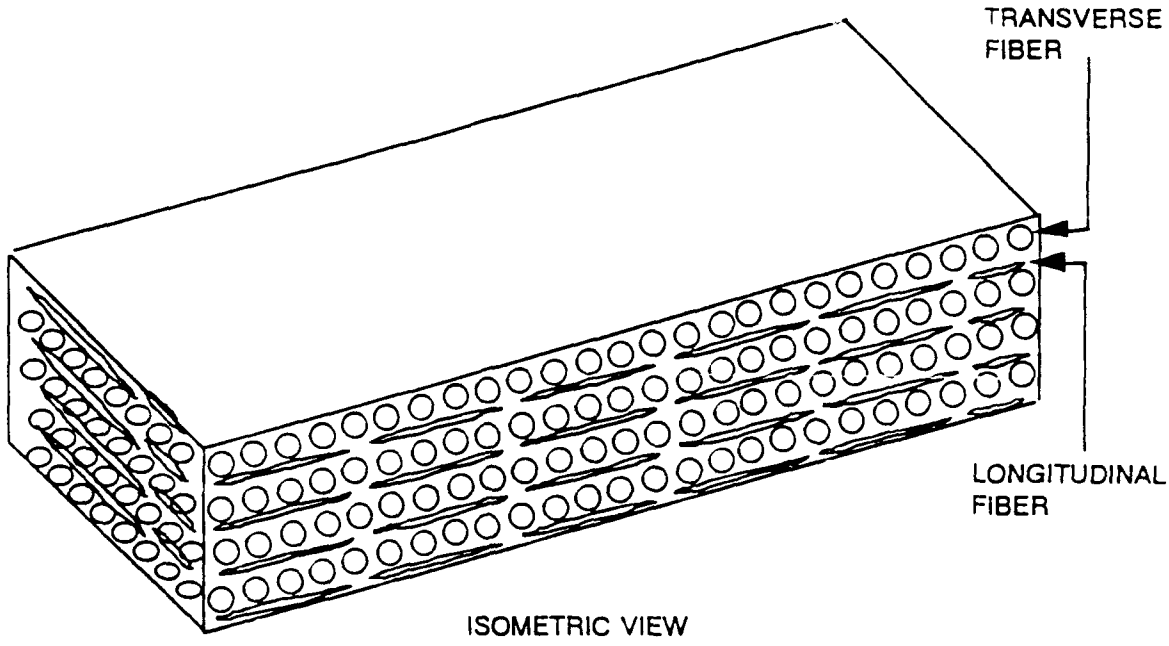

ISOMETRIC VIEW

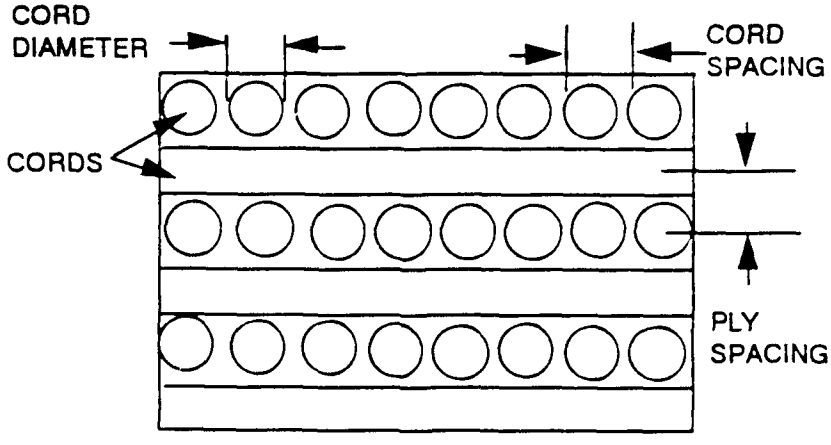

CROSS SECTION

Fig. 29 Tire carcass coupon

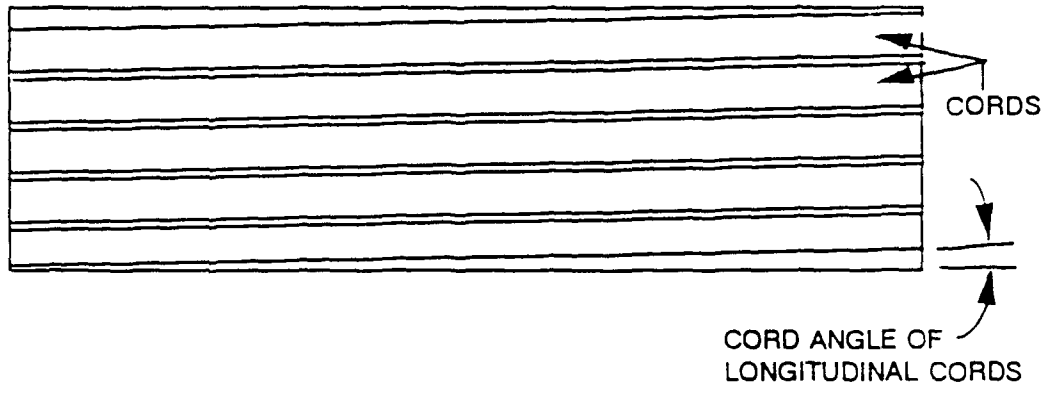

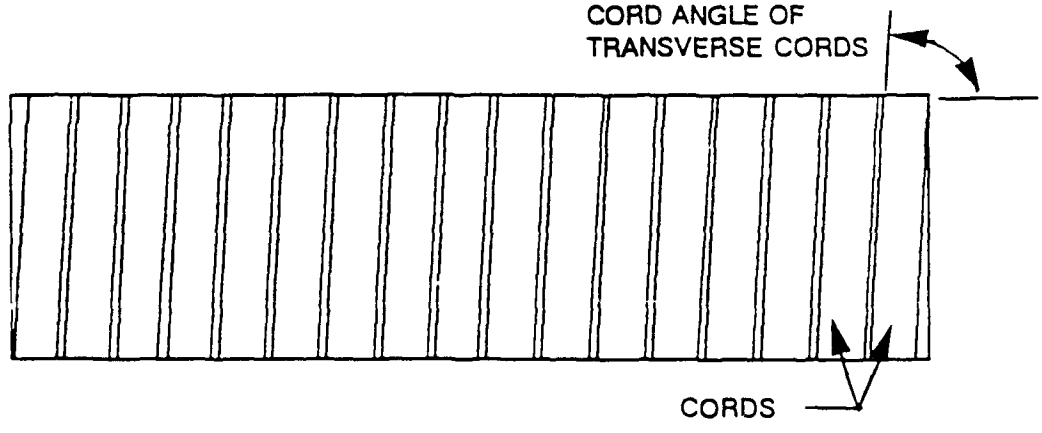

Fig. 30 Cord angle measurement

4.4.4 Cord Diameter

The test specimens were cut to size 1 X 1 X 5/8" and squared so that the plies became parallel or perpendicular to the surfaces for accurate measurement. Cord diameter was also measured using a toolmaker's microscope, as shown in Fig. 29.

4.4.5 Ply Spacing Measurement

The test specimens were cut to size 1 X 1 X 5/8" and squared so that the plies became parallel or perpendicular to the surfaces for accurate measurement. Ply spacing was measured for nine coupons taken from three tires (3 coupons/tire). Ply spacing was measured using a toolmaker's microscope as shown in Fig. 29.

4.4.6 Damping Coefficient and Shear Modulus

Rubber tread and carcass material were cut into rectangular specimens of dimensions 3.0 X 0.5 X 0.25" to suit the requirements of the Dynamic Mechanical Analyzer (DMA). The testing was performed by Michigan Molecular Institute of Midland, MI using a Du Pont 982 Dynamic Mechanical Analyzer by using the resonance method and a vibration amplitude of 0.2 mm. A schematic of the clamped in the DMA is shown in Fig. 31.

4.4.7 Tensile Modulus

Rectangular coupons of size 1 X 0.5 X 10" were used because they were convenient for gripping in the tensile testing machine. Coupons were cut separately from the tread and the carcass. The tensile modulus was measured

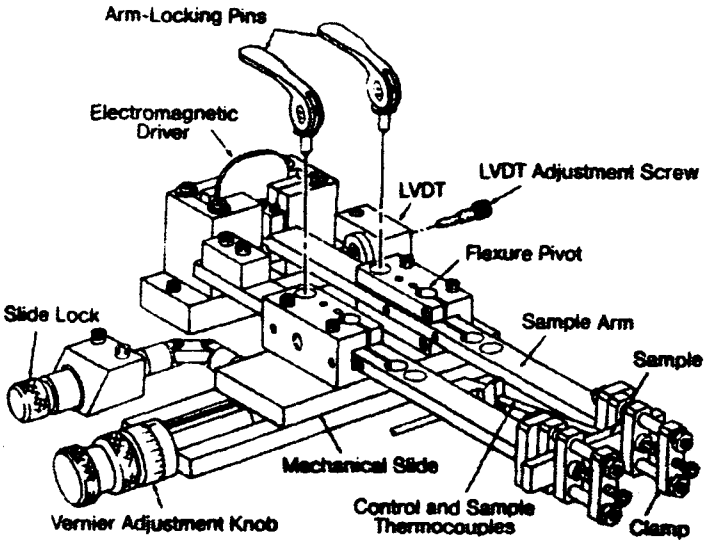

Fig. 31 DMA coupon clamping fixture (from DMA manual)

using the tensile test. This test was carried out on MTS - 810 testing machine. Since large strains were involved, the strain was measured by using the displacement of the actuator as against using strain gages or extensometers. The machine was operated in strain control mode at a strain rate of 0.01 in./in./min. Load cell and extensometer were used to measure the load and transverse strain for tread and carcass specimens respectively. Using the data thus obtained, the tensile moduli were calculated. The axial and transverse strains were used in computing Poisson's ratio.

4.4.8 Thermal Analysis

Thermal analysis of the tire samples involved the measurement of thermal conductivity and specific heat capacity. Specimens of size 4.0 X 4.0 X 0.3" were chosen to suit the instrument requirements. Tread and carcass materials were tested separately.

Thermal conductivity was measured using a thermal conductivity instrument (Anacon Model 88). The specimen was placed in the instrument chamber. The top and bottom platens at hot and cold temperatures placed on the specimen and the temperatures were allowed to stabilize. This took two hours, after which the temperature and the heat flow was measured and the conductivity was calculated.

Specific heat was calculated using the principle of conservation of total heat in a system. The thermal conductivity specimens were also used in this test. The specimen was heated in a water bath and allowed to soak at a fixed temperature for 30 mins. It was then transferred to the calorimeter which contained water at

room temperature. The temperature was noted for that point at which it stopped rising and started falling. Using this, the specific heat was calculated. These tests were performed separately on rubber and carcass specimens.

4.5 Peel Coupon Design and Test Configurations

Baseline peel coupons were used to find the peel strength between different ply levels. All coupons were cut in the direction of fibers because there is less wandering of the fracture between ply levels with this orientation. The width of the specimen is 1", in accordance with ASTM 413-88. The standard does not specify the coupon length. 10" long coupons were cut because 3 to 4 tests can be performed on the same ply level. The dimensions are shown in Fig. 11.

The present work was directed toward finding the most consistent (least scatter) method of peeling from amongst the following three methods:

4.5.1 180° Peel

The coupon was attached to the coupon holder of the fixture by nine pins inserted through the tread compound. The fixture was gripped vertically in a testing machine. A minimum of two plies were peeled off the coupon at 180° each time as shown in Fig. 32. This procedure is described in detail below.

The coupon was held in the fixture holder. The location of the holes were marked for pins with a sharp white marker. Holes were then drilled in the tread. The specimen was re-inserted into the coupon holder, and steel pins were inserted into the coupon holder to firmly retain the coupon. Ply levels were counted from

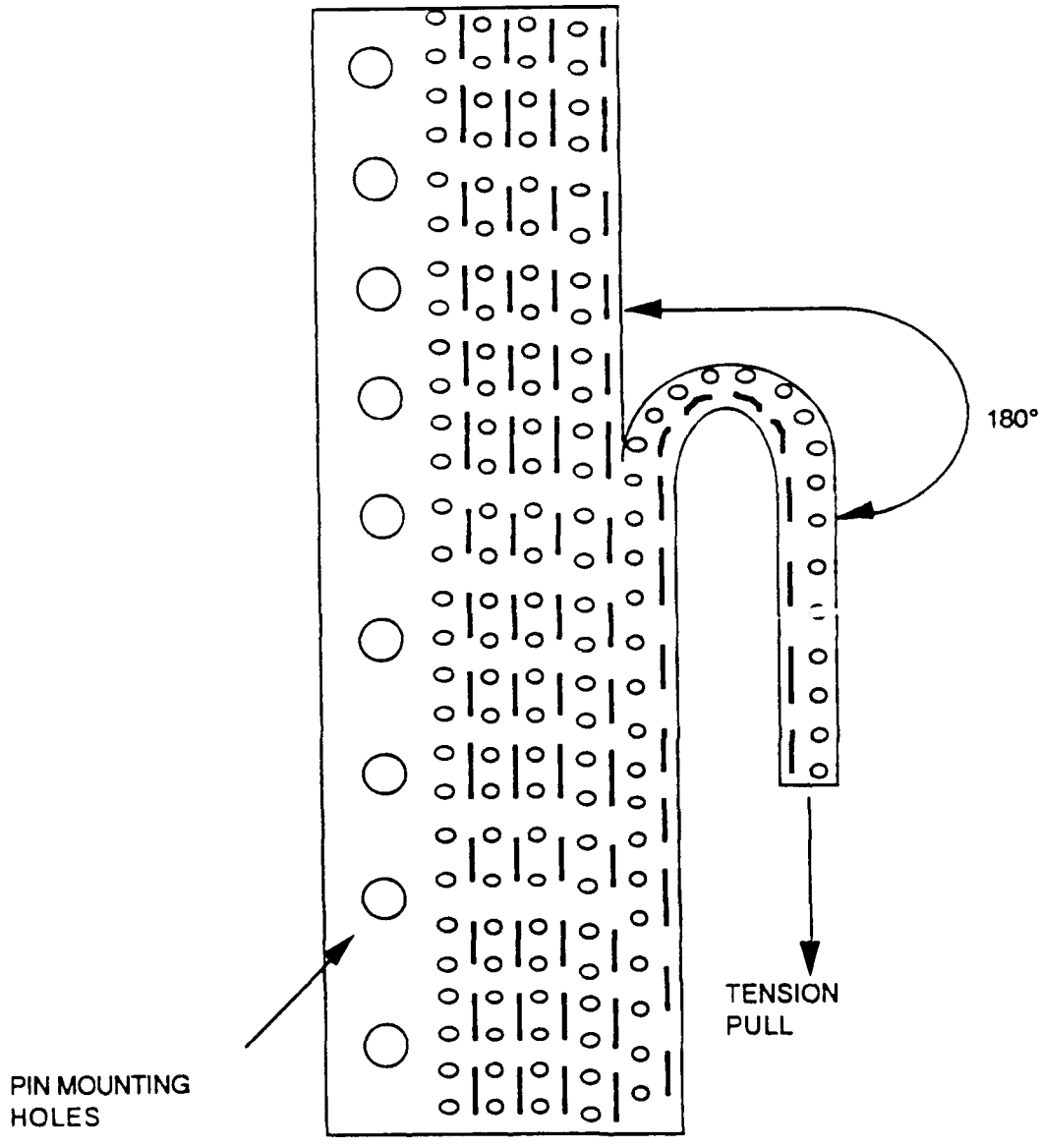

Fig. 32 180° peel configuration

the pressurized side of the tire to the ground side. The first ply had transverse fibers, the second ply had fibers oriented longitudinally and so on. A sharp knife was used to open a horizontal cut between the third and fourth ply for a depth of about 1.5" of the ply so as to obtain a grip with ply holder. The fixture was then gripped in the crosshead of the testing machine. The gripped part of the ply was connected to the load cell and the load cell connected to the actuator of the machine. The actuator control (Microprofiler) program was used to move the actuator at a rate of 2 in/min. The test was run stroke control mode. Load and displacement were collected and stored using Lab Tech data acquisition software. Each test was run through a minimum 3" displacement. Load displacement values were similarly obtained between plies 7-8, 11-12, 15-16.

4.5.2 90° Peel

The coupon was attached to the coupon holder of the moving trolley mechanism using nine pins. The fixture was gripped horizontally in the crosshead. A minimum of two plies were peeled off the coupon at 90° each time. The 90° peel test configuration is shown in Fig. 33. The moving trolley translated so as to maintain the peel angle at 90°.

4.5.3 +/- 90° Peel

In this method, three sets of four plies each were gripped firmly with plier and rolled off the carcass. An opening was made between the two middle plies of each set. Both ends were gripped in the ply holders and then the plies were separated. The +/-90° peel test configuration is shown in Fig. 34. The procedure

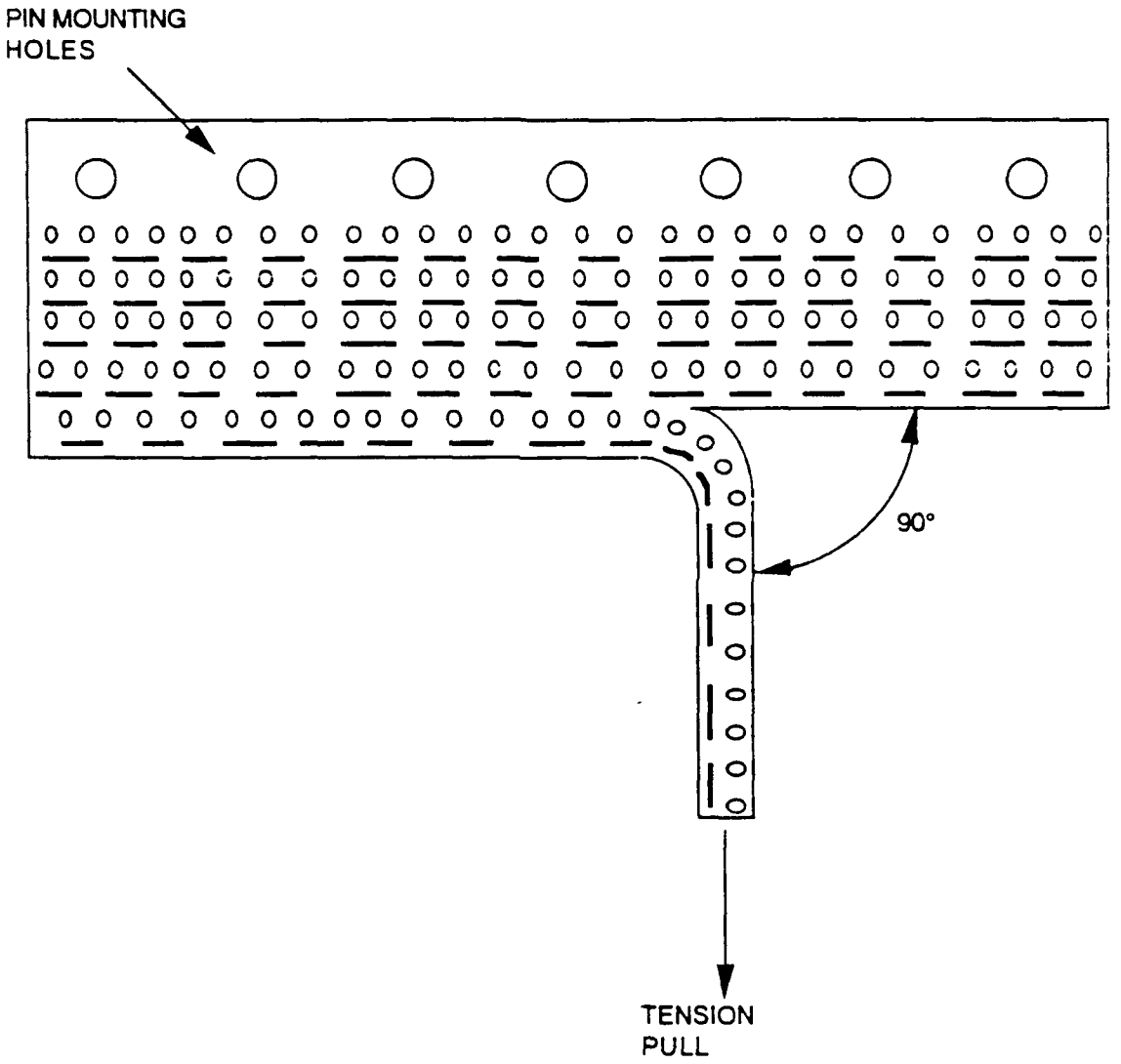

Fig. 33 90° peel configuration

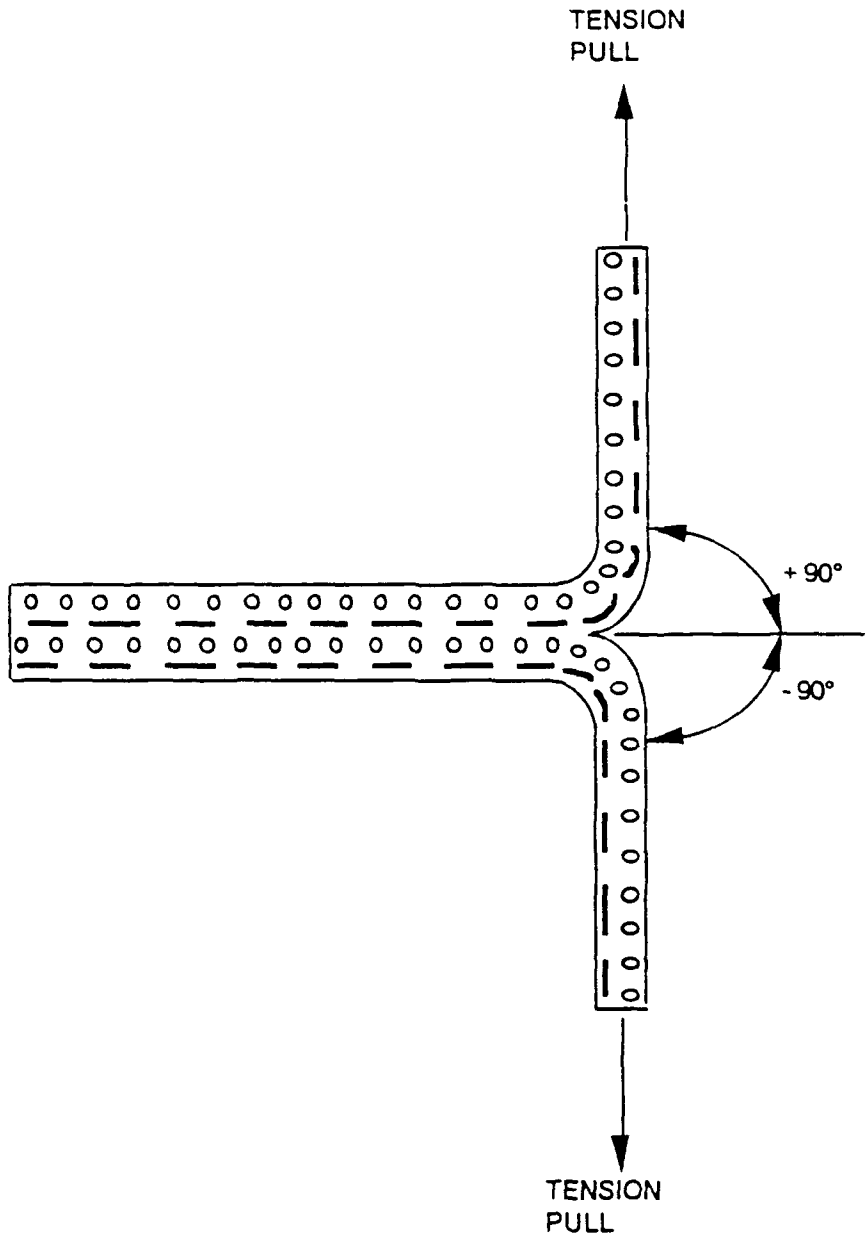

Fig. 34 +/-90° peel configuration

is described in detail below.

The coupon was clamped in a machine vise. Using pliers and a sharp knife, an opening was made between the first layer of ply and second ply level. The rubber tread and the first ply were then removed. An opening was made between the third and fourth ply about 1.5" deep. Openings were similarly made between the fifth and sixth ply levels and by using pliers the above mentioned set of four plies was removed. The next two sets of four plies each were removed similarly. There was no need for a fixture in this case. Two ply holders were used, one attached to the crosshead grip and the other attached to the actuator through the load cell.

4.6 Conditioning Coupon Design and Aging Methods

To simulate actual service conditions, two types of conditioning methods were chosen as follows:

4.6.1 Thermal Aging under Tensile Load

After a lot of trial and error, it was determined that a bone shape was satisfactory because tensile stress concentration at bolt holes can be reduced by squeezing the flared end of the coupon in the coupon holder. The width of the coupon in the gage length area was taken to be 1" and the gage length was chosen 2 1/2", so that three peel tests could subsequently be performed on a given ply level. The dimensions are shown in Fig. 11.

The coupon was preloaded with a tensile load proportional to the tire

inflation pressure and aged at various temperatures for different time durations as shown in Table 1. This test simulates the combined effect of inflation pressure and elevated temperature. It should be noted at this point that the test matrix was expanded to include a 21 hour time duration in order to provide an equitable comparison between thermal aging and flex fatigue conditioning. Additionally, when preliminary results from thermally aged coupons showed rapid deterioration of peel strength between 200°F and 250°F, an additional aging temperature of 225°F was added to the test matrix.

Procedure: Coupons(Fig. 11) taken from virgin aircraft tires were gripped in the following manner: 5/16" holes were drilled into both ends of the coupon to accommodate coupon holder bolts. The coupon holders were inserted into the frame of the aging fixture. The coupon was fixed in the coupon holders using four nuts tightened enough to sustain a 3000 lbf tension force. The three calibrated compression springs were inserted and compressed between one arm of the fixture and spring holder by tightening the 1/2" nuts which were suitably lubricated. The tensile load required to simulate tire inflation was calculated as shown below. The load was applied using compression springs of known stiffness. Coupons were aged at different temperatures and for different time durations as shown in Table 1.

Calculation of Static Tension Load to Simulate Inflation Pressure:

The static tension load was computed by modelling the inflated aircraft tire as a thin-walled pressure vessel. 170 psi inflation pressure was assumed. Hoop

Table 1 Test matrix for coupon conditioning

Thermally aged coupons

Aging temperature (°F)	Number of coupons aged			Peel levels/ coupon	Total data points
	Aged 21 hrs	Aged 100 hrs	Aged 200 hrs		
150	1	3	3	3	63
200	1	3	3	3	63
225	1	3	3	3	63
250	1	3	3	3	63

Flex fatigue coupons

Flex temperature (°F)	Frequency (Hz)	Number of coupons	Peel levels/ coupon	Total data points
75	5	3	3	27
75	10	3	3	27
150	10	3	3	27
200	10	3	3	27
225	10	3	3	27
250	10	3	3	27

stresses and longitudinal stresses were calculated. Since the coupons were cut at 45° to the circumferential direction, these two stresses were transformed to the normal stress in the 45° direction using the standard stress transformation equation as shown below.

Inflation pressure assumed (p)	= 170 psi.
Internal diameter of tire (d)	= 45.75 in.
External diameter	= 49 in.
Effective carcass thickness(t)	= 0.95 in.
Cord angle (Θ)	= 45°
Hoop stress (σ_H)	= pd/2t
Longitudinal stress (σ_L)	= pd/4t
Hoop stress (σ_H)	= 4094 lb/in^2
Longitudinal stress (σ_L)	= 2047 lb/in^2
Normal stress($\sigma_H\cos^2\Theta + \sigma_L\sin^2\Theta$)	= 3070 lb/in^2
Area of cross - section (A)	= 0.95 in^2
Static tension load(σ_{normal} * A)	= 2917 lbf.

4.6.3 Flex Fatigue Conditioning

Flex fatigue coupons have to be subjected to a combination of longitudinal tensile load and lateral flexing, so a bone shape was chosen as described above for thermally aged coupons. However, the gage length was designed to be 5" due to the size limitation on the flexing rollers. The dimensions are shown in Fig. 11. The static load was applied to the coupons taken from virgin aircraft tires as

described in the aging test. It was flexed laterally (to simulate rolling) at room temperature and at elevated temperatures. The tests at elevated temperatures are meant to simulate inflation pressure and distance of roll as well as temperature rise due to braking and flexing of the tire.

Procedure: Coupons(Fig. 11) were gripped in the flex fatigue fixture by the same procedure as for thermal aging. The same static load was applied. Any vertical movement of the coupons holders was restricted by rigid side arms. The fixture was attached to the crosshead of the MTS testing machine and raised sufficiently to install the heater jacket. The actuator gripped the coupon in the center using two rollers. The lower roller was installed first. Then the heater jacket was put around the actuator. The crosshead was lowered until the fixture was enclosed by the jacket. The actuator was moved slowly and stopped when the machine was checked and zeroed. The other gripping roller was then installed and tightened enough to grip the specimen well. The load channel value of the MTS machine was set to zero by moving the actuator very slowly by rotating the zero knob of the displacement controller. Channel 1 of a thermocouple was attached to the specimen surface using lead tape and the second channel was held in air very close to the specimen. The thermostat thermocouple tip was inserted in the entry zone of the heat stream in the specimen section. The heater jacket covers were fitted tightly using tape. The thermostat was set to the required elevated temperature(Table 1). The heater was turned on until the system attains equilibrium. The specimen surface temperature was noted. The controller program

on the testing machine was set to move the actuator at a frequency of 10 Hz for 741,000 cycles. The calculations are listed below. The actuator movement stops automatically when the set number of cycles is completed. The heater was then turned off and the system allowed to cool. The upper covers of the heater jacket were removed, the moving roller arm was unscrewed and the upper roller was removed. The crosshead was raised sufficiently to remove the heater jacket. The roller arms were removed from the actuator and the crosshead was lowered. The fixture was removed from the crosshead. The specimen was removed and squared with a band saw.

Calculation of Flex Fatigue Amplitude and Frequency:

Tire diameter (D)	= 49 in.
Taxiing distance - assumed (L)	= 6 miles
Number of cycles per landing ($L/\pi D$)	= 2470 cycles
Assumed tire life	= 300 landings
Total number of cycles	= 741,000 cycles
Deflection of tire	= 3.7 in.
Effective length of coupon	= 5.5 in.
Required deflection amplitude	= 0.42 in.
Amplitude achieved (machine limitations)[1]	= 0.31 in.(at 5 Hz)
	= 0.14 in.(at 10 Hz)

[1] Refer to valve characteristics in Appendix A. Amplitude drops off rapidly with increasing frequency. The existing valving and hydraulic pump on the testing machine are insufficient to produce the large deflections desired at 5 and 10 Hz.

Ground speed	Frequency	Time for flex fatigue test
220 mph	25.2 Hz	8 hrs 10 min
150 mph	17.2 Hz	11 hrs 57 min
100 mph	11.4 Hz	18 hrs 3 min
88 mph	10.0 Hz*	20 hrs 35 min
44 mph	5.0 Hz*	41 hrs 10 min
25 mph	2.9 Hz	70 hrs 59 min

* Frequencies actually used. Higher frequencies were not used because of severe drop off in amplitude. Lower frequencies were not used because of excessive test duration.

Chapter 5

RESULTS AND ANALYSIS

This chapter presents the results of the experiments described in Chapter 4. First, the constitutive properties are reported. The procedure for obtaining mean peel strength and standard deviation from raw load-displacement data is outlined. The results of the baseline peel tests are presented. Analysis of the baseline data is discussed. This analysis was the basis for choosing the +/- 90° test for the conditioned coupons. Finally, peel strength results for conditioned coupons, and the associated data analysis are presented.

5.1 Constitutive Properties

The results and analysis for all the constitutive properties are given below. These have been obtained using the procedures mentioned in the previous chapter.

5.1.1 Specific Gravity

The specific gravity of rubber tread and carcass is given in Table 2. From the results, it is seen that the tread (1.115) has higher specific gravity than the carcass (1.074).

5.1.2 Cord Spacing

The cord spacing is the average distance between two neighboring cords in the same ply. The results are given in Table 3. The cord spacing for casing plies, breaker plies and tread reinforcing plies varies from 0.036" to 0.040", 0.034"

Specimen number	Wt. of tread in air(gms)	Wt. of tread in water(gms)	Specific gravity
1	10.043	0.989	1.109
2	10.295	1.076	1.117
3	10.974	1.155	1.118

Average specific gravity of tread rubber = 1.1145

Specimen number	Wt. of carcass in air(gms)	Wt. of carcass in water(gms)	Specific gravity
4	10.287	0.892	1.095
5	10.982	0.930	1.093
6	12.348	0.422	1.035

Average specific gravity of carcass (nylon + rubber) = 1.0743

Table 3 Cord spacing

Ply type	Ply #	Cord spacing (in)		Average cord spacing (in)
		Minimum Observed	Maximum Observed	
Casing ply	1	0.033	0.043	0.039
	2	0.035	0.043	0.040
	3	0.035	0.046	0.039
	4	0.034	0.041	0.038
	5	0.034	0.042	0.038
	6	0.033	0.043	0.039
	7	0.033	0.041	0.038
	8	0.036	0.042	0.039
	9	0.031	0.045	0.038
	10	0.033	0.042	0.038
	11	0.032	0.041	0.038
	12	0.031	0.047	0.036
Breaker ply	13	0.031	0.039	0.035
	14	0.030	0.038	0.034
Tread reinf. Ply	15	0.031	0.039	0.035
	16	0.031	0.040	0.036
	17	0.031	0.043	0.036

Data obtained from 9 coupons (from 3 tires), 3 readings per ply level, 17 ply levels.

to 0.035", and 0.035" to 0.036" respectively. No particular trend is observed.

5.1.3 Cord Angle

The cord angle is measured with respect to the longitudinal edge of the specimen. The results are given in Table 4. The cord angle for longitudinal plies increases from 0° to about 18° and for transverse plies, decreases from about 88° to 71° in going from the pressure side to the ground side of tire. The maximum deviation was seen in the reinforcing and breaker plies.

5.1.4 Cord Diameter

The cord diameter results are given in Table 5. The cord diameter of casing plies, breaker plies and tread reinforcing plies varies from 0.023" to 0.026", 0.022" and 0.021" to 0.023" respectively. No trend is observed.

5.1.5 Ply Spacing

The ply spacing is the distance between neighboring plies. The results are given in Table 6. From the results it is seen that the distance between pressure side surface and first ply is 0.101". Ply spacing for 1-2, 2-3, 3-4, 4-5, 5-6, 6-7, 7-8, 8-9, 9-10, 10-11, 11-12, 12-13, 13-14 plies varies from 0.031" to 0.052". The spacing between the last breaker ply (#14) to the first tread reinforcing ply (#15) is 0.133". Ply spacing for 15-16 and 16-17 is 0.051". The ply spacing between last tread reinforcing ply (17th) and the eage (ground side) is 0.815".

Table 4 Cord angle

Ply type	Ply #	Cord angle (°)		Avg. cord angle (°)
		Minimum Observed	Maximum Observed	
Trans-verse ply	1	84.5	88.0	87.7
	3	84.5	87.0	85.5
	5	84.5	88.0	86.1
	7	84.5	88.0	85.8
	9	82.5	88.0	84.8
	11	84.5	88.0	85.8
	13	66.0	81.0	70.9
	15	66.5	74.5	71.2
	17	65.5	76.0	70.6
Longi-tudinal ply	2	0.0	1.0	0.6
	4	0.0	4.5	1.6
	6	0.5	4.0	1.7
	8	0.0	4.0	2.0
	10	0.5	4.5	3.0
	12	2.5	8.5	5.8
	14	14.5	20.0	17.8
	16	14.5	19.5	16.3

Cord angle is measured with reference to the longitudinal edge of the coupon. 27 readings per ply level.

Table 5 Cord diameter

Ply type	Ply	Cord diameter (in)		Average cord diameter (in)
		Minimum Observed	Maximum Observed	
Casing ply	1	0.026	0.027	0.026
	2	0.025	0.026	0.026
	3	0.025	0.027	0.026
	4	0.025	0.027	0.026
	5	0.025	0.027	0.025
	6	0.026	0.027	0.026
	7	0.025	0.027	0.026
	8	0.025	0.027	0.026
	9	0.025	0.027	0.026
	10	0.025	0.026	0.025
	11	0.022	0.023	0.023
	12	0.022	0.026	0.023
Breaker ply	13	0.021	0.024	0.022
	14	0.021	0.026	0.022
Tread reinf. Ply	15	0.021	0.025	0.023
	16	0.020	0.025	0.021
	17	0.021	0.026	0.022

Data obtained from 3 coupons, 3 readings per ply level, 17 ply levels.

Table 6 Damping coefficient and shear modulus

Material	Sample #	Damping coeff.	Shear storage modulus psi (MPa)	Shear loss modulus psi (MPa)
Carcass	1	0.22	1940.7 (13.35)	2003.3 (13.78)
	2	0.24	1533.7 (10.55)	1606.4 (11.05)
Tread	1	0.26	770.5 (5.30)	726.9 (5.00)
	2	0.24	799.6 (5.50)	690.5 (4.75)

Values are for room temperature (25°C)

5.1.6 Damping Coefficient and Shear Modulus

The results of damping coefficient and shear modulus at room temperature are given in Table 7. Typical DMA output for damping and shear (from 20 to 130°C temperature range) are seen in Fig. 35 to 36.

Damping coefficient is the resistance of material (tirsurface) to displacement (radial) due to material visco-elasticity. Damping coefficient (at 25°C) of tread is 0.25 and that of the carcass is 0.23.

Shear modulus (shear storage modulus) is the measure of energy stored and recovered per cycle when different systems are compared at the same strain amplitude. Shear modulus (at 25°C) for tread varies from 771 - 800 psi (5.3 - 5.5 MPa) and that for carcass varies from 1534 - 1941 psi (10.6 - 13.4 Mpa).

Shear loss modulus is a measure of energy dissipated or lost as heat per cycle of sinusoidal deformation when different systems are compared at the same strain amplitude. Shear loss modulus (at 25°C) for the tread varies from 691 - 727 psi (4.8 - 5.0 MPa) and that for carcass varies from 1606.4 - 2003 psi (11.1 - 13.78 MPa).

5.1.7 Tensile modulus

Tensile modulus for tread and carcass are specified in Table 8. The elastic modulus of the tread rubber is 1744 psi (12 MPa) and that of the carcass is 29164 psi (201 MPa). The elastic modulus of carcass material is approximately seventeen times that of tread material.

Table 7 Ply spacing

Ply type	Ply spacing (in)		Average ply spacing (in)
	Low	High	
Edge-1	0.090	0.109	0.101
1-2	0.026	0.039	0.031
2-3	0.029	0.040	0.035
3-4	0.031	0.042	0.036
4-5	0.033	0.047	0.037
5-6	0.028	0.045	0.036
6-7	0.029	0.046	0.038
7-8	0.028	0.041	0.035
8-9	0.029	0.043	0.036
9-10	0.030	0.040	0.036
10-11	0.027	0.045	0.038
11-12	0.032	0.048	0.037
12-13	0.026	0.050	0.042
13-14	0.047	0.062	0.052
14-15	0.122	0.147	0.133
15-16	0.040	0.061	0.051
16-17	0.036	0.061	0.051
17-edge	0.810	0.858	0.815

Data obtained from 9 coupons (from 3 tires),
3 readings per ply level, 17 ply levels.

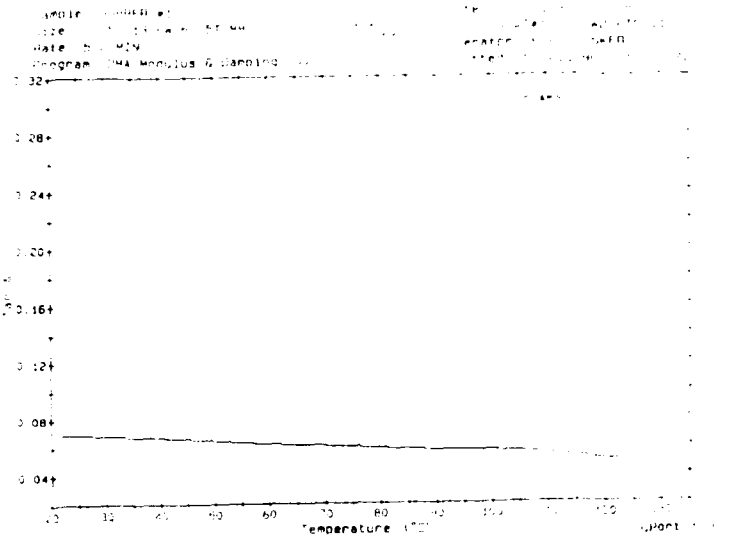

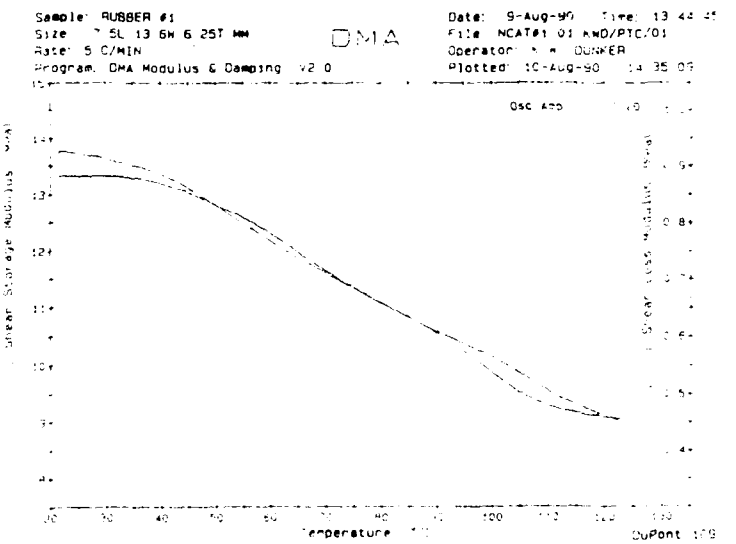

Fig. 35 DMA plots for carcass material

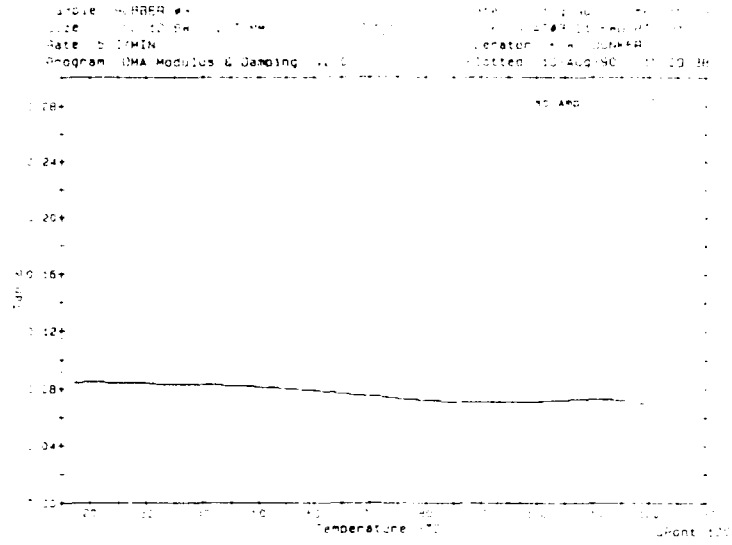

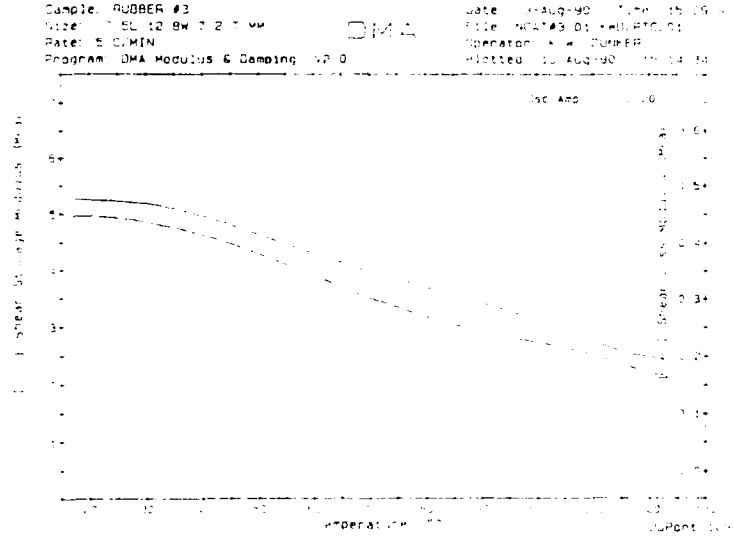

Fig. 36 DMA plots for tread rubber

Table 8 Tensile modulus

Elastic modulus for the tread:

Test no.	Elastic modulus psi (MPa)	Poisson's ratio (μ)
1	1605 (11.1)	0.348
2	1874 (12.9)	0.340
3	1753 (12.1)	0.361

Average elastic modulus = 1744 psi = 12 MPa
Poisson's ratio (μ) = 0.35

Elastic Modulus for the carcass:

Test no.	Elastic modulus psi (MPa)	Poisson's ratio (μ)
1	30987 (213.4)	0.706
2	28230 (194.4)	0.671
3	28274 (194.7)	0.550

Average elastic modulus = 29164 psi = 201 MPa
Poisson's ratio (μ) = 0.631

5.1.8 Thermal Properties

The thermal properties of rubber and tread material are given in Table 9. Thermal conductivity of tread is 1.088 kcal.m/m^2.hr.°C and for carcass is 1.002 kcal.m/m^2.hr.°C.

Specific heat of tread is 0.43 cal/gr.°C and for carcass is 0.48 cal/gr.°C.

5.2 Baseline Test Results

Baseline data analysis is the most important part of this work. A uniform rate of peeling (2"/min) was selected for all tests. The test was performed in stroke control mode and data was sampled at a sampling rate of 3 Hz. The data for load and displacement was acquired and stored in an ASCII file. The load increases to a level corresponding to the peel strength and fluctuates about this level as the fracture propagates. The mean and standard deviation of the fracture load data between points B and C (shown in Fig. 37) was calculated using a PC-based spreadsheet program. Using this procedure, the mean peel strength values were obtained for various configurations of peel test. The results are given in Table 10 to 12. These results are summarized in Table 13. Two different criteria were used to identify the optimal test configuration: minimal standard deviation of data and minimal range. The raw data (Table 13) shows a difference in peel strength values between the three test configurations, as would be expected from the differences in test geometry. The average peel strength was found for each test configuration and used to normalize the raw standard deviation and range data (Table 14). The normalized standard deviation and range for the three tests are seen in Table 15.

Table 9 Thermal conductivity and specific heat

Thermal conductivity:

Specimen	Hot temp (°C)	Cold temp (°C)	Thickness mm	Conductivity kcal.m/m^2.hr°C
Tread	37.7	16.6	17.0	1.088
Carcass	37.7	17.6	9.9	1.002

(Conversion 1 kcal. m/$m.^2$hr. °C = 8.063 BTU. in/$ft.^2$hr. °F)

Specific heat:

Sample	Specific heat cal/gr. °C
Tread	0.43
Carcass	0.48

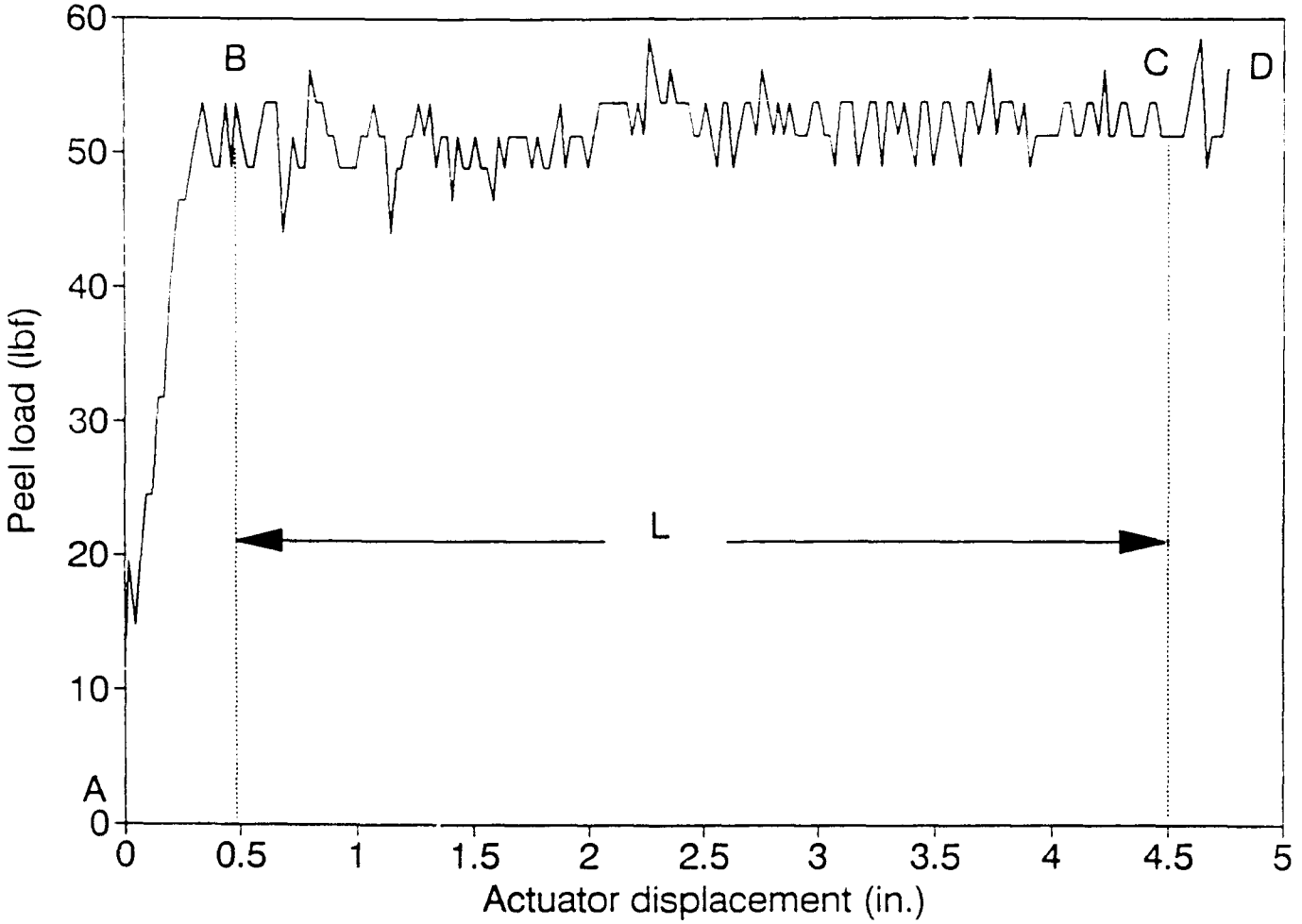

Fig. 37 Typical peel test load-displacement data

Table 10 Baseline peel data (180° peeling)

Tire #	Sector	Ply 3-4	Ply 7-8	Ply 11-12	Ply 15-16
3	A	42.7	40.0	50.7,43.6,43.0	70.3,73.5,74.3, 52.1,49.1,48.9
3	B	43.6,41.3,46.1, 46.0,40.2	47.4,52.5,52.2, 45.1	44.0,44.9,50.0, 48.1	65.2,56.8,51.0, 47.5, 51.5
3	C	47.8,52.5,59.2, 50.3,51.1	47.5,51.3,48.7, 49.5,43.0	53.0,50.6,50.7	85.6,75.4,58.2, 52.6
3	D	44.0,47.0,48.1, 49.8,47.6	50.9,46.1	48.7,47.4,43.2, 45.3,46.1	75.1,66.2,61.0, 59.0,54.5,55.2
3	E	49.6,48.1,47.6, 40.7	58.4,52.0,40.3	42.1,41.6,40.0, 42.4,48.4,49.3	63.6,53.0,53.5, 52.5,56.4
4	A	46.2,45.0,41.0, 39.0	55.2,54.9,48.0, 53.0,49.8	42.1,38.0,43.9, 34.0	65.2,55.6,47.4, 44.0
4	B	76.3,71.9,66.7	70.7,81.1,67.1,	49.2,57.7,44.0,	54.5,46.8,43.7
4	C	48.8,46.9,51.8	54.0,50.2,44.4	41.6,38.0,39.3	51.1,49.4,51.0
4	D	37.9,39,7,40.5	45.9,43.0,42.7	41.8,39.1,38.6	63.4,56.0,47.5
4	E	70.7,60.0,54.2	38.5,42.4,41.8	47.0,52.0,42.5	50.1,50.7,47.4
5	A	50.2,46.7,54.2	41.8,47.1,51.1	32.6,42.3,46.2	67.3,59.1,49.0
5	B	38.8,38.9,40.3	47.3,50.6,49.3	44.1,40.2,38.5	69.0,60.2,50.5
5	C	36.6,37.8,39.1	42.7,42.3,50.1	37.0,38.5,44.0	55.6,52.7,53.0
5	D	50.3,44.0,40.1	43.9,42.5,43.1	41.8,35.1,36.6	49.5,46.2,46.4
5	E	50.7,51.6,48.4	44.8,52.4,46.7	38.7,34.9,37.3	52.4,49.0,44.7

Table 11 Baseline peel data (90° peeling)

Tire #	Sector	Ply 3-4	Ply 7-8	Ply 11-12	Ply 15-16
3	A	96.0,101.1,61.2	67.0,75.0	54.2,63.5,73.6	84.7,76.4
3	B	77.9,78.2,69.4	63.8,53.4,53.2	64.8,90.3,85.8	138.5,86.5,89.8
3	C	58.2,55.1,68.1	87.6,71.1,76.6	78.8,82.2,97.6	84.6,87.3,88.3
3	D	74.7,78.8,77.4	84.3,80.9,66.4	66.8,63.6,87.1	88.5,79.7
3	E	59.5,62.9,65.4	69.5,89.4,59.1	62.0,63.4,93.0	111.4,89.5,92.9,
4	A	78.4,68.6,69.8	77.7,86.4,69.5	63.7,85.3,98.7	123.8,76.7, 78.0
4	B	61.5,63.2,71.2	67.3,69.5,67.2	60.1,71.6,69.7	111.2,75.9,69.9
4	C	61.3,64.1,64.0	64.0,70.3,74.3	73.8,70.1,67.2	114.4,82.395.8
4	D	64.0,65.0,67.1	71.1,75.7,67.5	79.0,80.4,75.7	101.1,77.7,85.7
4	E	54.0,54.7,55.9	64.0,71.9,70.8	50.7,90.6,90.5	93.0,96.4,95.5
5	A	94.0,89.0,67.9	67.6,77.1,65.9	57.2,94.7,72.4	93.3,91.6,86.0
5	B	57.1,57.8,60.5	66.8,67.0,73.1	60.2,61.2,75.1	112.7,92.9,94.5
5	C	54.6,48.5,83.2	67.8,70.6,79.1	59.8,69.5,68.7	104.6,85.4,88.8
5	D	85.6,99.0,78.5	70.0,67.9,65.6	64.2,66.8,75.0	92.3,90.8,84.3
5	E	63.2,60.0,60.4	67.8,67.9,65.6	64.2,66.8,75.0	92.3,90.8,84.3

Table 12 Baseline peel (+/-90° peeling)

TIRE #	SECTR	PLY 3-4	PLY 7-8	PLY 11-12
3	A	48.4,48.8,52.4	53.6,52.1,48.4	54.2,49.1,48.1
3	B	51.4,52.4,51.7	48.9,44.5,47.7	50.6,49.4,53.1
3	C	56.0,55.4,54.0	49.8,46.5,48.3	49.8,50.1,52.5
3	D	46.0,51.6,52.7	46.7,45.2,46.7	50.3,51.6,50.5
3	E	50.9,49.2,50.0	52.1,49,0,50.4	49.3,53.5,46.8
4	A	53.6,51.1,47.5	49.4,49.2,48.2	51.6,49.5,45.0
4	B	53.9,49.6,46.4	49.17,47.7,47.8	46.0,45.4,47.6
4	C	48.7,53.1,56.2	50.2,49.4,50.7	47.4,51.5,50.7
4	D	50.0,50.5,47.6	49.1,51.1,50.3	54.8,47.3,49.4
4	F	58.9,56.7,52.6	48.8,47.9,46.0	51.0,50.7,49.4
5	A	49.9,48.8,47.6	51.4,47.0,48.7	52.0,52.6,58.2
5	B	49.8,51.1,46.4	50.0,47.8,46.1	54.1,54.1,56.3
5	C	46.8,43.5,46.3	46.7,47.8,47.3	48.2,44.6,50.5
5	D	48.0,48.1,46.9	51.1,45.1,46.8	49.1,48.4,46.8
5	E	40.3,42.0,39.3	43.5,42.5,42.1	43.9,41.9,41.5

Table 13 Data analysis for baseline peel data

Tire number	Ply level	Peel strength* (lbf/in)		
		180° peel test	+/-90° peel test	90° peel test
3	3,4	47.2	51.4	70.2
3	7,8	47.6	48.7	71.2
3	11,12	46.3	50.6	75.1
4	3,4	43.7	51.8	64.2
4	7,8	47.4	49.0	71.1
4	11,12	42.1	49.2	75.1
5	3,4	43.8	46.3	71.3
5	7,8	46.4	46.9	71.0
5	11,12	39.2	49.5	75.2

*Each based on 15 data points

Peel test orientation	Average peel strength
180°	= 45.0 lbf/in
+/-90°	= 49.3 lbf/in
90°	= 71.6 lbf/in

Table 14 Standarad deviation of peel strength values

Standard deviation of peel strength values

Tire number	Ply level	Standard deviation* (lbf/in)		
		180° peel test	+/-90° peel test	90° peel test
3	3,4	4.51	2.77	10.7
3	7,8	4.42	2.65	11.8
3	11,12	3.65	2.12	13.7
4	3,4	4.81	3.60	4.48
4	7,8	2.22	1.39	5.57
4	11,12	4.67	2.63	13.1
5	3,4	5.47	2.35	15.5
5	7,8	3.78	1.99	5.71
5	11,12	3.78	2.95	12.2

Normalized standard deviation of peel strength values

Tire number	Ply level	Standard deviation* (%)		
		180° peel test	+/-90° peel test	90° peel test
3	3,4	10.0	5.6	14.9
3	7,8	9.8	5.4	16.5
3	11,12	8.1	4.3	19.2
4	3,4	10.7	7.3	6.3
4	7,8	4.9	2.8	7.8
4	11,12	10.4	5.3	18.3
5	3,4	12.6	4.8	21.6
5	7,8	8.4	4.0	8.0
5	11,12	8.4	6.0	17.0

*Each based on 15 data points

Table 15 Range of peel strength values

Range of peel strength values

Tire number	Ply level	Range* (lbf/in)		
		180° peel test	+/-90° peel test	90° peel test
3	3,4	19.0	10.0	40.9
3	7,8	12.5	9.10	36.2
3	11,12	13.0	7.4	43.4
4	3,4	13.9	12.5	24.4
4	7,8	16.7	5.1	22.4
4	11,12	18.0	9.8	18.0
5	3,4	15.0	11.8	44.4
5	7,8	10.6	9.3	18.9
5	11,12	13.6	16.7	39.9

Normalized range of peel strength values

Tire number	Ply level	Range* (%)		
		180° peel test	+/-90° peel test	90° peel test
3	3,4	42.2	20.3	57.1
3	7,8	27.8	18.5	50.6
3	11,12	28.9	15.0	60.6
4	3,4	30.9	25.4	34.1
4	7,8	37.1	10.3	31.3
4	11,12	40.0	19.9	67.0
5	3,4	33.3	23.9	62.0
5	7,8	23.6	18.9	26.4
5	11,12	30.2	33.9	55.7

*Each based on 15 data points

The +/-90° test is found to be best from the standpoint of both criteria.

Statistical Model (Analysis Of Variance, ANOVA) for +/- 90° Peel:

Analysis of variance models are versatile statistical tools used in experimental studies to find the effect of different independent variables (ply levels, sectors and tires in this case) on dependent variables (peel strength in this case). Tests of significance allow us to draw conclusions about the significance of each factor.

In this work, statistical analysis of the results for +/- 90° peel test was performed using the SAS (Statistical Analysis Software) package on a VAX/VMS computer to find the effect of ply levels, sectors and tires on the dependent variable peel strength. The procedure and results are listed below:

The model has as its three factors tires [tire #3 (i=1), tire #4 (i=2), tire #5 (i=3)], sectors [A (j=1), B (j=2), C (j=3), D (j=4), E (j=5)], and plies [3-4 (k=1), 7-8 (k=2), 11-12 (k=3)].

Here each data point is the average of three values. By inputting this data to the SAS Program, the ANOVA output shown on next page is obtained.

ANOVA INPUT:

```
DATA ONE;
INPUT TIRES SECTORS PLIES STRENGTH;
CARDS;
```

Table 16 SAS input for +/-90° baseline peel test

Tires	Sectors				
	j = 1 (A)	j = 2 (B)	j = 3 (C)	j = 4 (D)	j = 5 (E)
	Ply level k=1 k=2 k=3 (3-4)(7-8)(11-12)	Ply level k=1 k=2 k=3 (3-4)(7-8)(11-12)	Ply level k=1 k=2 k=3 (3-4)(7-8)(11-12)	Ply level k=1 k=2 k=3 (3-4)(7-8)(11-12)	Ply level k=1 k=2 k=3 (3-4)(7-8)(11-12)
3	49.9 51.4 50.5	51.8 47.0 51.0	55.1 48.2 50.8	50.1 46.2 50.5	50.0 50.5 49.9
4	50.7 48.9 48.7	50.0 48.4 46.3	52.7 50.1 49.9	49.4 50.2 50.5	56.1 47.6 50.4
5	48.7 49.0 54.3	49.1 48.0 54.8	45.5 47.3 47.8	47.7 47.7 48.1	40.5 42.7 42.4

(Tire #3 (i=1), tire #4 (i=2), tire #5 (i=3))

Table 17 SAS output for +/-90° baseline peel test

SAS 22:37 TUESDAY, OCTOBER 2, 1990

GENERAL LINEAR MODELS PROCEDURE

CLASS LEVEL INFORMATION

CLASS	LEVELS	VALUES
TIRES	3	1 2 3
SECTORS	5	1 2 3 4 5
PLIES	3	1 2 3

NUMBER OF OBSERVATIONS IN DATA SET = 45

GENERAL LINEAR MODELS PROCEDURE

DEPENDENT VARIABLE: STRENGTH

SOURCE	DF	SUM OF SQUARES	MEAN SQUARE	F VALUE	PR > F	R-SQUARE	C.V.
MODEL	28	334.12577778	11.93306349	2.78	0.0178	0.829401	4.2079
ERROR	16	68.72622222	4.29538889		ROOT MSE		STRENGTH MEAN
CORRECTED TOTAL	44	402.85200000			2.07253200		49.25333333

SOURCE	DF	TYPE I SS	F VALUE	PR > F	DF	TYPE III SS	F VALUE	PR>F
TIRES	2	63.80400000	7.43	0.0052	2	63.80400000	7.43	0.0052
SECTORS	4	31.83422222	1.85	0.1681	4	31.83422222	1.85	0.1681
PLIES	2	24.40133333	2.84	0.0880	2	24.40133333	2.84	0.0880
SECTORS*PLIES	8	14.49644444	0.42	0.8911	8	14.49644444	0.42	0.8911
TIRES*SECTORS	8	152.32711111	4.43	0.0055	8	152.32711111	4.43	0.0055
TIRES*PLIES	4	47.26266667	2.75	0.0647	4	47.26266667	2.75	0.0647

The important terms used in this model are described below:

SOURCE	=	Sources of variation
MODEL	=	All the treatments (sectors, plies and tires)
ERROR	=	Error within all above treatments
CONNECTED TOTAL	=	Sum of all the treatments and errors
SUM OF SQUARES	=	Sum of squares (SS) for model and the sum of squares for errors within treatments
F VALUE	=	Value of F statistic
DF	=	Degrees of freedom
PR > F	=	Probability of getting observed F (level of significance α)
C.V.	=	Coefficient of variation
R-SQUARE	=	Coefficient of multiple determination

The level of significance α is the probability of making a Type I error in the test of hypothesis ie rejecting null hypothesis when it is true. The coefficient of variation is a measure of relative dispersion for a data set.

C.V. = (Standard deviation/Mean)*100

The coefficient of multiple determination measures how much variation in the dependent variable (peel strength) can be accounted for by the model.

R-SQUARE = SS(model)/SS(corrected total)

The level of significance (α) for the whole model is α = 0.018, and [(1-0.018)*100] = 98.2% is the confidence level for the whole model. In the same way, the levels of significance for tires, sectors, plies, sectors * plies, tires * sectors, tires * plies are 0.005, 0.168, 0.088, 0.891, 0.006, 0.065 respectively. Hence at the 95% confidence level only tires and tires*sector interaction are seen to have a significant influence on peel strength.

The coefficient of multiple determination (R-SQUARE) for the whole model is 0.83. It is obtained using the formula

R-Square = SS (treatment)/SS (corrected total)

The variance 83% in the peel strength is due to parameters such as sectors, plies, tires, and their interactions.

Individually, the variances in peel strength values due to tires, sectors, plies, sectors * plies, tires * sectors, tires * plies are 16%, 8%, 6%, 4%, 4% and 12% respectively. So, there is a variance of 17% in the data due to error and uncontrolled variables.

5.3 Conditioned Coupon Peel Tests

The results for conditioned coupons were compared with the +/- 90° room temperature peel test results given in Table 18. For each test a quantity called the "% Peel strength retained" is computed. This is defined as follows;

% Peel strength retained = (Peel strength of conditioned coupon/peel strength of virgin coupon) * 100

Table 18 Room temperature peel test data for tire #6

+/-90° peel test data (tire #6)

Coupon number	Peel strength values for ply levels (lbf/in)		
	3-4	7-8	11-12
1	48.1,47.2,46.4	49.4,48.7,49.0	48.5,49.0,46.4
2	48.6,49.0,49.3	47.8,47.1,49.1	49.0,48.5,48.6
3	48.3,48.7,50.2	50.1,47.8,48.2	48.6,48.7,52.2
Average	48.4	48.6	48.8

The results are described below:

5.3.1 Thermally Aged Coupons

Thermal aging durations varied between 21 hours and 200 hours. The temperature ranged between room temperature (77°F) and 250°F. The results are shown in Tables 19 to 21.

Fig. 38 show the variation in peel strength retained in three different ply levels (3-4, 7-8, and 11-12) with various times and temperatures. At 250°F, peel strength degradation (100% - % peel strength retention) of 23% was obtained after 21 hours, 60% after 100 hours and 70% after 200 hours. Most of the peel strength degradation seems to take place in the initial portions of the test.

5.3.2 Flex Fatigue Aged Coupons

Flex fatigue conditioning was done at two frequencies (5 Hz and 10 Hz) at room temperature for 741,000 cycles. It was done at 10 Hz for elevated temperatures ranging between 150 and 250°F. The results are shown in Table 22. Fig. 39 shows the variation in peel strength retention for three different ply levels (3-4, 7-8 and 11-12) as a function of temperature. At 150°F about 13%, at 200°F about 16% and at 250°F, about 24% peel strength degradation (100 % - % peel strength retention) was obtained. For each frequency, the maximum amplitude achievable was employed. The results indicate that even the maximum amplitudes did not have a large effect on peel strength at room temperature. Therefore it was decided not to try lower amplitude levels. Also, only the normal inflation pressure (170 psi) was simulated. Hence data is not currently available on the effect of

Table 19 Thermally aged (21 hrs) coupons peel test data

Temperature (°F)	Ply level	Peel* strength (lbf/in)	% Peel strength retained
150	3,4	43.9	90.7
150	7,8	45.1	92.8
150	11,12	46.5	95.3
200	3,4	44.8	92.6
200	7,8	40.7	83.7
200	11,12	47.8	98.0
225	3,4	38.6	79.8
225	7,8	39.4	81.1
225	11,12	43.7	89.5
250	3,4	35.3	73.0
250	7,8	37.6	77.4
250	11,12	38.9	79.7

*Each value is average of 3 tests.

Table 20 Thermally aged (100 hrs) coupons peel test data

Temp. (°F)	Ply level	Peel strength*			Mean peel strength (lbf/in)	% peel strength retained
		Coupon number 1	2	3		
150	3,4	45.7	46.3	46.2	46.1	95.2
150	7,8	46.6	45.3	46.2	46.0	94.7
150	11,12	45.8	49.4	49.0	48.1	98.6
200	3,4	41.7	43.0	41.2	42.0	86.8
200	7,8	43.8	40.9	38.8	41.2	84.8
200	11,12	46.1	45.2	45.2	45.5	93.2
225	3,4	34.1	38.7	36.3	36.4	75.2
225	7,8	39.3	40.7	37.5	39.2	80.7
225	11,12	35.7	41.4	35.6	37.6	77.0
250	3,4	15.0	19.1	14.7	16.3	33.7
250	7,8	21.3	23.6	15.7	20.2	41.6
250	11,12	15.8	18.9	21.3	18.7	38.3

*Each value is average of 3 tests.

Table 21 Thermally aged (200 hrs) coupons peel test data

Temp. (°F)	Ply level	Peel strength*			Mean peel strength (lbf/in)	% peel strength retained
		Coupon number 1	2	3		
150	3,4	44.0	39.1	45.6	42.9	88.6
150	7,8	45.2	41.0	46.1	44.1	90.7
150	11,12	43.7	41.9	45.9	48.1	89.7
200	3,4	36.1	36.6	30.5	34.4	71.1
200	7,8	34.4	40.3	31.0	35.2	72.4
200	11,12	40.7	39.8	34.6	38.4	78.7
225	3,4	30.8	16.0	23.2	23.3	48.1
225	7,8	29.9	24.4	27.4	27.2	55.9
225	11,12	30.2	22.2	29.0	27.1	55.5
250	3,4	13.3	15.2	12.5	13.7	28.3
250	7,8	17.7	15.9	13.9	15.8	32.5
250	11,12	17.4	13.2	12.7	14.3	29.3

*Each value is average of 3 tests.

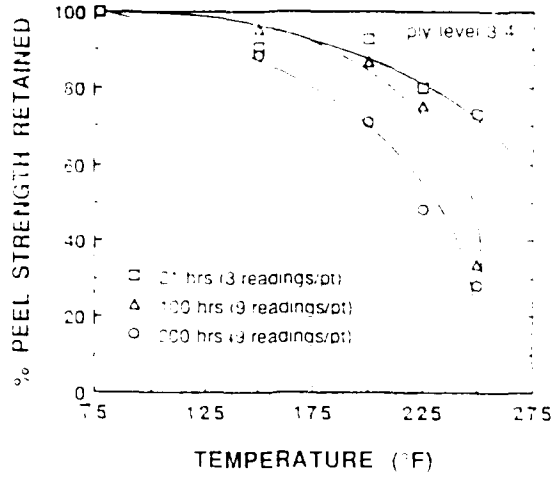

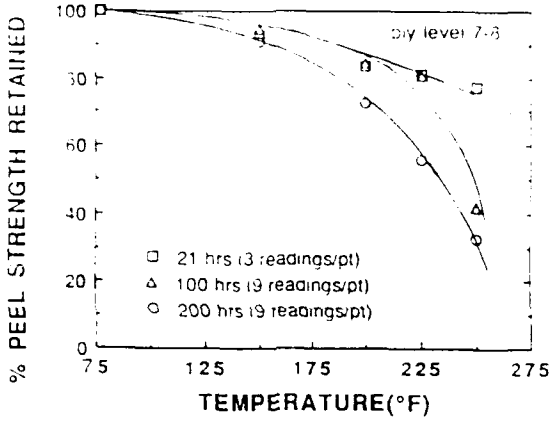

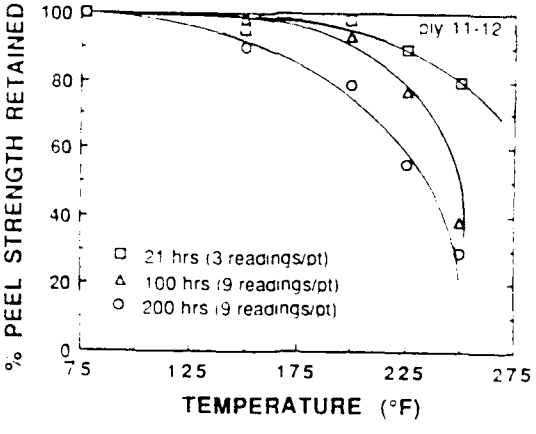

Fig. 38 Effect of thermal aging on peel strength

Table 22 Flex fatigue coupons peel test data

Room temperature flex fatigue

Freq. (Hz)	Ply level	Peel strength* Coupon number 1	2	3	Mean peel strength (lbf/in)	% peel strength retained
5	3,4	42.4	44.6	45.2	44.1	91.1
5	7,8	42.0	44.9	46.4	44.4	91.4
5	11,12	48.3	48.1	48.2	48.2	98.8
10	3,4	42.7	41.0	39.0	40.9	84.5
10	7,8	46.5	41.8	43.8	44.0	90.5
10	11,12	45.6	46.5	40.9	44.3	90.7

Elevated temperature flex fatigue at 10 Hz

Temp. (°F)	Ply level	Peel strength* Coupon number 1	2	3	Mean peel strength (lbf/in)	% peel strength retained
150	3,4	39.5	39.6	43.6	40.9	84.5
150	7,8	41.7	40.5	44.8	42.3	87.0
150	11,12	45.1	41.5	46.4	44.3	90.8
200	3,4	41.3	35.5	38.7	38.5	79.5
200	7,8	42.1	41.7	40.0	41.3	84.9
200	11,12	42.9	44.4	40.4	42.6	87.3
250	3,4	34.7	40.7	28.4	34.6	71.5
250	7,8	38.5	40.9	33.7	37.7	77.6
250	11,12	43.1	40.9	33.3	39.1	80.1

*Each value is average of 3 tests.

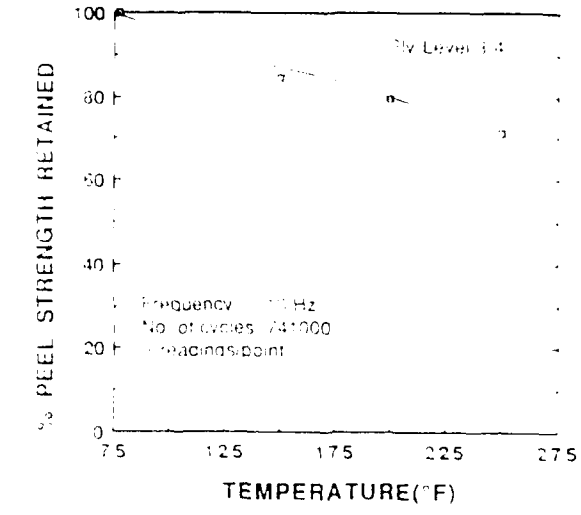

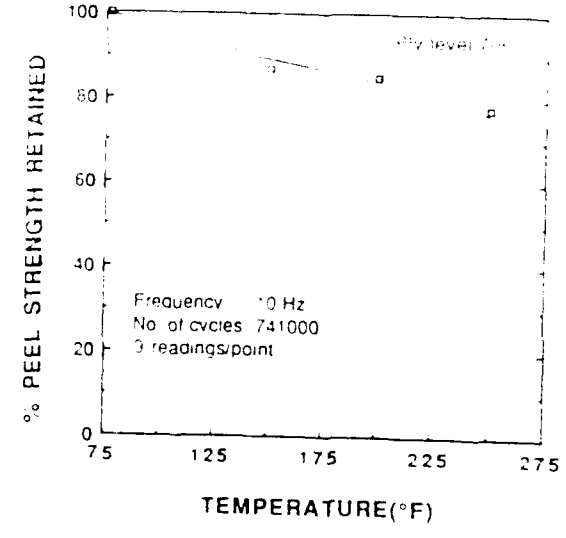

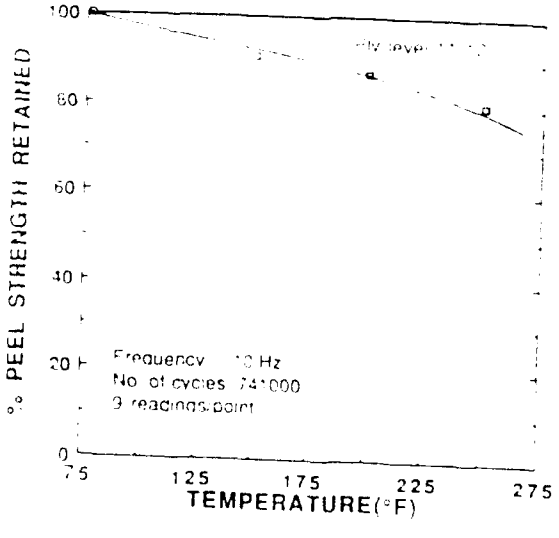

Fig. 39 Elevated temperature flex fatigue effect

amplitude and mean load on peel strength.

Fig. 40 shows peel strength retention in different ply levels (3-4, 7-8 and 11-12) as a function of frequency. This test shows that the peel strength degraded 6% at 5 Hz and 11% at 10 Hz.

5.3.3 Comparison of Thermal Aging and Flex Fatigue Tests

The tests show the difference between thermally aged and flex fatigued coupons. Fig. 41 compares the degradation of peel strength induced by thermal aging and by flex fatigue. It is seen that conditioning by thermal aging and by flex fatigue with heating have approximately the same effect on peel strength.

Earlier work on the thermal aging test of aircraft tire coupons done by Clark[3] used samples taken from tires that had been rejected for cuts or foreign object damage. The tests were performed only between third and fourth ply levels using the +/-90° peeling method. No tensile load was applied during these experiments to simulate inflation pressure. The comparison of these results with our data is shown in Fig. 42. From the plot, it can be seen that two results are comparable.

Analysis of variance is used to find the effect of flex fatigue and thermal aging temperature. The model is set up with i=1 for no flex (purely thermal aging) and i=2 for flex fatigue and thermal aging. The other factor j, the thermal aging temperature has four levels (room temp., 150°F, 200°F, 250°F).

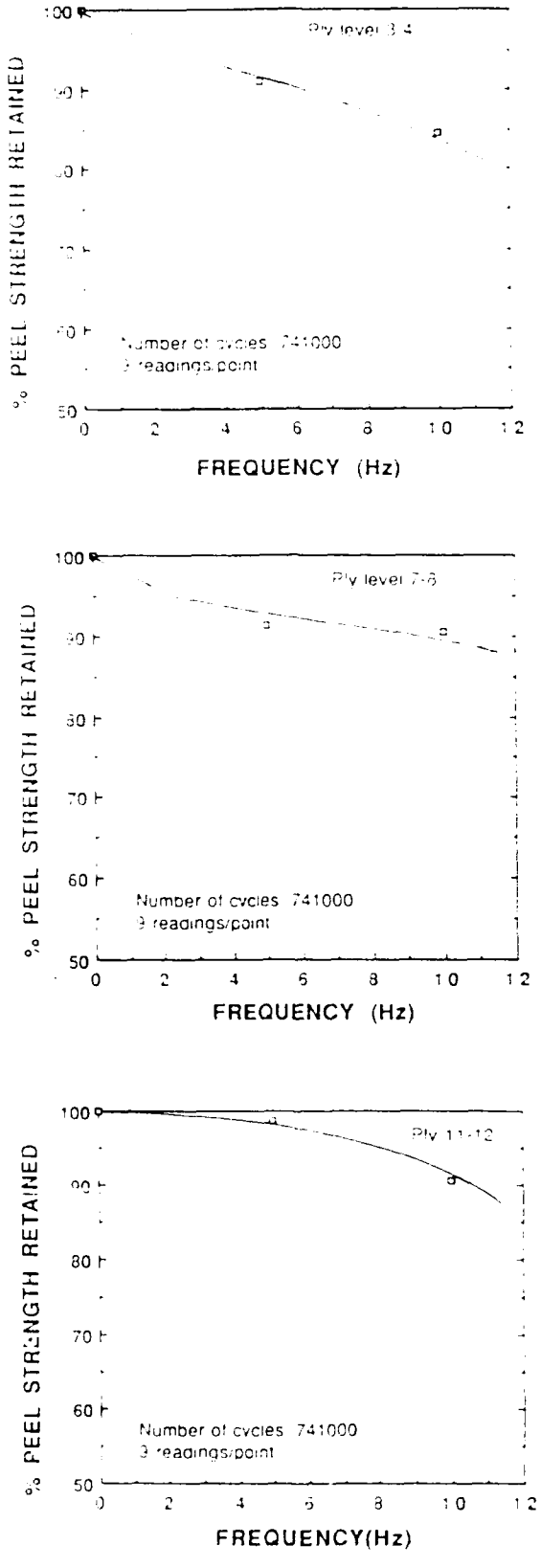

Fig. 40 Room temperature flex fatigue effect

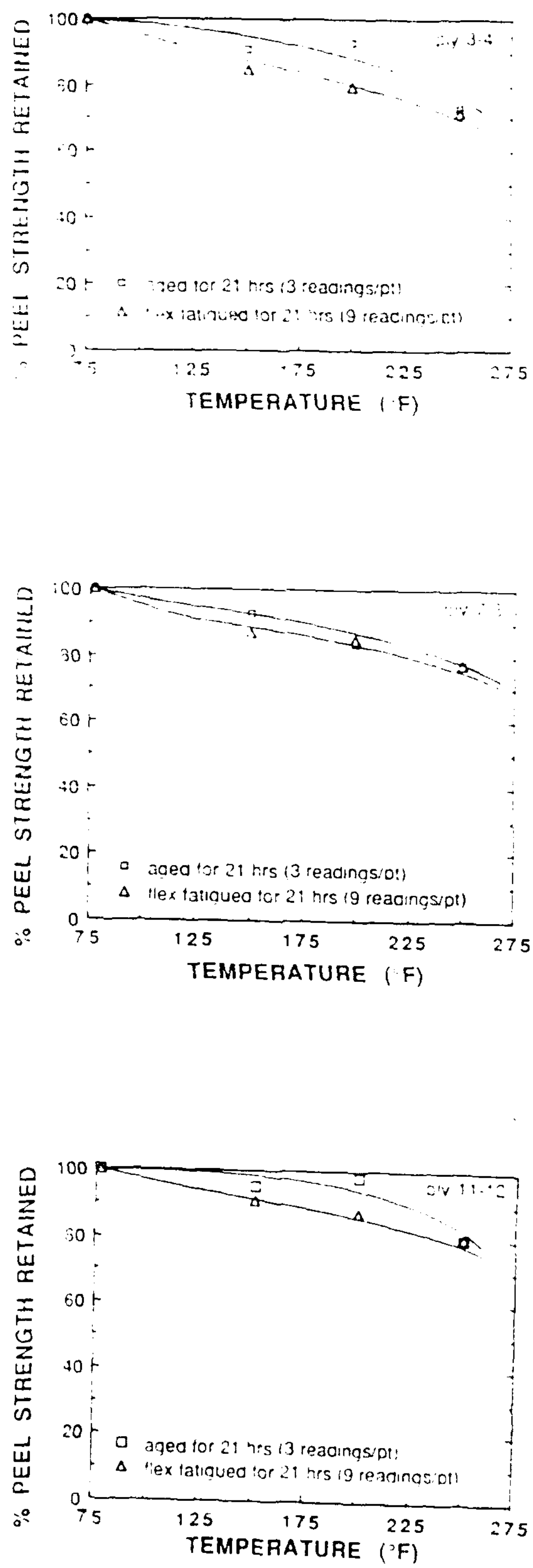

Fig. 41 Thermal aging vs flex fatigue aging

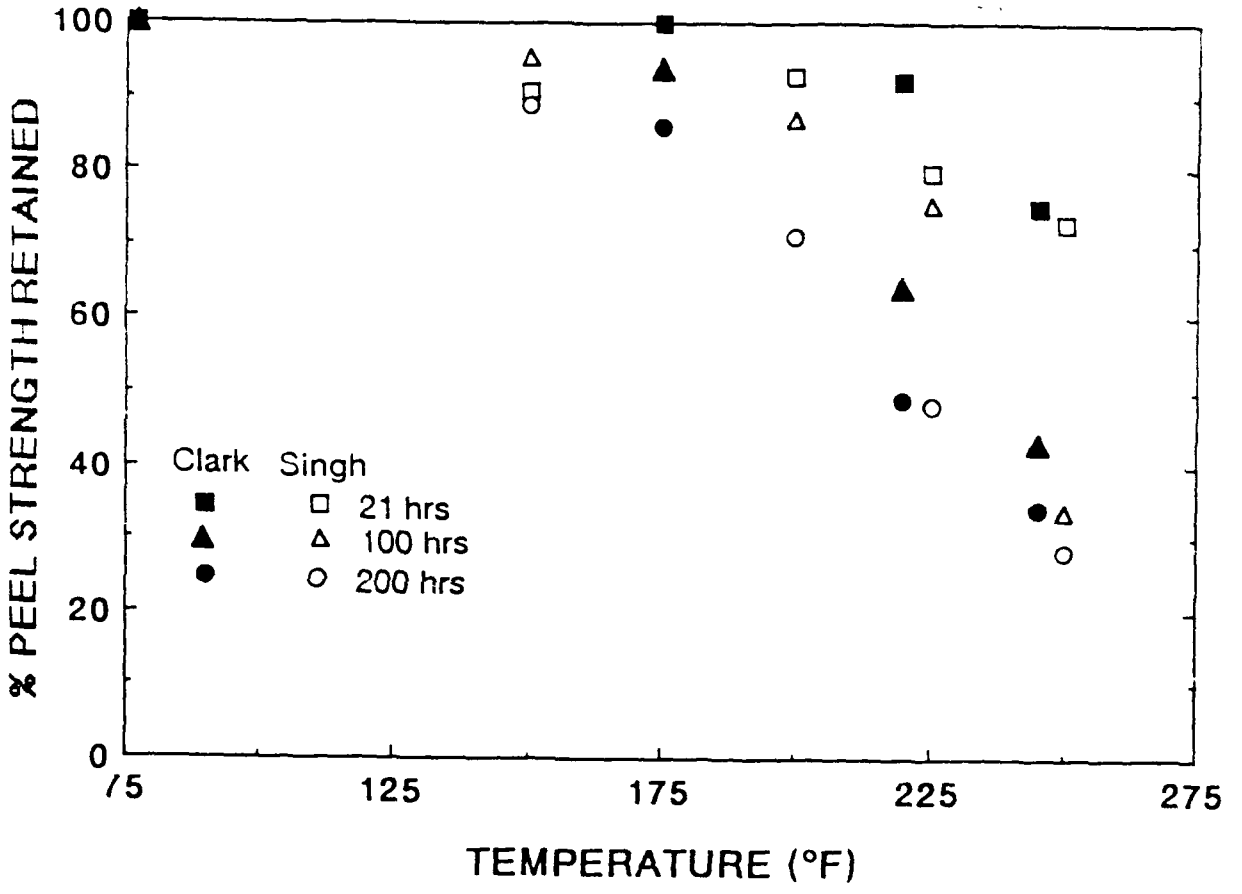

Fig. 42 Thermal aging

ANOVA INPUT:

```
DATA ONE;
INPUT TESTYPES PLYLVL TEMPS STRENGTH;
CARDS;
1 1 1 48.4    1 1 2 43.9    1 1 3 44.8
1 1 4 35.3    1 2 1 48.6    1 2 2 45.1
1 2 3 40.7    1 2 4 35.3    1 3 1 48.8
1 3 2 46.5    1 3 3 47.8    1 3 4 38.9
2 1 1 48.4    2 1 2 40.9    2 1 3 38.5
2 1 4 34.6    2 2 1 48.6    2 2 2 42.3
2 2 3 41.3    2 2 4 37.7    2 3 1 48.8
2 3 2 44.3    2 3 3 42.6    2 3 4 39.1
;
PROC GLM;
CLASSES TESTYPES PLYLVL TEMPS;
MODEL STRENGTH=TESTYPES TEMPS;
```

[Output of SAS Model is shown in Table 23]

Table 23 SAS output for conditioned coupons peel tests

SAS 11:57 MONDAY, NOVEMBER 12, 1990 1

GENERAL LINEAR MODELS PROCEDURE

CLASS LEVEL INFORMATION

CLASS	LEVELS	VALUES
TESTYPES	2	1 2
PLYLVL	3	1 2 3
TEMPS	4	1 2 3 4

NUMBER OF OBSERVATIONS IN DATA SET = 24

DEPENDENT VARIABLE: STRENGTH

SOURCE	DF	SUM OF SQUARES	MEAN SQUARE	F VALUE	PR > F	R-SQUARE	C.V.
MODEL	4	434.62500000	108.65625000	25.22	0.0001	0.841525	4.8305
ERROR	19	81.84833333	4.30780702		ROOT MSE		STRENGTH MEAN
CORRECTED TOTAL	23	516.47333333			2.07552572		42.96666667

SOURCE	DF	TYPE I SS	F VALUE	PR > F	DF	TYPE III SS	F VALUE	PR > F
TESTYPES	1	12.04166667	2.80	0.1109	1	12.04166667	2.80	0.1109
TEMPS	3	422.58333333	32.70	0.0001	3	422.58333333	32.70	0.0001

The important terms used in this model are described below:

TESTYPE = Thermal aging and flex fatigue aging

TEMPS = Elevated temeprature levels

The level of significance (α) for the whole model is α = 0.0001, and [(1-0.0001)*100] = 99.9% is the confidence level for the whole model. In the same way, the levels of significance for testypes and temps are 0.11 and 0 respectively. Hence at the 95% confidence level only temperature is seen to have a significant influence on peel strength. But test type does not have a significant influence on peel strength.

The coefficient of multiple determination (R-SQUARE) for the whole model is 0.0.842. It is obtained using the formula

R-Square = SS (treatment)/SS (corrected total)

5.4 Nature of Peel Fracture

Scanning electron microscopy was used to examine the nature of the delamination between plies. A circular specimen of pairs of peeled plies was cut from selected tire coupons. The pairs of plies were separated and mounted on a SEM side by side to compare the peaks and valleys where the cord and matrix had once mated. These are seen for the various baseline tests in Fig. 43 to Fig. 46. The 180° peel test (Fig. 43) shows almost exclusively matrix-matrix fractures. The 90° peel test (Fig. 44) shows mostly cord-matrix debonding and some matrix-matrix fractures. The +/-90° peel test (Fig. 45) shows almost exclusively cord-matrix debonding. The micrographs from the conditioned

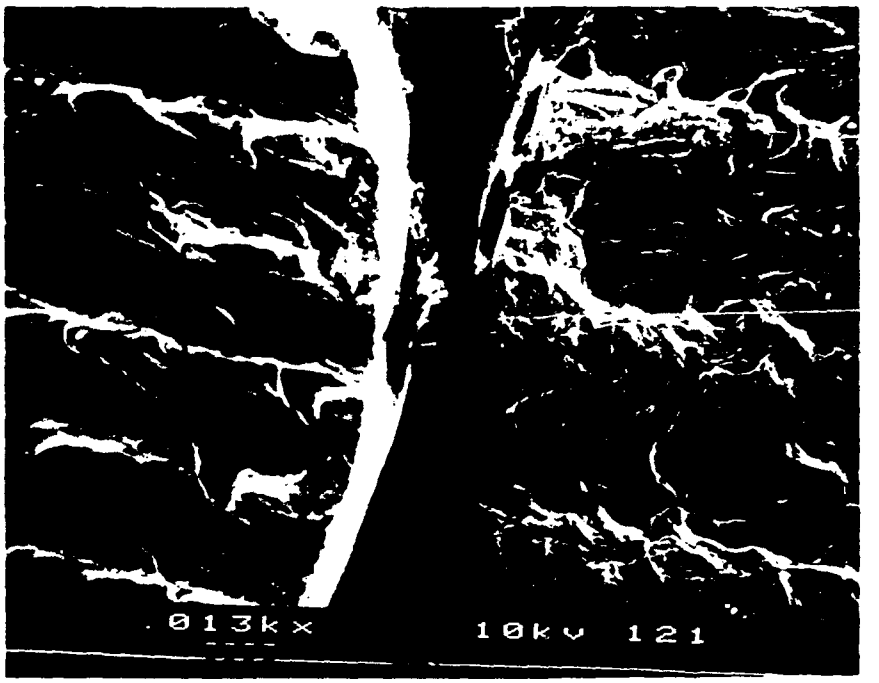

Fig. 43 Micrograph of 180° baseline peel coupon

Fig. 44 Micrograph of 90° baseline peel coupon

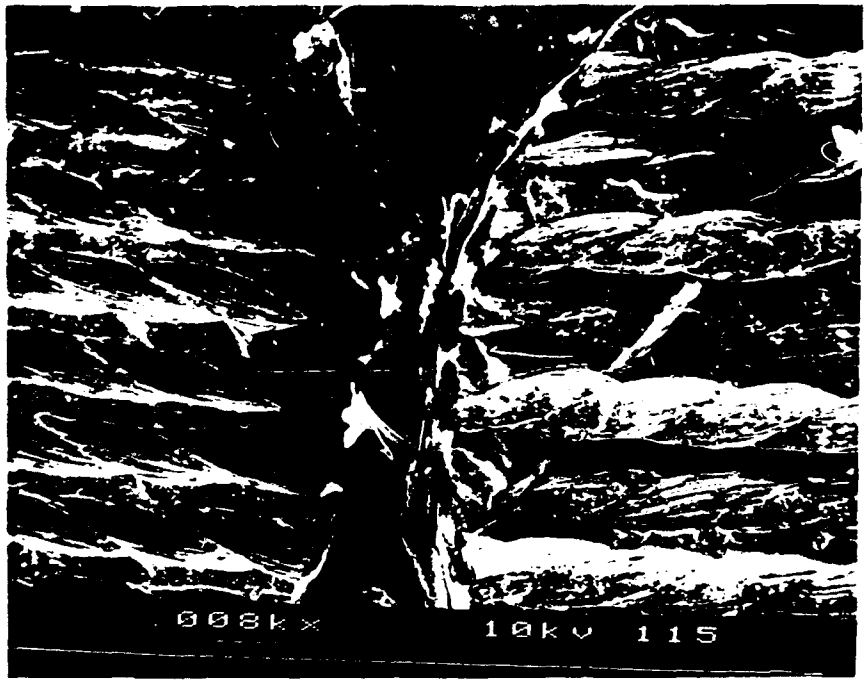

Fig. 45 Micrograph of +/-90° baseline peel coupon

coupons (Fig. 46) shows some signs of melting. The fracture appears to be largely matrix-matrix.

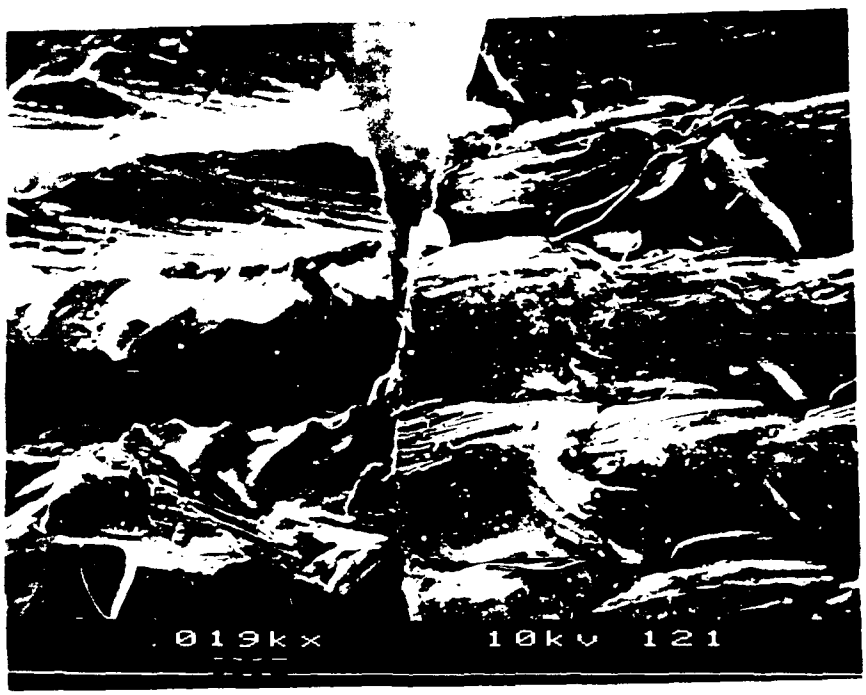

Fig. 46 Micrograph of flex fatigue coupon

Chapter 6

CONCLUSIONS AND RECOMMENDATIONS

The following conclusions can be drawn:

1) The laboratory procedure developed at NC A&T State University for coupon extraction was found to be satisfactory and reasonably convenient.

2) Three peel test configurations were compared for consistency of peel test results. The baseline data from tests performed on virgin tire coupons reveals that the +/- 90° test (recommended by ISO) gives data with the least scatter and range. This test configuration was used to peel conditioned coupons.

3) Statistical analysis performed on baseline data also reveals the influence of variables such as tire, sector and ply level on peel strength. At a 95% confidence level, peel strength was found not to depend on the sector of the tire nor on the ply level used for the peel test. There was a significant variation between the peel strength for different tires, indicating that manufacturing variability exists.

4) The fixtures designed for coupon conditioning were found to be satisfactory and are expected to hold up well for even higher amplitude and frequency of test.

5) A statistical analysis of the conditioned coupon peel strength data indicates that thermal aging temperature has a strong influence on peel strength at the 95% confidence level. However, for the frequency and amplitude achieved, flex fatigue conditioning does not significantly accelerate the degradation any more than just thermal aging at the 95% confidence level.

6) Earlier work done by Clark [3] measured peel strength retention as a function of thermal aging temperature. No tensile preload was applied during those experiments. The results from the test at NC A&T, where a preload was applied, do not appear to be significantly different. A reason for this could possibly be that Clark used tires that were on their first cycle of retreading while the NC A&T study used brand new tires.

7) Constitutive properties of tire tread and carcass material were measured and found to compare favorably with results in the literature where such data was available.

8) Scanning electron microscopy to study the fracture mode in peel testing reveals cord-matrix debonding or matrix-matrix fracture depending on the test type.

Recommendations for future work:

The present study provides a starting point for future

experimentation at greater depth.

1) Development of an expanded database containing peel strength of virgin coupons and of coupons artificially conditioned in the laboratory.

2) Construction/acquisition of a high frequency/high amplitude flex fatigue conditioning unit.

3) Testing of coupons from tires used in the field.

4) Comparison of the results from (1) and (3) to determine the validity of the artificial conditioning environment.

BIBLIOGRAPHY

1. Bhakuni, R.S., Rya, G.W., and Domchick, S.J.,"Adhesive and Processing Concepts for Tire Reinforcing Materials," Tire Reinforcement and Tire Performance, ASTM STP 694, p. 122-138, 1979.
2. Wake, C.W., "Adhesion Science and Tires," Rubber Industry, The City University, London, pp. 242-252, December, 1973.
3. Clark, S.K., "Loss of Adhesion of Cord-Rubber Composites in Aircraft Tires," Tire Science and Technology, Vol. 14, No. 1, pp. 33-43, January-March 1986.
4. Clark, S.K., Dodge, R.N., "Tire Modeling and Contact Problems - Heat Generation in Aircraft Tires," Computers and Structures, Vol. 20, No. 1-3, pp. 535-544, University of Michigan, Ann Arbor, MI, 1985.
5. "Goodyear Aircraft Tire Data," General Data, The Goodyear Tire and Rubber Company, Akron, OH.
6. "Tire Construction," Handbook of Off-the-Road Tires and Their Performance Characteristics, pp. 47-77, The Goodyear Tire and Rubber Company, Akron, OH.
7. Woods, E.C., Pneumatic Tyre Design, pp. 1-60, The Institution of the Rubber Industry, 12 Whitehall, London, England.
8. McPherson, A.T., "Engineering Uses of Rubber," Tires, pp. 296-299, NIST, Washington, DC.

9. Gehman, S.D., "Rubber Structure and Properties," Mechanics of Pneumatic Tires, pp. 1-36, edited by Clark, S.K., University of Michigan, Ann Arbor, MI, 1975.

10. Bhakuni, R.S., Rye, G.W., and Bomchick, S.J., "Adhesive and Processing Concepts for Tire Reinforcing Material," Tire Reinforcement and Tire Performance. pp. 122-138., ASTM, 1979.

11. Kovac, F.J., "Tire Manufacture," Tire Technology, pp. 81-87, The Goodyear Tire and Rubber Company, Akron, OH.

12. Miller, C., Popper, P., Gilmour, P.W., and Scheffers, W.J., "Textile Mechanics Model of a Pneumatic Tire," Tire Science and Technology, pp. 187-226, Vol. 13, No. 4, October-December, 1985.

13. Gough, V.E., "Structure of the Pneumatic Tire," Mechanics of Pneumatic Tires, edited by Clark, S.K., University of Michigan, Ann Arbor, MI, 1975.

14. Curtiss, W.W., "Principles of Tire Design," Tire Science and Technology, Vol. 1, No. 1, pp. 77-98, February, 1973.

15. Noor, A.K., Anderson, F.M., "Finite Element Modeling and Analysis of Tires," Tire Modeling, Tanner, J.A., Langley Research Center, Hampton, VA, September, 1982.

16. Noor, A.K., Tanner, J.A. "Tire Modeling and Contact Problem - Advanced and Trends in The Development of Computational Models for Tires," Computers for Structures, Vol. 20, No. 1-3, pp. 517-533, 1985.

17. Noor, A.K., Anderson, C.M, Tanner, J.A., "Mixed Models and Reduction

Technique for Large Rotation, Nonlinear Analysis of Shells of Revolution with Application to Tires," Langley Research Center, Hampton, VA.

18. Tielking, J.T., Martin, R.E., and Schapery, R.A., "A Note on Tire Carcass Mechanical Properties," Tire Science and Technology, Vol. 6, No. 4, pp. 248-262, November, 1978

19. Vorachek, J.J., "Role of Tire Reinforcement on Composite Static and Dynamic Characteristics," Tire Reinforcement and Tire Performance, ASTM, pp. 180-199, 1979.

20. Kovac, F.J., O'Neil, K.B., Predicting the Fatigue Performance of Tires, Material Research & Standards, Vol. 8, No. 6, pp. 27-32, June, 1968.

21. Brewer, H.K., "Measurement of Steady State and Transient Aircraft Tire Forces," Tire Science and Technology, Vol. 3, No. 2, pp. 111-127, May, 1975.

22. Bobo, S.N., "Adhesion of Aircraft Tires," Tire Modeling, NASA Conference Publications 2264, 1983.

23. "Rubber, Vulcanized - Determination of Adhesion to Textile Fabric," International Standard, ISO 36-1985(E).

24. "Rubber Property - Adhesion to Flexible Substrate," ASTM D413 82 and 88.

25. Harcsar, F.G., "The Harcsar-Reiger Method for Determination of Tire Components Adhesion," Test Engineering, November, 1970.

26. Gardon, J.L., "Peel Adhesion," Journal of Applied Polymer Science, Vol. 7, pp. 625-641, Textile Research Laboraatory, Rohm and Haas Company,

Philadelphia, Pennsylvania, 1963

27. Gent A.N., Hamed, G.R., "Peel Mechanics for an Elastic-Plastic Adherend," Rubber Chemistry and Technology, Vol. 52, pp. 1057-1071, Institute of Polymer Science, The University of Akron, Akron, OH, 1979.

28. Takashigarashi, "Mechanics of Peeling of Rubbery Material - Peel Strength and Energy Dissipation," Journal of Polymer Science, Polymer Physics Edition, Vol. 13, pp. 2129-2134, Research Laboratory, Hitachi Cable Ltd., Hidakaco, Hitachi, Ibaraki-Ken, JAPAN, 1975.

29. Iyengar, "Adhesion Behavior of Nylon Tire - Cord/Adhesive/Rubber Systems," Journal of Applied Polymer Science, Vol. 13, pp. 353-663, Industrial Products Research Laboratory, E.I. du Pont de Nemours & Company, Inc., Wilmington, DE, 1969.

30. Iyengar, Y., "Adhesion of Kevlar Aramid Cord to Rubber," Journal of Applied Polymer Science, Vol. 22, pp. 801-812, Industrial Products Research Laboratory, E.I. du Pont de Nemours & Company, Inc., Wilmington, DE, 1978.

31. Gent, A.N., Hamed, G.R., "Some Rheological Aspects of The Peel Strength of Rubbery Adhesives," Rubber Chemistry and Technology, Vol. 55, pp. 483-493, Institute of Polymer Science, The University of Akron, Akron, OH, 1982.

32. Schreuder-Stacer, H.L., "Peel Strength Of Composite Layered Joints," Rubber Chemistry and Technology, Vol. 61, pp. 794-811, Institute of

Polymer Science, The University of Akron, Akron, OH, 1988.

33. Gent, A.N., Hamed, G.R., "Adhesion of Elastomers with Special References to Triblock Copolymers," Rubber Chemistry and Technology, Vol. 51, pp. 354-364, Institute of Polymer Science, The University of Akron, Akron, OH.

34. Breidenbach, R.F., Lake, G.J., "Mechanics of Fracture in Two - Ply Laminates," Rubber Chemistry and Technology, Vol. 52, pp. 96-109, The Firestone Tire & Rubber Company, Central Research Laboratories, Akron, OH, 1979.

35. Iyengar, Raj, "Adhesion of Tire Cords - The Total Picture," Rubber World, pp. 24-29, November, 1987.

36. Brodsky, G.I., "Comprehensive Evaluation of Cord - to - Rubber Adhesion," Rubber World, pp. 29-39, Hercules Inc., Wilmington, DE, August, 1984.

37. Watton, D.B., "The Adhesion of Textile Tire Materials," Rubber World, pp. 36-41, Milliken Industries Ltd., Bury, England, April, 1984.

38. Lake, G.J., Thomas, A.G., " Strength Properties of Rubber," Natural Rubber Science and Technology, pp. 731-772, 1988.

APPENDIX A

MTS - 810 Testing Machine

The 810 Material Testing System is a hydraulic testing machine. Closed loop control is provided for the servohydraulic system. This system includes load unit, load cell, grips, servovalve, hydraulic power supply, and hydraulic service manifold.

Load Unit: Figure A.1 shows a schematic of the Series 318 Load Unit used in this system. Table A.1 lists important dimensions and weights.

Load Cell: Several load cells were available for the load unit described above. Table A.2 lists the characteristics for the two load cells used in this study.

Hydraulic Power Supply:

Model Number	610.21B
Serial Number	210
Flow Rate	21.2 gpm
Continuous operating pressure	3,000 psi.

Servo Valves: Series 252 Servovalves are used in this unit. Specification are listed in Table A.3. The displacement vs frequency curve for the valve is shown in Fig. A.2.

Servovalve Flow rating:

Model Number	252.24C
Full-Flow Rating	10 gpm (37 l/m)
90° point at 10% command	140 Hz

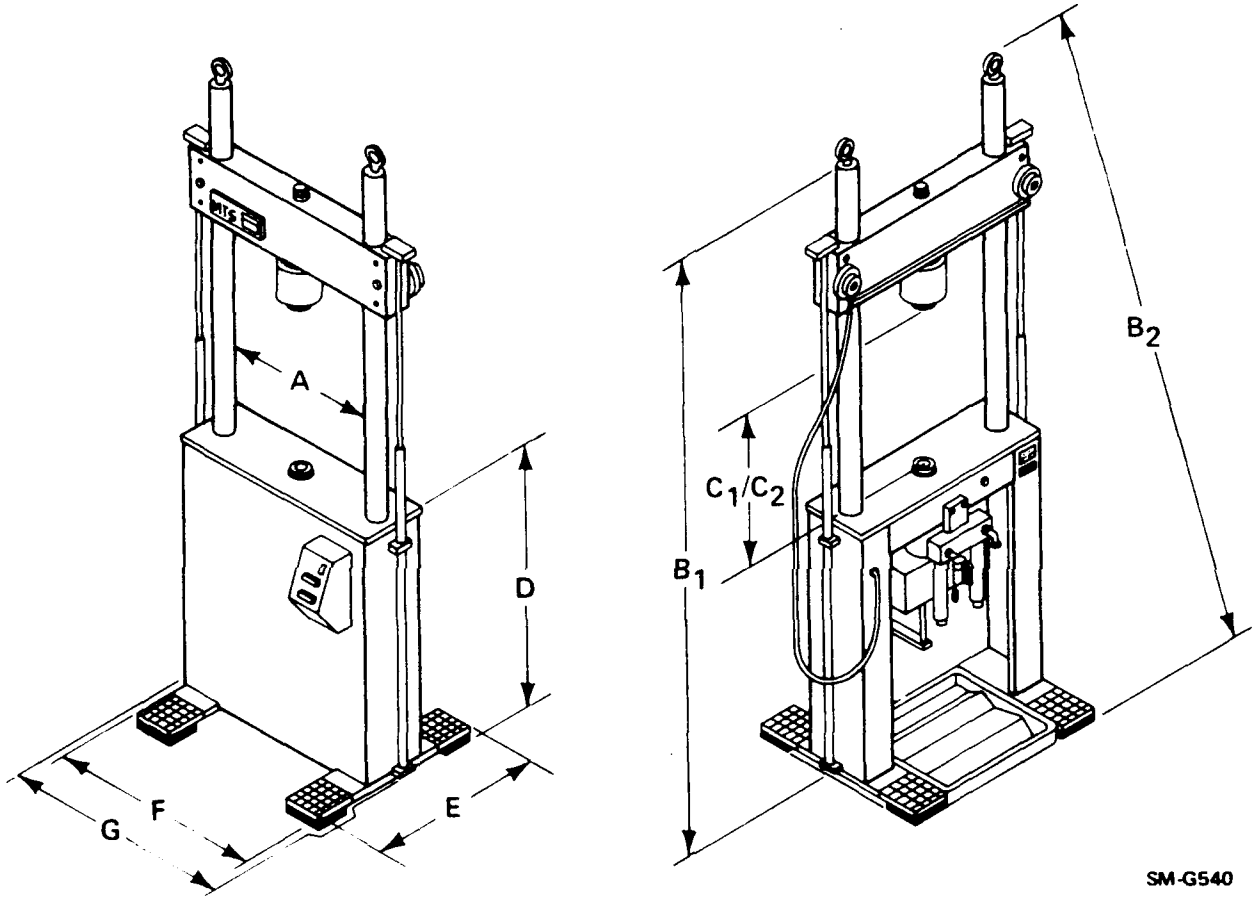

Fig. A.1 Load Unit Dimensional Drawing

Table A.1 Load Unit Dimensions and Weights

Parameter	Model 318.25	
Maximum actuator force rating	55 kip	250 kN
Weight Load unit (approx.) Crosshead (approx.)	 2000 lbs 225 lbs	 960 kg 102 kg
Clearance Between columns(A)	25 in.	0.6 m
Load Frame height Vertical without lift ring (B_1)	119 in.	3.0 m
Diagonal with lift rings (B_2)	128 in.	3.2 m
Specimen and grip space Minimum (C_1) Maximum (C_2)	 9.75 in. 65 in.	 0.25 m 1.6 m
Platen height from floor (D)	35 in.	0.9 m
Base depth (E)	30 in.	0.7 m
Base width (F)	34 in.	0.8 m
Width including lifts (G)	40 in.	1.0 m

Table A.2 Load Cell Specifictions

	Load cell for baseline peel testing	Load cell for flex fatigue testing
Model Number	661.19C-01	661.23A-01
Serial Number	49608	2381
Capacity	1 kip	55 kip
Load cartridg/s available	5,000, 1,000, 500, 200, 100 lbs.	1,000, 500, 200,100 lbs.
Load cartridg/s used	100 lbs.	500 lbs.

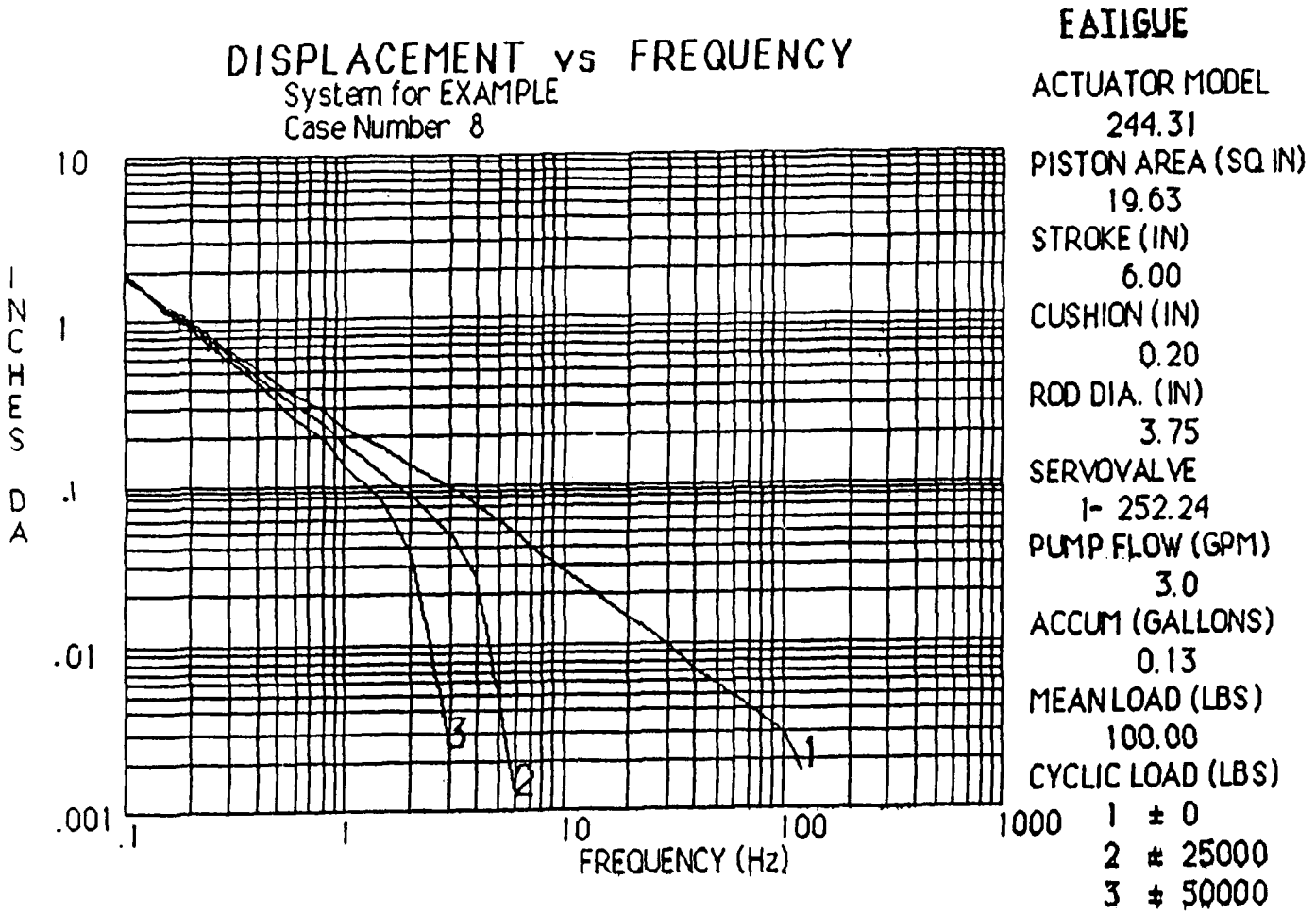

Fig. A.2 Servovalve Displacement vs Frequency

Table A.3 Servovalve Specifications

Servovavle Specifications	
Operating supply pressure	3,000 psi (20.7 MPa)
Temperature range	-65 to 275°F (-53 to 135°F)
Rated full flow input signal current (per coil)	25 mA (series) 50 mA (differential)
Coil resistance	80 ohms
Weight 252.2X/0.4X 252.3X	 2.3 lbs (1.03 kg) 7.75 lbs (3.5 Kg)